

INFORMATION TO USERS

This dissertation was produced from a microfilm copy of the original document. While the most advanced technological means to photograph and reproduce this document have been used, the quality is heavily dependent upon the quality of the original submitted.

The following explanation of techniques is provided to help you understand markings or patterns which may appear on this reproduction.

1. The sign or "target" for pages apparently lacking from the document photographed is "Missing Page(s)". If it was possible to obtain the missing page(s) or section, they are spliced into the film along with adjacent pages. This may have necessitated cutting thru an image and duplicating adjacent pages to insure you complete continuity.
2. When an image on the film is obliterated with a large round black mark, it is an indication that the photographer suspected that the copy may have moved during exposure and thus cause a blurred image. You will find a good image of the page in the adjacent frame.
3. When a map, drawing or chart, etc., was part of the material being photographed the photographer followed a definite method in "sectioning" the material. It is customary to begin photoing at the upper left hand corner of a large sheet and to continue photoing from left to right in equal sections with a small overlap. If necessary, sectioning is continued again — beginning below the first row and continuing on until complete.
4. The majority of users indicate that the textual content is of greatest value, however, a somewhat higher quality reproduction could be made from "photographs" if essential to the understanding of the dissertation. Silver prints of "photographs" may be ordered at additional charge by writing the Order Department, giving the catalog number, title, author and specific pages you wish reproduced.

University Microfilms

300 North Zeeb Road
Ann Arbor, Michigan 48106

A Xerox Education Company

73-11,574

SEVAK, Nitin Mohanlal, 1942-
OPTIMAL SYNTHESIS OF FLEXIBLE LINK MECHANISMS WITH
LARGE STATIC DEFLECTIONS.

The Ohio State University, Ph.D., 1972
Engineering, mechanical

University Microfilms, A XEROX Company, Ann Arbor, Michigan

OPTIMAL SYNTHESIS OF
FLEXIBLE LINK MECHANISMS
WITH LARGE STATIC DEFLECTIONS

DISSERTATION

Presented in Partial Fulfillment of the
Requirements for the Degree Doctor of
Philosophy in the Graduate School of
The Ohio State University

By

Nitin Mohanlal Sevak, B.E., M.Sc.

* * * * *

The Ohio State University
1972

Approved by



Adviser
Department of Mechanical
Engineering

PLEASE NOTE:

Some pages may have

indistinct print.

Filmed as received.

University Microfilms, A Xerox Education Company

To my late parents Sumanben and Mohanlal

ACKNOWLEDGEMENTS

The author wishes to express his indebtedness to his advisor, Prof. C. W. McLarnan for his guidance, valuable suggestions and generous assistance provided throughout the development of this investigation.

The author would like to take this opportunity to express his appreciation to his supervisor, Dr. D. R. Bussman of the National Cash Register Company, for his support throughout the doctoral program and for his interest and encouragement in this investigation. He extends his sincere thanks to his colleagues, Dr. C. Mei, for many hours of consultation and Mr. D. Filsinger for his assistance in the experimental work. Also, many thanks to Mrs. Margaret Smith for her skillful typing of this manuscript.

To his wife, Ulupi, a very special gratitude is expressed for her patience, understanding and moral support during the course of this study.

VITA

June 27, 1942 Born - Surat, India
1964 B.E.(M.E.), The M.S.
University of Baroda, India
1965 M.Sc., The University of
California, Berkeley,
California
1965 Mechanical Engineer, The
National Cash Register Co.,
Dayton, Ohio

PUBLICATIONS

"Mechanism Case Studies - Detent Mechanism". ASME paper
No: 72-Mech-59.

FIELDS OF STUDY

Major Field: Mechanical Engineering

Studies in Kinematics of Mechanisms.

Professors C. W. McLarnan, A.S. Hall, J.M. Shah

Studies in Mechanical Design.

Late Professor K.G. Hornung, Professor W.L. Starkey,
J.L. Costanza, R.T. Shah

Studies in Engineering Mechanics.

Professors W.E. Clausen, P.E. Korda,
D.M. Cunningham

Studies in Mathematics.

Professor H.D. Colson, H.D. McNiven

TABLE OF CONTENTS

	Page
ACKNOWLEDGEMENTS	ii
VITA	iii
LIST OF TABLES	vi
LIST OF FIGURES	vii
LIST OF SYMBOLS	ix
 Chapter	
I. INTRODUCTION	1
1.1 Flexural Joints and Flexible Link Mechanisms	
1.2 Background	
1.3 Scope of the Investigation	
II. NONLINEAR ANALYSIS BY THE FINITE ELEMENT METHOD	13
2.1 Introduction	
2.2 Basic Equations of the Finite Element Method	
2.3 Coordinate Transfer	
2.4 Formulation of the Finite Element Method for a Structure	
2.5 Solution Procedure for the Nonlinear Analysis	
III. ANALYSIS OF NONLINEAR SPRINGS	38
3.1 Cantilever Beam	
3.2 Attempts to Improve the Results	

TABLE OF CONTENTS (Continued)

IV.	ANALYSIS OF FLEXIBLE LINK MECHANISMS	49
4.1	One Flexible Member - Flexible Strip as a Coupler	
4.2	Two Flexible Members - Rigid Coupler Supported on two Flexible Input and Output Links	
4.3	Two Flexible Members - Flexible Members as Flexural Joints	
V.	OPTIMIZATION METHODS IN THE SYNTHESIS OF MECHANISMS	67
5.1	Introduction	
5.2	Formulation of Equations for the Optimization Method	
5.3	Variable Metric Method	
VI.	OPTIMUM DESIGN OF NONLINEAR SPRINGS.	81
6.1	Design of Cantilever Beam	
VII.	OPTIMUM DESIGN OF FLEXIBLE LINK MECHANISMS	88
7.1	Synthesis for Function Generation, $y=x^2$	
7.2	Synthesis of a Flexible Coupler Mechanism	
7.3	Synthesis of a Flexible Coupler Mechanism from a Different Starting Design	
7.4	Study of the Remaining Design Variables of the Flexible Link Mechanism	
7.5	Synthesis of a Flexural Joint Mechanism	
7.6	Common Characteristics of the Results	
VIII.	CONCLUSION	106
8.1	Discussion of the Results	
8.2	Possibilities for Future Research	
APPENDIX		
A.	COMPUTER PROGRAM	111
BIBLIOGRAPHY		136

LIST OF TABLES

Table	Page
1. Joints and Their Corresponding Nodal Displacements	50
2. Optimum Design of a Cantilever Beam Using the Objective Function, E_A . . .	84
3. Comparison of the Three Objective Functions	87
4. Optimum Synthesis of a Flexible Coupler Mechanism	92
5. Optimum Synthesis of a Second Flexible Coupler Mechanism	95
6. Optimum Synthesis of a Flexural Joint Mechanism.	101

LIST OF FIGURES

Figure	Page
1. Flexural Joint Four-Bar Linkage	3
2. Mechanical Adder Linkage	3
3. Hammer Guide Spring Mechanism	3
4. Flexible Link Mechanism	3
5. Nonlinear Analysis by the Linear Incremental Method	15
6. Planar Beam Element with Six Degrees of Freedom	17
7. Displacement Relationship Between the Local (x-y) and the Global (X-Y) Coordinate Systems	24
8. Three-member Planar Structure with 7 Nodal Displacements	29
9. Flow Diagram of the Finite Element Method Using the Linear Incremental Procedure	37
10. Cantilever Beam Subjected to a Large Deflection	39
11. Results of Nonlinear Analysis for a Cantilever Beam	41
12. Comparison of Experimental and Analytical Results	42
13. Shapes of a Cantilever Beam	44
14. Effects of the Number of Elements and Increments on the Convergence of the Results	48
15. Flexible Coupler Mechanism	52
16. Results of the Flexible Coupler Mechanism Analysis	54
17. Deflected Shapes of the Flexible Coupler . .	56
18. Flexible Input and Output Link Mechanism . .	58
19. Shapes of the Flexible Input and Output Link Mechanism During Displacement	60

LIST OF FIGURES (Continued)

Figure	Page
20. Flexural Joint Mechanism	63
21. Results of the Flexural Joint Mechanism Analysis	65
22. Desired and Generated Functions	74
23. Flow Diagram of the Variable Metric Method	76
24. Design of a Cantilever Beam for a Desired Force vs. Displacement Relationship . . .	82
25. Design Variables for a Flexible Coupler Mechanism	91
26. Relationship Between E_A and θ_s	91
27. Synthesis of a Flexible Coupler Mechanism	93
28. Second Flexible Coupler Mechanism	95
29. Synthesis of a Second Flexible Coupler Mechanism	97
30. Study of Effects of the Fixed Length d_o and Coupler Thickness h on the Maximum Stress in the Coupler	99
31. Design Variables for a Flexural Joint Mechanism	101
32. Synthesis of a Flexural Joint Mechanism . .	103

LIST OF SYMBOLS

a_i	Constants for the horizontal displacement function
A	Area of the beam element
b	Width of the beam element
b_i	Constants for the vertical displacement function
$\{d\}$	Design variables
E	Elastic modulus
E_A	Sum of the absolute values of the error curve
E_M	Maximum value of the error curve
E_R	Root-mean square value of the error
$\{F\}$	Element nodal forces
$\{G\}$	Gradients of the objective function
h	Thickness of the beam element
$[H]$	Approximate Hessian matrix
I	Area moment of inertia
$[I]$	Identity matrix
$[k]$	Element stiffness matrix
$[K]$	Stiffness matrix of the structure
$[k_E]$	Elastic stiffness matrix for the element
$[k_G]$	Geometric stiffness matrix for the element
L	Length of the beam
M	Bending moment

LIST OF SYMBOLS (Continued)

[M]	Correction to the approximate Hessian matrix
[N]	Correction to the approximate Hessian matrix
{P}	Nodal forces in the global system
{q}	Nodal displacements in the global system
{R}	Difference between the gradients for two consecutive steps
S	Direction of the line of search
[T]	Coordinate transformation matrix
u	Horizontal displacement of the beam element
U	Strain energy
v	Vertical displacement of the beam element
x,y	Local coordinate system
X,Y	Global coordinate system
α	Increment along the line of search
[β]	Matrix which relates the element and the structure displacements in the global system
γ	Element orientation angle in the global coordinate system
{ δ }	Element nodal displacements
ϵ	Strain
θ	Rotation of the input link
ϕ	Rotation of the output link
Δ	Increment
{ }	Column vector

LIST OF SYMBOLS (Continued)

$[\]$	Matrix
$[\]^{-1}$	Inverse of the matrix
$[\]^{-T}$	Transpose of the matrix

CHAPTER I

INTRODUCTION

1.1 Flexural Joints and Flexible Link Mechanisms

A new era in mechanism design has begun where pin (revolute, pivoted) joints of the linkage are replaced by flexural (flexible) joints. Problems of backlash and wear are inherent with pivoted joints. In many applications the lubrication of joints is difficult because of small rotations of the linkage or because of hostile environmental conditions. This results in excessive frictional forces at the joints, which oppose the motion of the linkage.

Bendix [1] produced flexural pivots as a replacement for the pin joints. These flexural pivots can perform as bearings, hinges, force sensing devices, torsional springs, or may serve many other functions. The flexural pivot solved most of the problems associated with pin joints but the relatively high cost of the flexural pivots and their limited rotation prevent their unanimous acceptance for pin joint replacement.

Hewlett Packard [2] designed a four-bar linkage with flexural joints for an adjustment of the mirror of the optical galvanometer in an ultraviolet recorder. The form of the linkage used by Hewlett Packard is depicted in Figure 1. The flexural joints deflect in this linkage to achieve $\pm 2.5^\circ$ of adjustment. This particular linkage was moulded of glass filled polycarbonate, which reduced the cost of manufacturing tremendously.

Infotechnics, Inc. [3] used flexural joints instead of pivots in their design of a random access prime mover. Levers, torsional springs and flexural joints were produced from a metal sheet by a chemical etching process to simplify fabrication. This reduced the inertia of the system which increased the speed of the prime mover's rotation with increased accuracy.

Many other companies have also used flexural joints in one form or other in their products. At NCR the flexural joint linkage as shown in Figure 2 was considered for the mechanical adder. Another unusual application of the flexible link mechanism was made to guide the hammer of a high speed printer. The linkage of

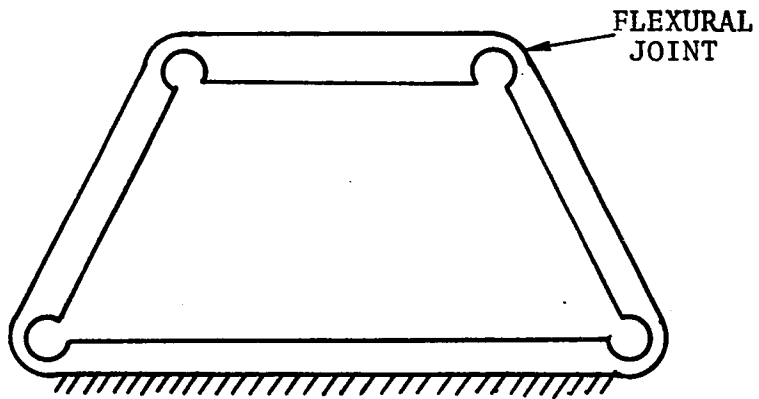


Figure 1. Flexural Joint Four-Bar Linkage

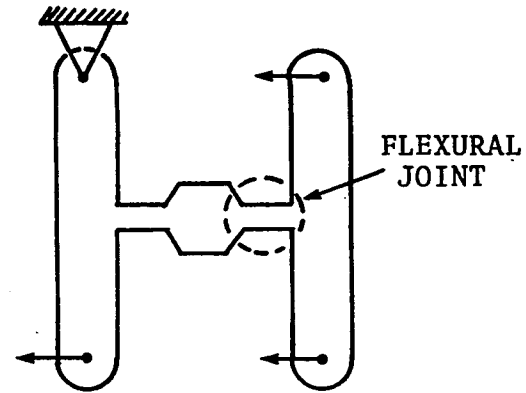


Figure 2. Mechanical Adder Linkage

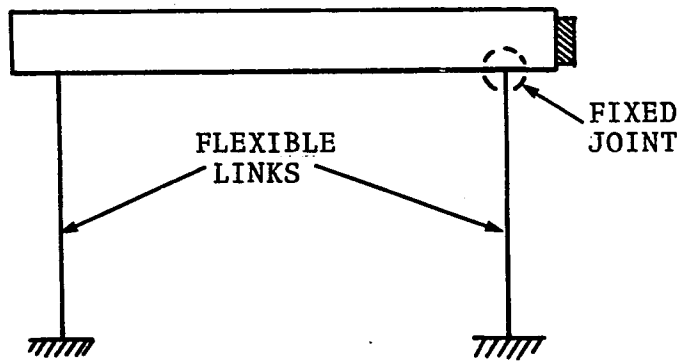


Figure 3. Hammer Guide Spring Mechanism

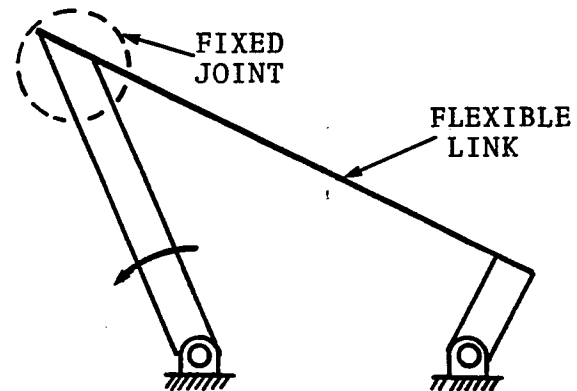


Figure 4. Flexible Link Mechanism

Figure 3 is the hammer guide spring mechanism whose flexible guide springs are bonded in the plastic hammer. The joints at the coupler are defined as fixed joints.¹

Another possible practical version of the flexible link mechanism is depicted in Figure 4 whose coupler is a flexible link which is connected by fixed joints to rigid input and output links. This type of linkage has the capability of large rotation which is necessary to demonstrate the technique of nonlinear analysis. The linkage can be used as a nonlinear spring but the author's interest is to use it as a function generator.

From the above applications it can be stated clearly that the flexural joint and flexible link mechanisms have the following advantages over pin joint linkages:

- A. Wear, lubrication and frictional losses diminish to near zero.
- B. Zero backlash makes increased accuracy and reduces noise levels.
- C. Lower manufacturing cost and better quality control can be achieved.
- D. Fewer parts in the mechanism make it mechanically simpler and increases the reliability.

¹Burns and Crossley [7] defined this type of joint as a fixed joint.

The distinction between pinned, fixed and flexural joints are clear from Figure 1 to 4. One more clarification the author would like to make is between rigid, elastic and flexible links. A rigid link is one which does not deform under the operating conditions. When a rigid link is deformed under static or dynamic loading then this link becomes an elastic link. A flexible link is an elastic link which must deflect to impart motion to the linkage as depicted in linkages of Figure 3 and 4.

From Grübler's criterion² for the number of degrees of freedom of a plane linkage it can be proven that linkages which have less than 4 links and a maximum of 3 pinned or prismatic joints (with the exception of fixed and flexure joints) will have zero or a negative number of degrees of freedom. The linkages shown in Figure 1 to 4 fall in this category, e.g. the linkage of Figure 1 is a one piece member or link with no joints which will have zero degrees of freedom. These linkages can move only due to the elastic deflection of the joints or the flexible links. More detailed discussion on the

²Grübler's criterion:

$$\text{Number of degrees of freedom} = 3(L-1) - 2J$$

Where L=Number of links, and J = Number of joints

number of degrees of freedom and the structural permutations of flexible link mechanisms is covered by Burns and Crossley [7] and Shoup and McLarnan [13].

A limitation of the flexible link mechanism is that the linkage will have relatively small rotation. Also with fixed or flexural joints at the coupler, as in linkage of Figure 4, the crank will not be able to make more than one revolution unless the flexible link winds up like a watch spring. So the flexible link mechanisms covered in Figure 1 to 4 can be used only as a "double-rocker" mechanism. If one of the joints at the coupler is permitted to be a pin joint then the mechanism can be used for a "crank-rocker" application. But this will not be covered in this investigation.

1.2 Background

Flexible link mechanisms with one or more flexible members were first explored by Burns and Crossley [7], [8]. They proposed a semi-graphical static synthesis technique for a flexible link four bar mechanism similar to linkage of Figure 4 whose coupler is a flexible link which acts as a cantilever beam (fixed-pin) or an encastered beam (fixed-fixed). Shockling [9] has utilized non-linear flexible beams to replace one or more

links or joints in a kinematic linkage. Shoup and McLarnan [10-13], applied the equations of the undulating and nodal elastica to a flexible strip subjected to very large displacements. The results are presented in terms of the non-dimensional variables which serve as a first approximation for the iterative synthesis of flexible link devices or flexible link mechanisms.

Boronkay and Mei [14] analyzed the motions of mechanical adder linkage of Figure 2. The finite element method was used to simulate the dynamic response of the mechanical adder linkage to the multiple inputs. Small displacement (linear) theory was sufficient to obtain a reasonable match between the theoretical and experimental results. The finite element method was combined by Winfrey [15] with the kinematics of rigid link mechanisms to predict the dynamics of elastic mechanisms. The method was demonstrated on a planar quick return mechanism and a spatial Bennett mechanism to determine the dynamic deflection of the coupler link under a constant speed of an input shaft. Also, he [16] reduced the computational time by modifying the method without appreciable loss of accuracy.

A similar technique was developed by Erdman, Sandor, et al [17-20] for dynamic synthesis. The method was based

on a new stretch rotation operator which includes kineto-elastodynamic effects. The technique provides a systematic iterative process for synthesis of an elastic mechanism.

Refs. [21-23] deal with the dynamic response and vibration analysis of the elastic connecting rod of a planar slider crank mechanism. Classical beam theory was used for the derivation of the motion equations which were solved by numerical methods. Refs. [24,25] carried out the stability analysis of the elastic coupler in a planar mechanism. Davidson [26] worked out the analysis and approximate synthesis of a slider-crank mechanism whose slider was connected to another slider through a spring. A survey article by Lowen and Jandrasits [27] covers the literature in the area of dynamic behavior of mechanisms with elastic links which are assumed to have a continuous distributed mass.

The background material thus far mainly pertains to the analysis of elastic and flexible link mechanisms. Now a brief background on the synthesis of rigid link mechanisms will be covered. Special attention will be given to the optimization methods. Rigid link mechanisms were used by many researchers to demonstrate the capability of optimization methods. It is the purpose of this investigation to apply one of the optimization methods to the

synthesis of flexible link mechanisms. A detailed discussion of optimization methods is included in chapter V.

There are several ways to synthesize rigid link mechanisms. The methods can be grouped into direct (classical) methods and indirect methods. The direct methods include graphical as well as analytical procedures, while the indirect methods include the optimization techniques. In the direct analytical method, characteristically, the linkage equation is derived in terms of the unknown dimensions (parameters) of the linkage. These parameters are determined from the solutions of a set of linear or nonlinear simultaneous equations for known conditions at the precision points. The solution may be obtained by one of several standard techniques.

Leading contributions in the direct synthesis methods have been made by Freudenstein, McLarnan, Sandor and Roth [40-44] who studied the synthesis of four-link, six-link and geared five-bar mechanisms. Since then more sophisticated methods have been developed to synthesize spatial and complex planar mechanisms, as accounted for in survey articles [49] and [50].

Recently indirect methods have been developed for mechanism synthesis whereby the synthesis is performed indirectly. An objective criteria for the synthesis is formulated indirectly in terms of the mechanism parameters. The mechanism synthesis is then achieved by driving the objective criteria to its minimum value by the process of successively readjusting the mechanism parameters based on one of the optimization methods (mathematical or non-linear programming methods).

The following is a list of the optimization methods and the major users of the method in the mechanism synthesis field.

- A. Least square method - Timko [52].
- B. Random methods - Tomas [61], Garrett and Hall [63].
- C. Rosenbrook's rotating coordinate method - Lakshminarayana and Narayanamurthi [66].
- D. Steepest Descent - Tull and Lewis [70].
- E. Fletcher and Powell's variable metric method - Fox and Willmert [79].

Some optimization methods are capable of handling design constraints such as limitations on the length of the links, location of the shafts, minimum or maximum

magnitude of the transmission angle, etc. References [61] and [79] have demonstrated the synthesis of mechanisms using design constraints for function and coupler curve generation problems.

Compared to the direct synthesis method, the indirect methods require only one formulation of the objective criteria for all synthesis problems (function generation, coupler curve generation or coupler positioning) regardless of the linkage type to be designed, whereas the evaluation of the objective criteria by way of analysis is unique for each problem. This makes it possible to use the indirect method for generalized computer-oriented synthesis of mechanisms. The limitation of the method is that the global minimum is not guaranteed, only the local minimum is attained, and that a good starting design is required for rapid convergence to the optimum design.

1.3 Scope of the investigation

In this dissertation, the analysis and synthesis of flexible link mechanisms, as depicted in Figure 1 to 4, will be investigated. The finite element method used by Boronkay and Mei [14], and Winfrey [15] will be extended for the static large rotation of the mechanism. Since

the large rotation makes the analysis nonlinear, the problem will be solved by the piecewise linear method. The synthesis of the mechanism will be attempted by Fletcher and Powell's variable metric method of optimization.

In the mechanism, the flexible link is assumed to be initially straight and without internal stresses. To avoid the buckling and snap-through behavior, the present investigation assumes that the flexible link will be under tension during the motion of the linkage. Also, it assumes that the flexible link will not be subjected to a twisting moment. The present formulation of analysis can only account for rectangular cross sections of the flexible links. But, with slight modification this restriction can be removed.

The derivation is general. Therefore, the method is capable of solving any complex mechanism assuming any combination of external loads. For simplicity, however, the four bar mechanism will be analyzed and it will not be subjected to external loading other than the driving force.

The analysis and synthesis procedures will be developed in the next chapters and will be demonstrated first on a cantilever beam subjected to the large deflections. The same technique then will be applied to the mechanism having one or more flexible links.

CHAPTER II

NONLINEAR ANALYSIS BY THE FINITE ELEMENT METHOD

2.1 Introduction

The finite element method was initially developed in the early Nineteen Fifties and is gaining a widespread acceptance in the field of structural analysis. Normally, links of the traditional pin-jointed linkage are assumed rigid, thus it does not deflect during the motion of the linkage. Therefore, the structural analysis method is not required for the analysis of a pin-jointed linkage but it is required for a flexural joint or flexible link mechanism. Because, as mentioned previously, the flexible members have to deflect to impart motion to a flexible mechanism. The finite element method has been shown to produce accuracies of the same order of magnitude as the classical methods. In addition, the finite element method is more general and is easier to apply than the classical methods. The finite element method for large (nonlinear) static deflections will be developed in this chapter and will be applied to the analysis of flexible link mechanisms.

The pioneering efforts in the field of the finite element methods were contributed individually by Argyris and Turner. Turner used a matrix displacement method, i.e. a direct stiffness method of finite element analysis to solve complex structures subjected to linear deflections. Since that time much progress has been made in linear and nonlinear analysis.

Basically there are two types of nonlinearity:

(1) geometrical nonlinearity and (2) material or physical nonlinearity. In geometrical nonlinearity, large displacements are normally accompanied by small strains and material nonlinearity is due to nonlinear elastic and plastic or viscoelastic behavior of the material. Material nonlinearity will be omitted in this investigation.

Geometrical nonlinearity results in two classes of problems, the large deflection problem and the problem of structural stability. It is the large deflection which is of interest for the analysis of a flexible link mechanism. The problem of stability will be avoided in this investigation for which the flexible links are assumed to be under tension.

In the large deflection problem, nonlinearity arises in two places. First, with respect to the equilibrium equation. The equilibrium equations are written in the

deformed configuration and a solution can be achieved by two procedures: (1) direct solution where iteration is done at the prescribed load level for force equilibrium, and (2) an incremental or piecewise linear procedure as depicted in Figure 5 where the final load level is reached by series of small steps.

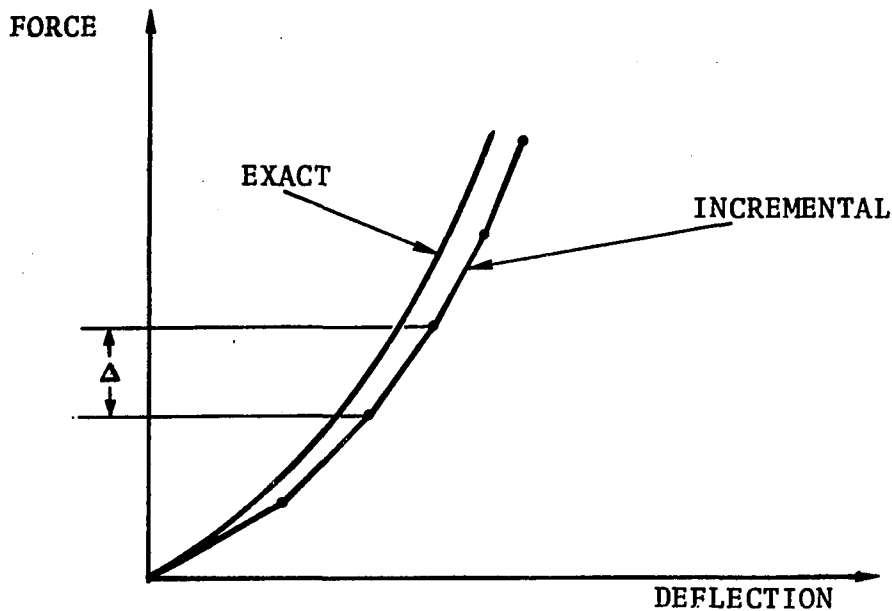


Figure 5. Nonlinear Analysis by the Linear Incremental Method

Turner et al [28] published the first article in the area of geometrically nonlinear problems, in which the problems were analyzed by the finite element method. Martin [29] presented a useful review of the efforts up to 1965 and revised it in 1970, [30]. Contributions

were also made by Argyris [31, 32], Jennings [33], Purdy and Przemieniecki [34], Mallett and Marcal [36], Powell [37], etc. Ebner and Ucciferro [38] compared the methods of Martin, Mallett and Marcal, Jennings and Powell for the solution of a variety of problems. Ebner concludes that the incremental procedure of Martin [29], performs the best for all classes of problems even though the procedure does not include the higher order terms in its formulation.

Martin's incremental procedure is the one which is used in this investigation for the analysis of flexible link mechanisms.

2.2 Basic Equations of the Finite Element Method

The complete derivation of the finite element method is covered by Martin [29] and Przemieniecki [35]. Only the fundamental equations and their results will be given in the following derivation.

The beam element selected for the analysis is shown in Figure 6. The element has six nodal degrees of freedom which is sufficient to model a flexible link of planar mechanisms. The beam element can be modified by adding extra degrees of freedom for spatial mechanism applications.

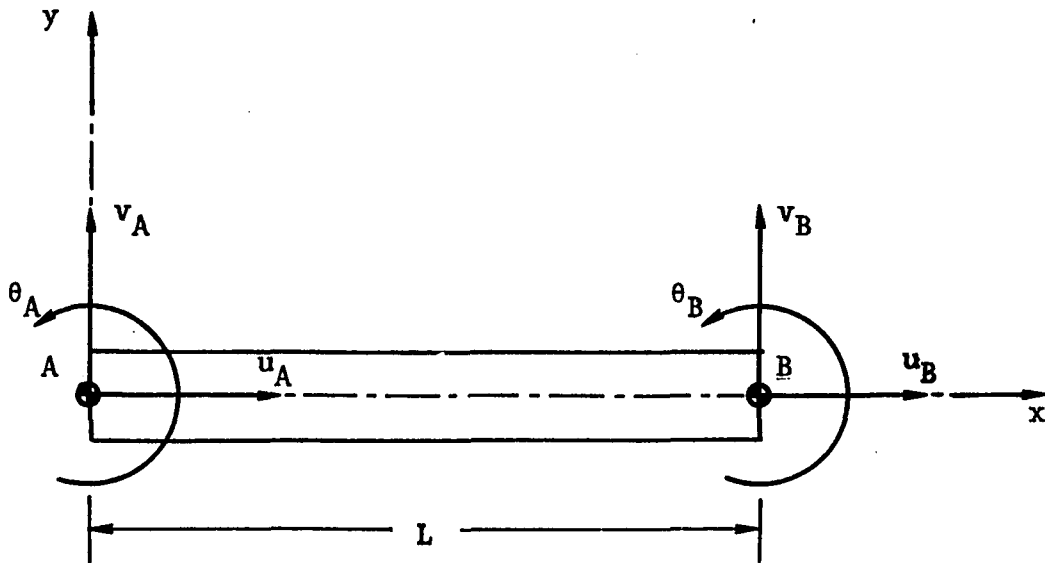


Figure 6. Planar Beam Element with Six Degrees of Freedom

The nodal displacement $\{\delta\}$, and force $\{F\}$, vectors of the beam element of Figure 6, are related by:

$$\{F\} = [k] \{\delta\} \quad (1)$$

where

$$\{\delta\} = \begin{Bmatrix} v_A \\ \theta_A \\ v_B \\ \theta_B \\ u_A \\ u_B \end{Bmatrix} \quad \text{and} \quad \{F\} = \begin{Bmatrix} F_{yA} \\ M_A \\ F_{yB} \\ M_B \\ F_{xA} \\ F_{xB} \end{Bmatrix} \quad (2)$$

where u and v are horizontal and vertical displacements and their corresponding forces are F_x and F_y respectively. θ is the end rotation and M is the corresponding moment.

The strain energy U of any elastic system can be expressed in a quadratic form in terms of the nodal displacements $\{\delta\}$, as:

$$U = \frac{1}{2} \{\delta\}^T [k] \{\delta\} \quad (3)$$

where $\{\delta\}^T$ is the transpose of the matrix $\{\delta\}$.

Taking the partial derivative of strain energy gives:

$$\frac{\partial U}{\partial \delta_i} = \{F\} \quad (4)$$

Equation (4) is the Castigliano's first theorem. The second partial derivative gives the stiffness coefficient k_{ij} as:

$$k_{ij} = \frac{\partial^2 U}{\partial \delta_i \partial \delta_j} \quad (5)$$

where k_{ij} is the element in the i^{th} row and j^{th} column of stiffness matrix $[k]$.

Now the derivation of the stiffness matrix $[k]$ of the beam element of Figure 6 will be presented. Let the

present strain in the element be ϵ_0 and the additional strain developed due to the load increment be ϵ_a , then the total strain ϵ will be

$$\epsilon = \epsilon_0 + \epsilon_a \quad (6)$$

By accounting in the nonlinear strain displacement equation for the longitudinal strain and the contribution due to bending, the additional strain can be expressed as:

$$\epsilon_a = \frac{\partial U}{\partial X} + \left(\frac{\partial v}{\partial X}\right)^2 - y \left(\frac{\partial^2 v}{\partial x^2}\right) \quad (7)$$

where the higher order term $\left(\frac{\partial U}{\partial X}\right)^2$ is neglected in comparison to $\left(\frac{\partial U}{\partial X}\right)$ but $\left(\frac{\partial v}{\partial X}\right)^2$ is retained.

A displacement function is selected which must be consistent with the beam theory. $u(x)$ should be linear to provide the constant strain along the length of the beam member and $v(x)$ should be cubic to provide the constant shear and linearly varying bending moment along its length. It will be:

$$\begin{aligned} u(x) &= a_0 + a_1 x \\ v(x) &= b_0 + b_1 x + b_2 x^2 + b_3 x^3 \end{aligned} \quad (8)$$

where a_0 , a_1 , b_0 , b_1 , b_2 and b_3 are six constants. By using the boundary conditions the constants can be expressed in terms of the nodal displacements as follows:

$$\begin{aligned}
 a_0 &= u_A \\
 a_1 &= \frac{u_B - u_A}{L} \\
 b_0 &= v_A \\
 b_1 &= \theta_A \\
 b_2 &= \frac{3}{L^2} (v_B - v_A) - \frac{1}{L} (2\theta_A + \theta_B) \\
 b_3 &= \frac{2}{L^3} (v_B - v_A) + \frac{1}{L^2} (\theta_A + \theta_B)
 \end{aligned} \tag{9}$$

The total strain energy U arising during the deformation is given by:

$$\begin{aligned}
 U &= \iiint \int_{\epsilon_0}^{\epsilon_0 + \epsilon_a} [\sigma \, d\epsilon] \, dx \, dy \, dz \\
 &= E\epsilon_0 \iiint \epsilon_a \, dx \, dy \, dz + \frac{E}{2} \iiint \epsilon_a^2 \, dx \, dy \, dz
 \end{aligned} \tag{10}$$

For constant cross sectional area A of a beam element, U can be simplified to:

$$U = AE\epsilon_0 \int_0^L \epsilon_a \, dx + \frac{AE}{2} \int_0^L \epsilon_a^2 \, dx \tag{11}$$

On substitution of equation (7) and grouping the terms it gives:

$$\begin{aligned}
 U = & AE\epsilon_o \int_0^L \left[\frac{\partial u}{\partial x} - y \left(\frac{\partial^2 v}{\partial x^2} \right) \right] dx + \frac{1}{2} AE\epsilon_o \int_0^L \left(\frac{\partial v}{\partial x} \right)^2 dx \\
 & + \frac{AE}{2} \int_0^L \left[\left(\frac{\partial u}{\partial x} \right)^2 - 2y \left(\frac{\partial u}{\partial x} \right) \left(\frac{\partial^2 v}{\partial x^2} \right) + y^2 \left(\frac{\partial^2 v}{\partial x^2} \right)^2 \right] dx \\
 & + \frac{AE}{2} \int_0^L \left[\frac{1}{4} \left(\frac{\partial v}{\partial x} \right)^4 + \left(\frac{\partial u}{\partial x} \right) \left(\frac{\partial v}{\partial x} \right)^2 + y \left(\frac{\partial v}{\partial x} \right)^2 \left(\frac{\partial^2 v}{\partial x^2} \right) \right] dx \quad (12)
 \end{aligned}$$

The partial derivatives in Equation (12) are first derived from Equation (8) and then expressed in terms of the nodal displacements with help of Equation (9). Upon substitution of the derivatives it is recognized that the first and the last integrals do not contain the quadratic terms and based on Equation (3) they can be omitted from Equation (12). Also, a symmetrical cross-sectional area is assumed for the beam element in the following simplification.

$$\begin{aligned}
 U = & \frac{1}{2} AE\epsilon_o \int_0^L \left(\frac{\partial v}{\partial x} \right)^2 dx + \frac{1}{2} AE \int_0^L \left[\left(\frac{\partial u}{\partial x} \right)^2 - 2y \left(\frac{\partial u}{\partial x} \right) \left(\frac{\partial^2 v}{\partial x^2} \right) \right. \\
 & \left. + y^2 \left(\frac{\partial^2 v}{\partial x^2} \right)^2 \right] dx \quad (13)
 \end{aligned}$$

which can be expressed as:

$$U = \frac{1}{2} \{\delta\}^T [k_G] \{\delta\} + \frac{1}{2} \{\delta\}^T [k_E] \{\delta\} \quad (14)$$

where $[k_E]$ is the elastic or linear stiffness matrix, and $[k_G]$ is the geometrical matrix or referred as the initial stress matrix. On comparison of Equations (14) and (3), the total stiffness matrix $[k]$ is

$$[k] = [k_E] + [k_G] \quad (15)$$

where $[k_E]$ and $[k_G]$ are expressed as follows:

$$[k_E] = \begin{bmatrix} \frac{12EI}{L^3} & & & & & \\ & \frac{6EI}{L^2} & \frac{4EI}{L} & & & \\ & & & \text{Symmetric} & & \\ & -\frac{12EI}{L^3} & -\frac{6EI}{L^2} & \frac{12EI}{L^3} & & \\ & \frac{6EI}{L^2} & \frac{2EI}{L} & -\frac{6EI}{L^2} & \frac{4EI}{L} & \\ & 0 & 0 & 0 & 0 & \frac{AE}{L} \\ & 0 & 0 & 0 & 0 & -\frac{AE}{L} & \frac{AE}{L} \end{bmatrix} \quad (16)$$

and

$$[k_G] = F_0 \begin{bmatrix} \frac{6}{5L} & & & & & \\ \frac{1}{10} & \frac{2}{15L^2} & & & & \\ & & \text{Symmetric} & & & \\ -\frac{6}{5L} & -\frac{1}{10} & \frac{6}{5L} & & & \\ \frac{1}{10} & -\frac{L}{30} & -\frac{1}{10} & \frac{2}{15L^2} & & \\ 0 & 0 & 0 & 0 & 0 & \\ 0 & 0 & 0 & 0 & 0 & 0 \end{bmatrix} \quad (17)$$

The incremental equation between force and displacement for Martin's method will be:

$$[k] \{\Delta\delta\} = \{\Delta F\} \quad (18)$$

where $\{\Delta\delta\}$ and $\{\Delta F\}$ are the increments in the nodal displacements and corresponding forces. So far the derivation of equations are only for the beam element. Now the derivation will be extended for a structure.

2.3 Coordinate Transformation Matrix

A structure (or mechanism) is composed of many beam elements which are oriented differently. Each of the elements is expressed in its local coordinate system and then related to the global coordinate system in which the

mechanism is oriented. The stiffness matrix, Equation (15) is expressed in the local coordinate system and transformation is essential because the displacement or loading on the mechanism is expressed in the global coordinate system. In Figure 7, the local coordinate system (x-y) is oriented at the angle γ to the global coordinate system (X-Y). In the following equations, the displacements in the global coordinate system are represented by a bar at the top.

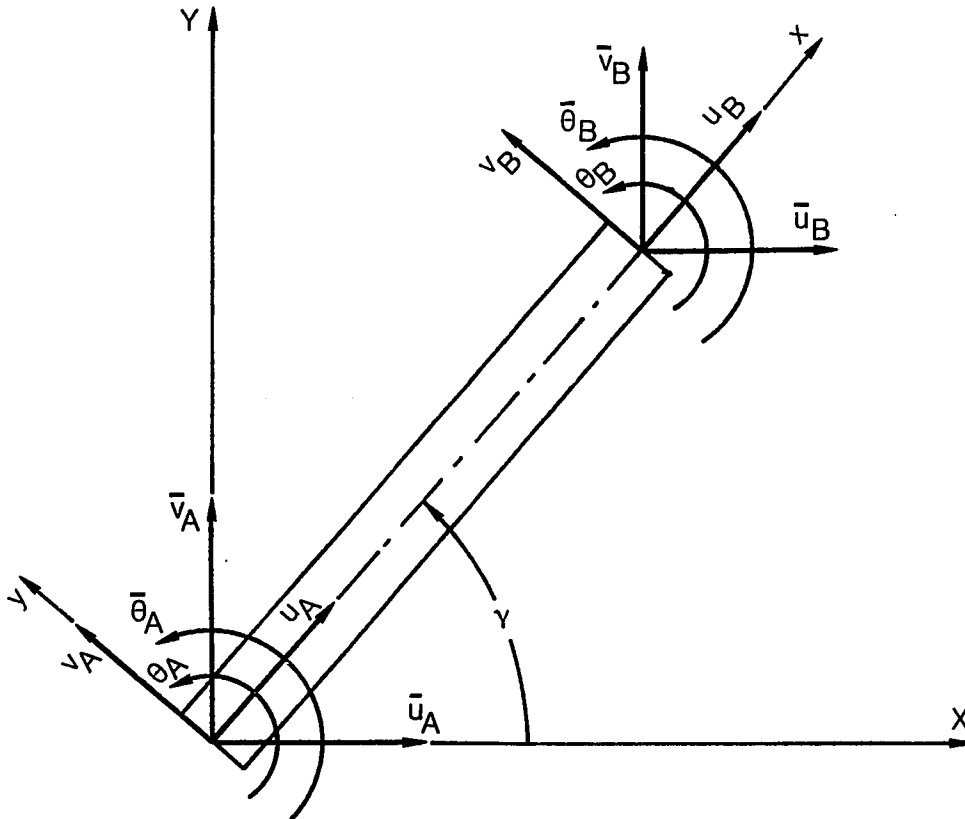


Figure 7. Displacement Relationship Between the Local (x-y) and the Global (X-Y) Coordinate Systems

$$\begin{aligned}
v_A &= \bar{v}_A \cos\gamma - \bar{u}_A \sin\gamma \\
u_A &= \bar{v}_A \sin\gamma + \bar{u}_A \cos\gamma
\end{aligned} \tag{19}$$

similar relations can be derived for u_B and v_B . Now the displacement vectors $\{\delta\}$ and $\{\bar{\delta}\}$ can be related by:

$$\{\delta\} = [T] \{\bar{\delta}\} \tag{20}$$

where $[T]$ is the coordinate transformation matrix whose elements are expressed as:

$$[T] = \begin{bmatrix} \cos\gamma & 0 & 0 & 0 & -\sin\gamma & 0 \\ 0 & 1 & 0 & 0 & 0 & 0 \\ 0 & 0 & \cos\gamma & 0 & 0 & -\sin\gamma \\ 0 & 0 & 0 & 1 & 0 & 0 \\ \sin\gamma & 0 & 0 & 0 & \cos\gamma & 0 \\ 0 & 0 & \sin\gamma & 0 & 0 & \cos\gamma \end{bmatrix} \tag{21}$$

The components of the displacement vector $\{\delta\}$ are expressed in Equation (2).

2.4 Formulation of the Finite Element Method for a Structure.

The basic equations for the beam element derived in the previous sections will now be extended to a structure.

The formulation of the stiffness matrix $[K]$ of the structure is derived from the stiffness matrix $[k]$ of the beam element in this section.

The strain energy of the structure can be expressed as:

$$U = \frac{1}{2} \{q\}^T [K] \{q\} \quad (22)$$

where $\{q\}$ is the nodal displacement vector of the structure in the global coordinate system. The strain energy of the i^{th} element can be expressed from Equation (3) as:

$$U_i = \frac{1}{2} \{\delta_i\}^T [k_i] \{\delta_i\} \quad (23)$$

Upon substitution of Equation (20) into the Equation (23), the strain energy will be transferred to the global coordinate system. This gives:

$$U_i = \frac{1}{2} \{\bar{\delta}_i\}^T [T_i]^T [k_i] [T_i] \{\bar{\delta}_i\} \quad (24)$$

The nodal displacement $\{\bar{\delta}\}$ in the global coordinate system is further related to $\{q\}$ by:

$$\{\bar{\delta}_i\} = [\beta_i] \{q\} \quad (25)$$

where $[\beta_i]$ is unique for each element and contains either one or zero. This will be explained in detail with an illustrative example in a latter part of this section. Substitution of Equation (25) into Equation (24) gives:

$$U_i = \frac{1}{2} \{q\}^T [\beta_i]^T [T_i]^T [k_i] [T_i] [\beta_i] \{q\} \quad (26)$$

The total strain energy of the structure will be the sum of the strain energies of the individual beam elements. For the structure with 'n' number of elements, it will be:

$$\begin{aligned} U &= \sum_{i=1}^n U_i \\ &= \frac{1}{2} \sum_{i=1}^n \{q\}^T [\beta_i]^T [T_i]^T [k_i] [T_i] [\beta_i] \{q\} \end{aligned} \quad (27)$$

The stiffness matrix of the structure can now be expressed in terms of the element stiffness matrices by comparing with Equation (22) and (27) as:

$$[K] = \sum_{i=1}^n [\beta_i]^T [T_i]^T [k_i] [T_i] [\beta_i] \quad (28)$$

The incremental equation for the structure is then:

$$[K] \{\Delta q\} = \{\Delta P\} \quad (29)$$

where $\{\Delta q\}$ and $\{\Delta P\}$ are respectively, the incremental nodal displacement and the force vector of the structure.

The finite element method of structural analysis will be demonstrated with the help of a simple structure as depicted in Figure 8. The structure is composed of three beam elements or members and has seven nodal displacements (q_1 to q_7) at the three nodal points. The local coordinate systems of the three elements are oriented by angles γ of 45, 0, and 315 degrees as depicted in Figure 8. When these values of γ are substituted in Equation (21), corresponding transformation matrices $[T_i]$ can be obtained.

From Figure 8 it is clear that \bar{u}_B and \bar{v}_B , the nodal displacements of the Element No. 1 in the global coordinate system, correspond to q_1 and q_2 respectively of the structural nodal displacements. Also $\bar{\theta}_B$ will be same as q_3 . Based on these relations the $[\beta_1]$ matrix for Element No. 1 is constructed as follows:

$$[\beta_1] = \begin{matrix} & \begin{matrix} 1 & 2 & 3 & 4 & 5 & 6 & 7 \end{matrix} \\ \begin{matrix} 1 \\ 2 \\ 3 \\ 4 \\ 5 \\ 6 \end{matrix} & \begin{bmatrix} 0 & 0 & 0 & 0 & 0 & 0 & 0 \\ 0 & 0 & 0 & 0 & 0 & 0 & 0 \\ 0 & 1 & 0 & 0 & 0 & 0 & 0 \\ 0 & 0 & 1 & 0 & 0 & 0 & 0 \\ 0 & 0 & 0 & 0 & 0 & 0 & 0 \\ 1 & 0 & 0 & 0 & 0 & 0 & 0 \end{bmatrix} \end{matrix} \quad (30)$$

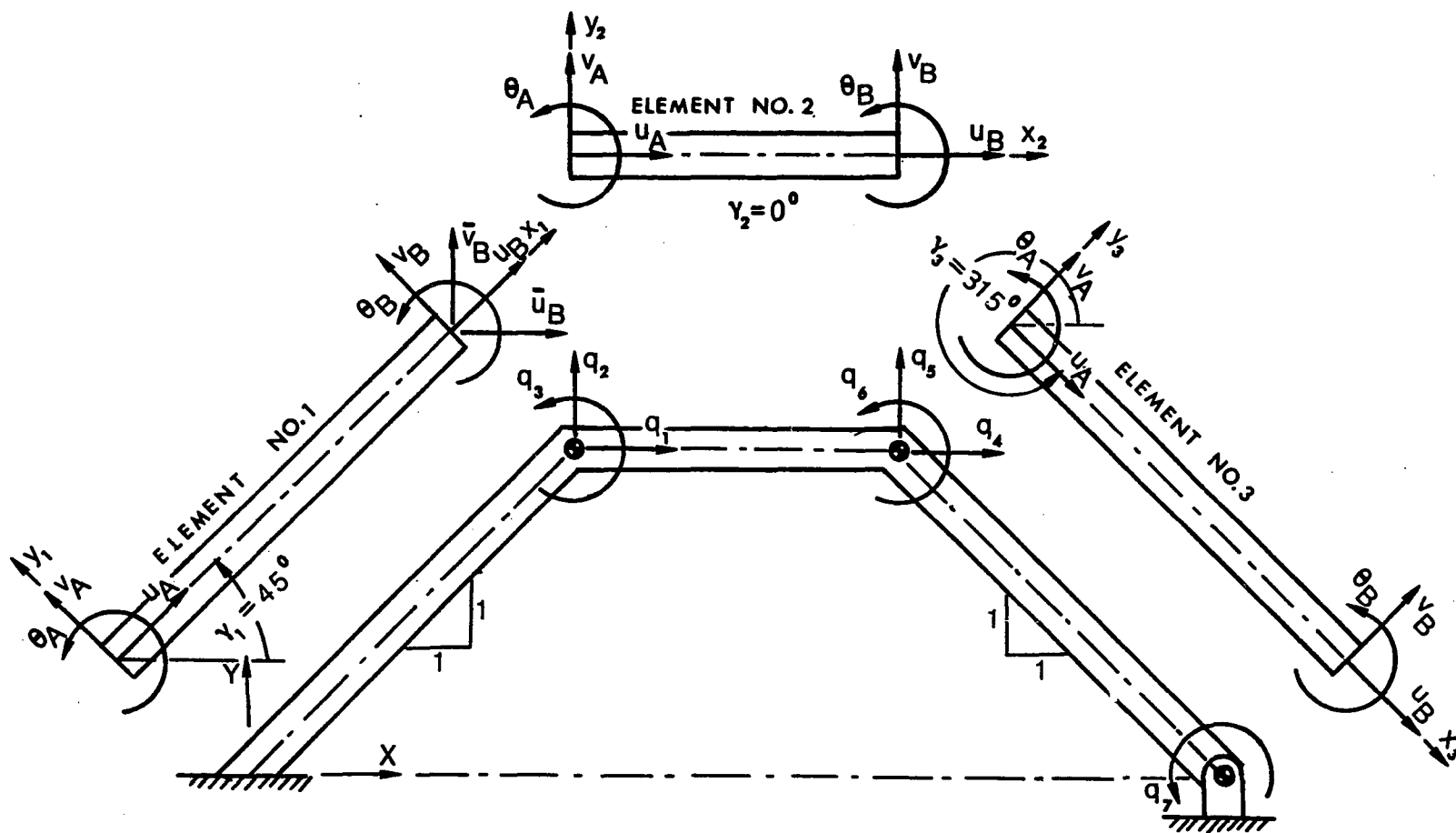


Figure 8. Three Member Planar Structure with 7 Nodal Displacements

similarly, $[\beta_2]$ and $[\beta_3]$ for the Elements No. 2 and 3 will be:

$$[\beta_2] = \begin{bmatrix} 0 & 1 & 0 & 0 & 0 & 0 & 0 \\ 0 & 0 & 1 & 0 & 0 & 0 & 0 \\ 0 & 0 & 0 & 0 & 1 & 0 & 0 \\ 0 & 0 & 0 & 0 & 0 & 1 & 0 \\ 1 & 0 & 0 & 0 & 0 & 0 & 0 \\ 0 & 0 & 0 & 1 & 0 & 0 & 0 \end{bmatrix}$$

$$[\beta_3] = \begin{bmatrix} 0 & 0 & 0 & 0 & 1 & 0 & 0 \\ 0 & 0 & 0 & 0 & 0 & 1 & 0 \\ 0 & 0 & 0 & 0 & 0 & 0 & 0 \\ 0 & 0 & 0 & 0 & 0 & 0 & 1 \\ 0 & 0 & 0 & 1 & 0 & 0 & 0 \\ 0 & 0 & 0 & 0 & 0 & 0 & 0 \end{bmatrix} \quad (31)$$

It should be noticed that in the above matrices for any row there is a maximum of one nonzero element and in the same way for any column there is a maximum of one nonzero element.

The stiffness matrix $[K]$ of the structure can be assembled by Equation (28) and the solution of the unknown parameters may be obtained from Equation (29). There are two types of incremental problems: (1) Find the nodal displacements under a given loading condition

and; (2) Find the necessary load corresponding to the desired displacements. Each of the two problems require a different solution procedure.

- (1) Force Input: Premultiply both sides of Equation (29) by $[K]^{-1}$ and the increment in the nodal displacement corresponding to the applied load increment can be evaluated as:

$$\{\Delta q\} = [K]^{-1} \{\Delta P\} \quad (32)$$

- (2) Displacement input: The solution procedure in this case is more complicated. The procedure is known as the reduction of coordinates by Guyan [39]. The basis for this procedure is that the forces corresponding to the unknown displacements are zero. Thus the nodal displacements corresponding to the unknown displacements can be eliminated from the Equation (29) as follows:

$$\begin{bmatrix} A & B \\ B^T & C \end{bmatrix} \begin{Bmatrix} \Delta q_I \\ \Delta q_{II} \end{Bmatrix} = \begin{Bmatrix} 0 \\ \Delta P_{II} \end{Bmatrix} \quad (33)$$

where $[A]$, $[B]$ and $[C]$ are submatrices of $[K]$ after the partitioning. $\{\Delta q_{II}\}$ are the known displacements and $\{\Delta P_{II}\}$ are the corresponding forces. $\{\Delta q_I\}$ are the remaining unknown displacements for which the forces are

zero. Equation (33) can be separated into:

$$[A] \{\Delta q_I\} + [B] \{\Delta q_{II}\} = \{0\} \quad (34)$$

and

$$[B]^T \{\Delta q_I\} + [C] \{\Delta q_{II}\} = \{\Delta P_{II}\} \quad (35)$$

Equation (34) can be rearranged as:

$$\{\Delta q_I\} = -[A]^{-1} [B] \{\Delta q_{II}\} \quad (36)$$

Substitution of Equation (36) into (35) gives:

$$\{\Delta P_{II}\} = ([C] - [B]^T [A]^{-1} [B]) \{\Delta q_{II}\} \quad (37)$$

Equations (36) and (37) give the remaining unknown displacements $\{\Delta q_I\}$ and unknown force $\{\Delta P_{II}\}$ corresponding to the displacement $\{\Delta q_{II}\}$.

2.5 Solution Procedure for the Nonlinear Analysis

In the previous sections the equations for the finite element method were derived for the beam element and were extended to the structure. Also, the solution procedures for the force and displacement input problems were explained. Now the solution procedure based on the previous section will be described.

The nonlinear analysis is performed by the linear incremental method as depicted in Figure 5, where the final load is reached in a series of small linear steps. The information from the previous step is utilized to update the stiffness matrix. The stiffness matrix is used to determine the increment in displacement under a given increment of load. The following steps describe the procedure in detail:

- A. The correction in the length of each element is made based on the deformation from the previous step. Corresponding to the new length, the elastic stiffness matrix $[k_E]$ is formed from Equation (16).
- B. At the end of the previous step, the total axial force F_0 is determined and, based on Equation (17), a new initial stress matrix $[k_G]$ is formed. This, when summed with $[k_E]$ will give the new stiffness matrix of the element, $[k]$.
- C. From the previous step, the new orientation of the beam element, γ , is determined and from Equation (21) a new coordinate transformation matrix $[T]$ is determined. The stiffness matrix $[k]$ now can be transferred into the global coordinate system by

following two steps:

$$(i) [T]^T [k] [T]^T \text{ and}$$

$$(ii) [\beta]^T [T]^T [k] [T] [\beta]$$

where $[\beta]$ remains constant throughout the analysis.

- D. These transformed matrices of elements are summed by Equation (28) to form the new stiffness matrix of the structure, $[K]$.
- E. The new stiffness matrix when used in conjunction with Equation (29) and solved by Equation (32) gives the increment in nodal displacements $\{\Delta q\}$ of the structure under a given load increment $\{\Delta P\}$. (If displacement is the input, the solution for $\{\Delta P_{II}\}$ and $\{\Delta q_I\}$ is obtained by Equations (36) and (37).)
- F. The displacement of the individual element $\{\Delta \delta\}$ in the global system can be evaluated from $\{\Delta q\}$ by Equation (25). $\{\Delta \delta\}$ can be transferred back to the local coordinate system, $\{\Delta \delta\}$, by transformation Equation (20). Now the correction of the length ΔL is applied as follows:

$$\Delta L = u_B - u_A \quad (38)$$

where u_B and u_A are the 5th and 6th components of vector $\{\Delta \delta\}$.

- G. With the help of Equation (1) the nodal forces $\{\Delta F\}$ of the element are calculated, from which the increment in the axial force will be:

$$\Delta F_o = \frac{AE}{L} (u_B - u_A) \quad (39)$$

which when added to the previous value will give the total axial force F_o . Similarly the increment in bending and axial stresses are determined by:

$$\Delta \sigma_b = \frac{M_B \frac{h}{2}}{\frac{1}{12}bh^3} \quad (40)$$

where $\Delta \sigma_b$ is the increment in the bending stress at nodal B of the element and M_B is 4th component of vector $\{\Delta F\}$. A similar expression for the bending stress at the nodal point A can be derived. The increment in the axial stress is determined by:

$$\Delta \sigma_a = \frac{F_{xB}}{bh} \quad (41)$$

where F_{xB} is the 6th component of vector $\{\Delta F\}$. According to the convention in Figure 6, the axial stress will be positive for tension and negative for compression. When the increment values of

stress are added to the previous values it will give the total magnitude of the stress.

- H. By adding $\{\Delta q\}$, the increment of the displacement, to the previous position of the structure, the new position of the structure and new orientation γ of the element can be determined.
- I. With the new values of γ , L and F_0 , the procedure is repeated for the next increment of load and the process is continued until the total load has been applied on the structure.

The basic computational flow diagram of the method is depicted in Figure 9.

A complete listing of the computer program is given in Appendix A. The flow diagram of Figure 9 is programmed into the subroutine FX4BAR. The subroutine FORDIS solves the increment equation for input of either force or displacement. In its present form it allows only one displacement input. Also, subroutine BEMREK is for $[k_E]$ and BEMRET is for $[k_G]$. The transformation matrix $[T]$ is programmed in a subroutine TRETTS. Subroutine A4BAR is for solving a pin-jointed four bar linkage with rigid links.

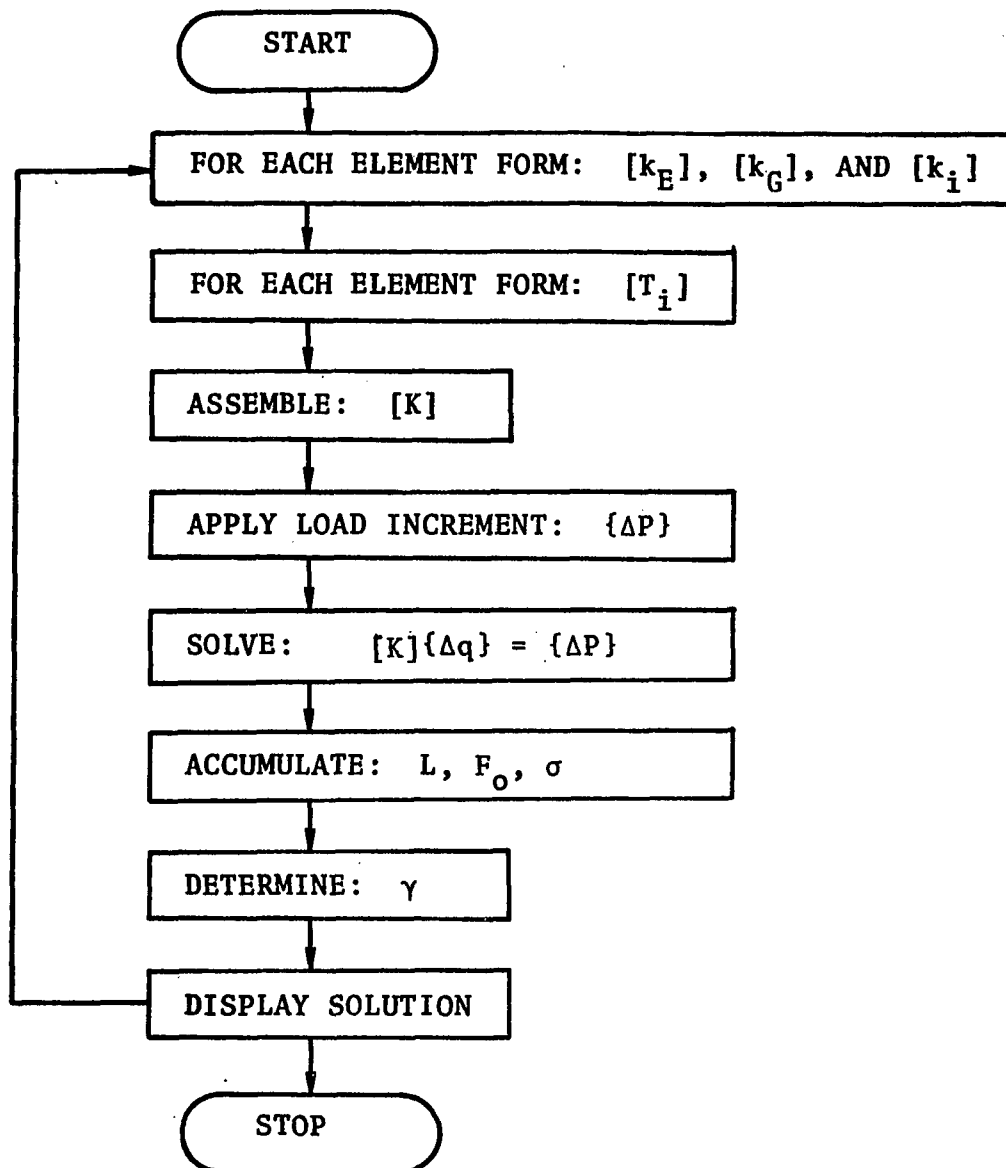


Figure 9. Flow Diagram of the Finite Element Method Using the Linear Incremental Method.

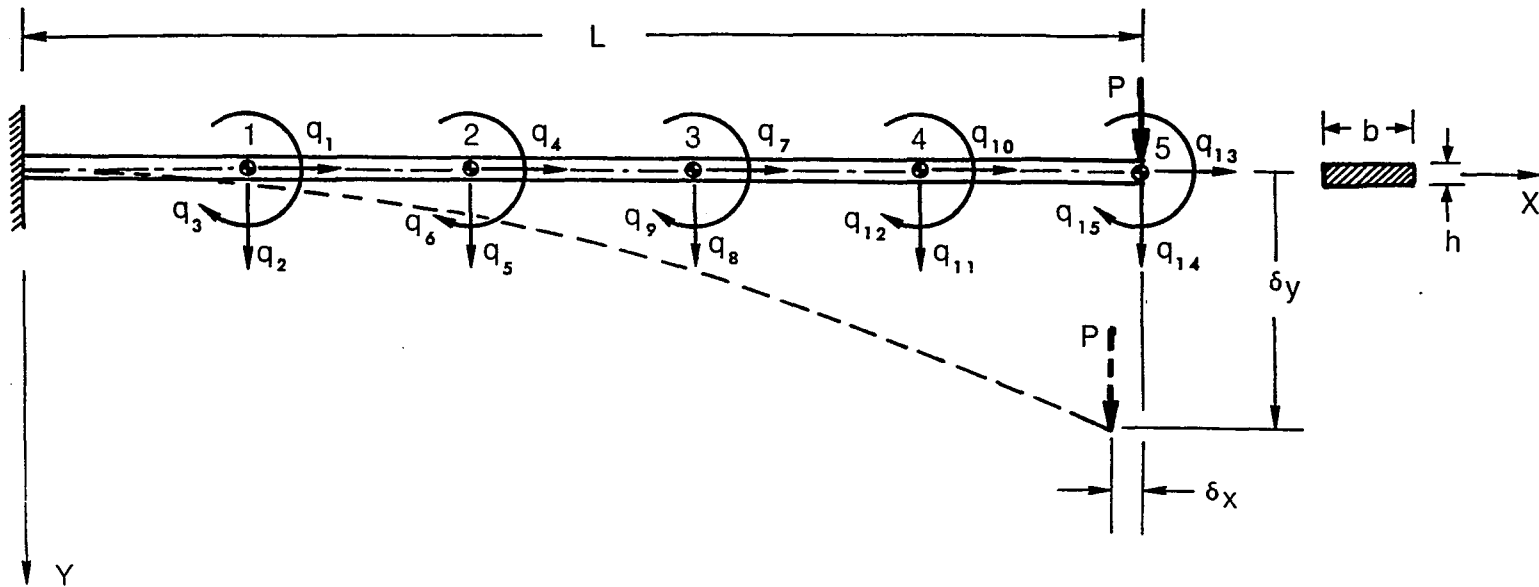
CHAPTER III

ANALYSIS OF NONLINEAR SPRINGS

3.1 Cantilever Beam

The finite element method for nonlinear analysis by the linear incremental procedure as developed in Chapter 2, will now be applied to a cantilever beam. A force vs. deflection relation is desired for a beam under a large deflection. A cantilever beam is selected as a preliminary test problem to check the accuracy of the method. The results of the finite element method are compared against the results of Bisshopp and Drucker [4] and with the experimental results.

The cantilever beam selected is a 0.5 inch wide strip of spring steel whose length L is 10 inches, and thickness h is 0.006 inch. The modulus of elasticity E for the spring steel is assumed to be 30×10^6 psi. The cantilever beam is divided into 5 elements of equal length as depicted in Figure 10. There is no displacement at the fixed end of the beam but there will be 15 nodal displacements, q_1 to q_{15} , at the 5 nodal points. A vertical load P is applied at the free end which moves with the free end and always acts in a vertical direction. The horizontal and vertical deflections, δ_x and δ_y which are indirectly



$b = 0.5''$
 $h = 0.006''$
 $L = 10.0''$
 $E = 30 \times 10^6 \text{ PSI}$

Figure 10. Cantilever Beam Subjected to a Large Deflection

$q_{1,3}$ and $q_{1,4}$, are determined at the end of each load increment ' ΔP ' by the procedure shown in Figure 9 of Chapter 2.

The results are converted in terms of the nondimensional parameters, $\frac{PL^2}{EI}$, $\frac{\delta_x}{L}$ and $\frac{\delta_y}{L}$, and are plotted in Figure 11. The conversion was necessary because the results of Bisshopp and Drucker [4], which are plotted in Figure 11, are in the same nondimensional parameters. The results by the finite element method compares within 6.6% to Bisshopp and Drucker's results in $\frac{\delta_y}{L}$ for $\frac{PL^2}{EI} = 3$ which amounts to a load P of 0.0081 lb. This final load was reached in a total of 90 load increments.

It should also be pointed out that a cantilever beam problem is solved by Frisch-Fay [5], Shoup [10] and Tada and Lee [6]. Bisshopp and Drucker, Frisch-Fay and Shoup have transferred the nonlinear bending moment equation of a cantilever beam into elliptical integrals which were solved by numerical methods, while Tada and Lee's solution is by finite element method based on Galerkin's method. The results of all the authors [4-6, 10] are in agreement except those of Tada and Lee, whose results in $\frac{\delta_x}{L}$ do not match with the others. The extension of a cantilever beam is very small and negligible. However, the finite element method developed in this investigation accounts for the extension of the beam, while the results of Bisshopp and Drucker and other authors assume an inextensible beam.

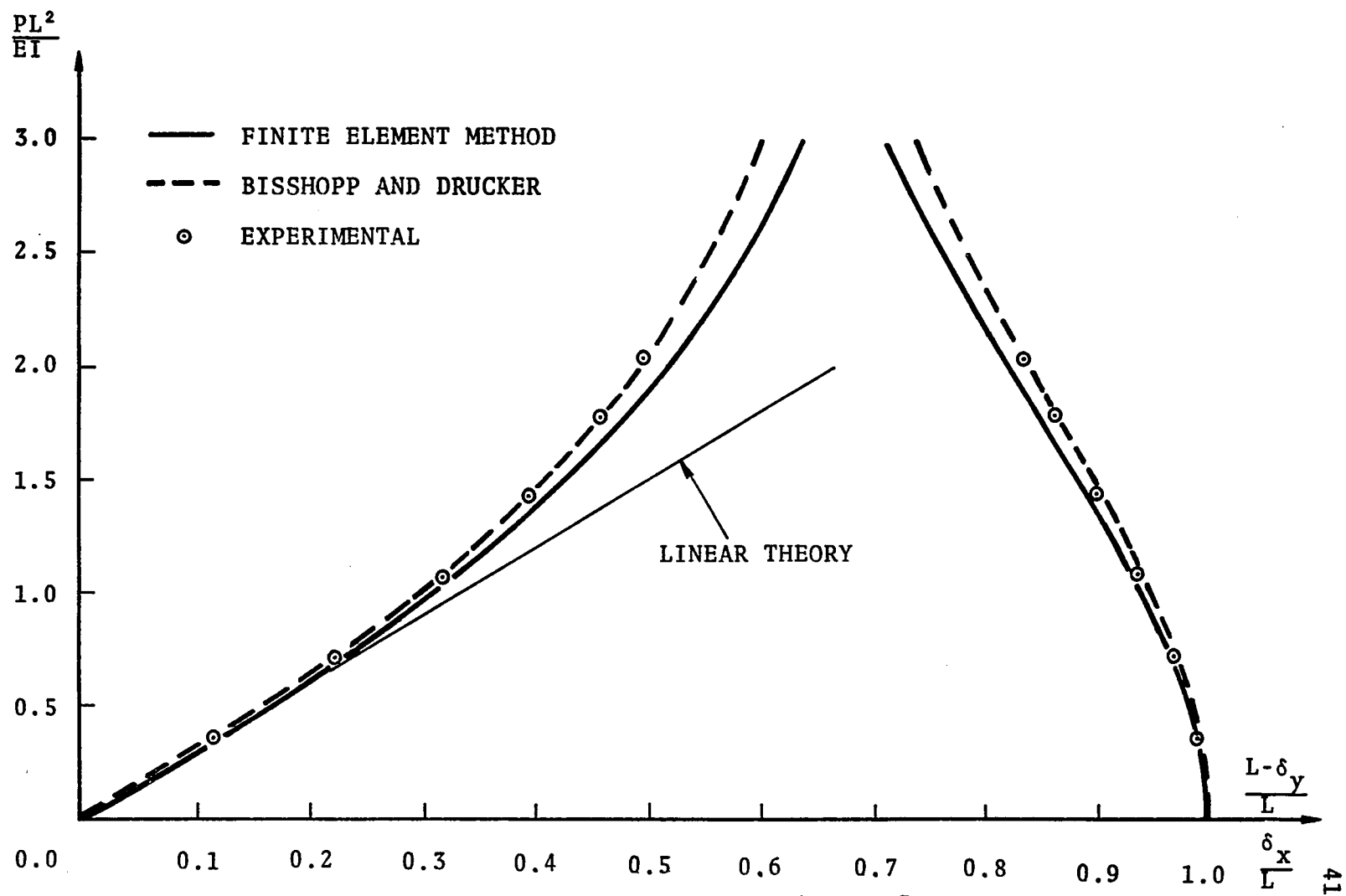


Figure 11. Results of Nonlinear Analysis for a Cantilever Beam

The results of the cantilever beam by the finite element method was further checked by an experimental result. The physical dimensions of the beam selected are given in Figure 12 along with its experimental and analytical results by the finite element method. Again, the comparison reveals that analytical results are in error of 5.13% for the deflection of 2.4 inches in δ_y for a 5.0 inch span of the beam. When the experimental results of Figure 12 are converted in terms of nondimensional parameters and plotted in Figure 11, it shows agreement with the results of Bisshopp and Drucker. It also indicates that the loading on the beam in the experiment reaches $\frac{PL^2}{EI}$ of 2 only and not 3. The modulus of elasticity E, for the spring steel beam used in the analysis, was determined to be 27.8×10^6 psi from the experimental results.

The cantilever beam shown in Figure 10 was analyzed for nonlinear deflection by incremental displacement input. A total of 128 increments were taken to displace the free end of the beam by 6.4 inches in δ_y . The results of displacement input perfectly matches results of the force input of Figure 11. The deflected shapes of the cantilever beam for increasing displacement in δ_y of the free end are depicted in Figure 13. When the number of increments are decreased from 128 to half that number, the results were in error by 1.24% to the previous results.

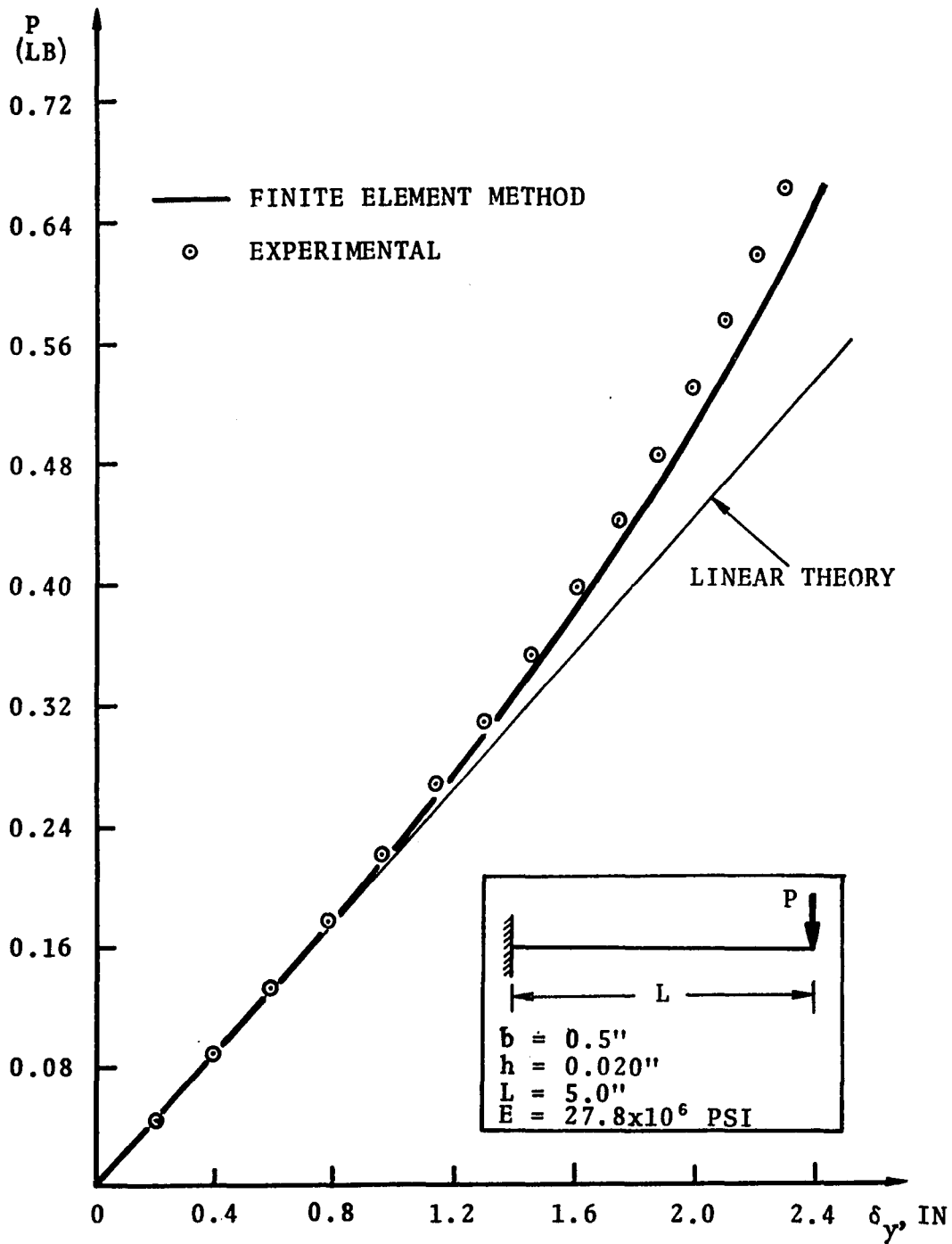


Figure 12. Comparison of Experimental and Analytical Results

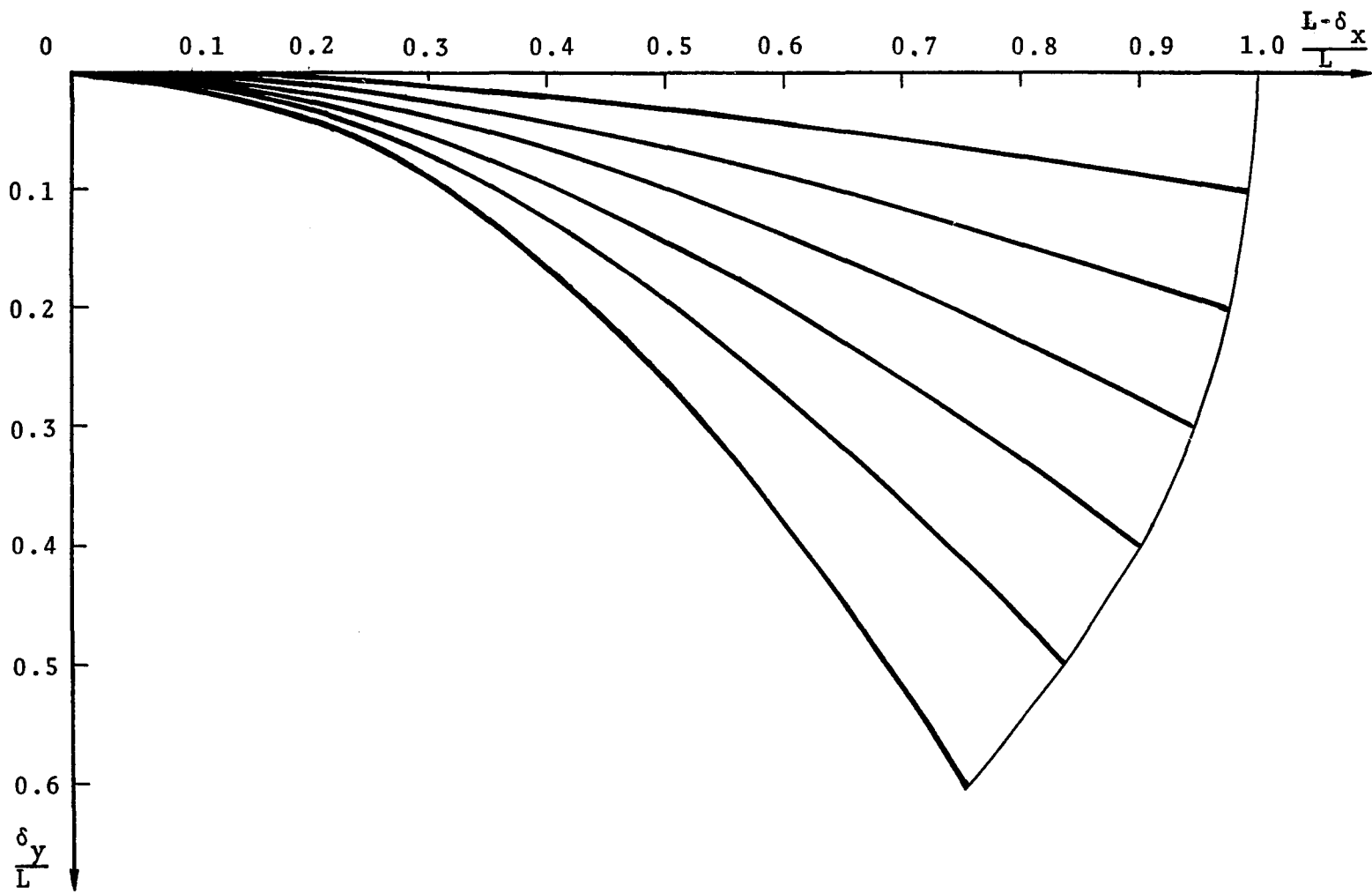


Figure 13. Shapes of a Cantilever Beam

3.2 Attempts to Improve the Results.

As mentioned previously, the nonlinearity comes from two areas: (1) the equilibrium equation and (2) the strain displacement equation. Many attempts were made to account for the nonlinearity in order to improve the results. The following are the results and conclusions of those attempts:

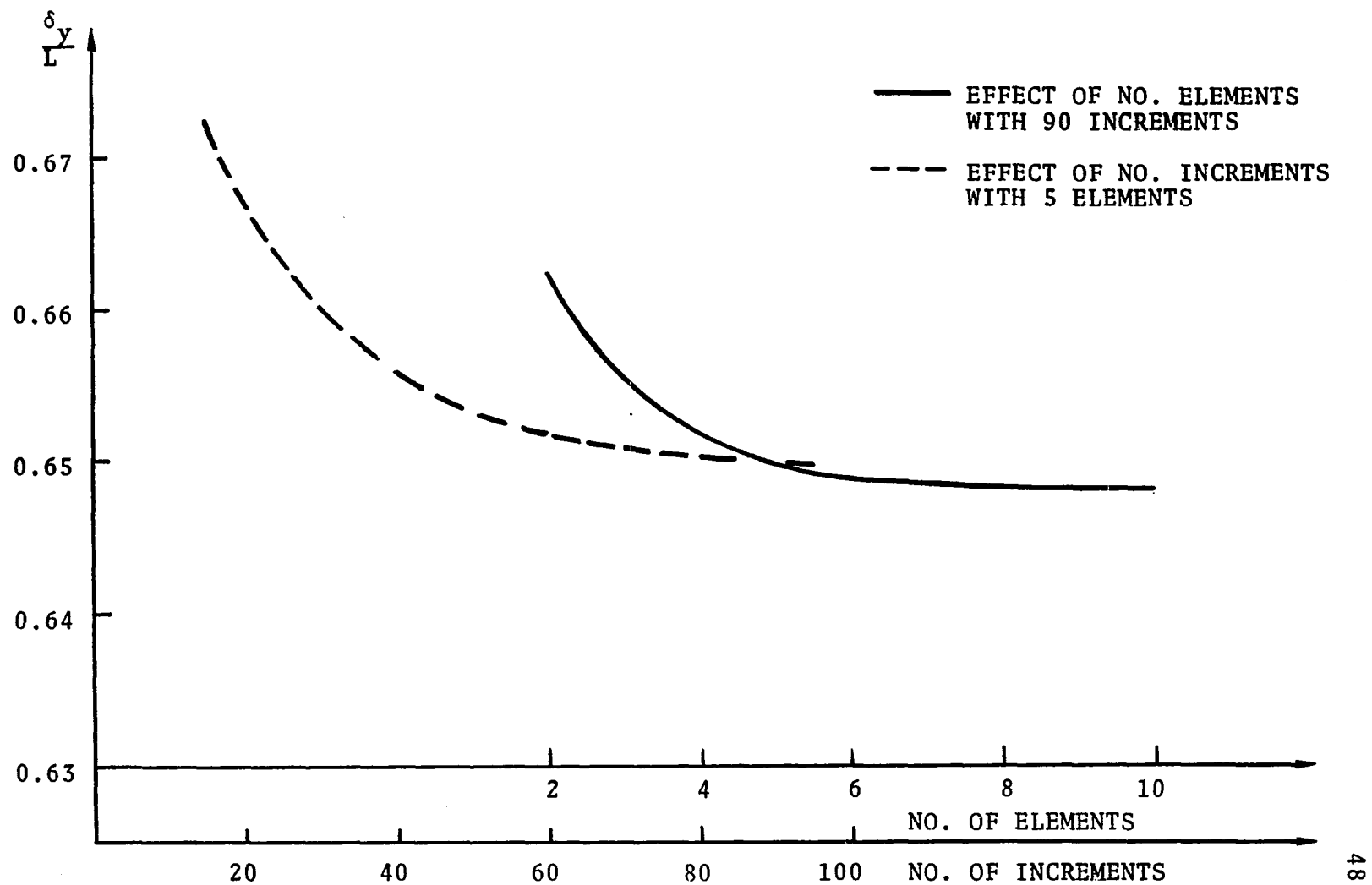
- A. The effect of an initial stress matrix and an extension of the beam were considered first. When the beam was assumed inextensible and without initial stress, matrix $[k_G]$ of Equation (17), i.e. only the coordinate transformation matrix $[T]$ of Equation (21) is accounted for in the analysis. An error of 14.6% was observed in the results compared to a 6.6% error if all of these factors are accounted for. It was further concluded that the improvement in error from 14.6% to 6.6% was mainly due to the initial stress matrix and not due to the extension of the beam. This also explains why the Bisshopp - Drucker's results with the assumption of an inextensible beam, are in good agreement with the experimental results.
- B. The derivation of the stiffness matrix was carried out based on the Mallet and Marshal method [36]. This method does not neglect the

higher order terms in Equation (12). When this stiffness matrix was used in the incremental procedure to analyze the cantilever beam of Figure 10, difficulties were experienced. The same conclusions were reached by Ebner and Ucciferro [38] for the Mallet and Marshal method.

- C. The finite element method, based on the stiffness method, guarantees continuous displacements but does not assure matching of forces at the nodal point. The method developed in Chapter 2 is based on the stiffness method and some error in matching external forces with the internal forces was expected. But the internal axial force near the free end of the cantilever beam is in large error relative to the applied load. The reasonable explanation for this large error in equilibrium of forces is not available at the present time.
- D. The analysis procedure was modified slightly by rotating the global coordinate system parallel to the free end of the cantilever beam. The vertical load at the free end is divided along the axes of the rotated global coordinate system, thus placing the load along the beam and perpendicular to it. By this modification, the equili-

brum of forces along the beam is achieved but it made the beam stiffer than Bisshopp and Drucker's beam and an error of larger magnitude resulted than that of Figure 11. No clear-cut conclusion can be reached from the above results but there are procedures available where the equilibrium of the forces can be achieved by iteration at the end of each or a few increment steps. Such a method will increase the computation time and thus was not considered in this preliminary investigation.

- E. Accuracy of the finite element method's results can be improved by: (1) dividing the beam into more elements and (2) by increasing the number of increments. The effect of these two parameters on the results of a cantilever beam are studied in Figure 14. Figure 14 shows the convergence of the results as the number of elements and increments increase. It also indicates that the results of Figure 11 with 5 elements and 90 increments are very close to the threshold values. Taking more elements or much smaller steps than the maximum indicated in Figure 14, might lead to numerical instability due to truncation errors.



48

Figure 14. Effect of the Number of Elements and Increments on the Convergence of Results

CHAPTER IV

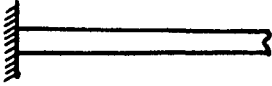
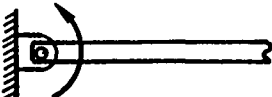
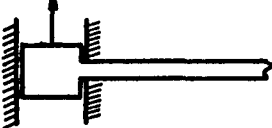
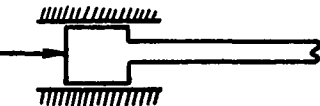
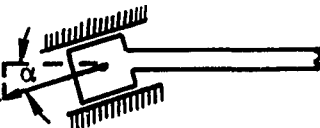
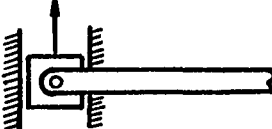
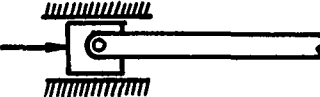
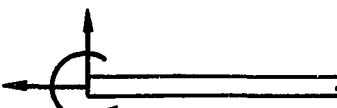
ANALYSIS OF FLEXIBLE LINK MECHANISMS

The finite element method will be applied to the analysis of a flexible link mechanism subjected to large displacements. The types of linkage under consideration are depicted in Figure 1 to 4 of Chapter 1. The couplers of these linkages are connected to the input and output links by flexural joints. Any or all three of the links in the linkage can be rigid or flexible. In this chapter, mechanisms with one flexible link and with two flexible links will be analyzed. A three flexible link mechanism would be impractical to use for many applications because of too much flexibility.

The input and output links of the planar mechanism can be grounded by pin, slider or fixed joints. Table 1 lists the various configurations of the joints and the nodal displacements associated with them; e.g. for a pin joint, the displacements u and v will be zero but rotation θ will be present. The mechanisms analyzed in the present investigation have not included any slider joints but without much effort a mechanism with slider joints can be analyzed.

TABLE 1

JOINTS AND THEIR CORRESPONDING
NODAL DISPLACEMENTS

JOINT	NODAL DISPLACEMENTS
FIXED 	$u = 0 \quad v = 0 \quad \theta = 0$
PINNED 	$u = 0 \quad v = 0$
TRANSVERSE SLIDER 	$u = 0 \quad \theta = 0$
LONGITUDINAL SLIDER 	$v = 0 \quad \theta = 0$
INCLINED SLIDER 	$u = v \tan \alpha \quad \theta = 0$
TRANSVERSE SLIDER & PIN 	$u = 0$
LONGITUDINAL SLIDER & PIN 	$v = 0$
FREE 	

The flexible links in the mechanism are assumed to have no pre-stresses and to be initially straight. Also, the mechanism is displaced such that the flexible members remain under tension. For a given displacement, analysis based on the finite element method, determines a required input (driving) force or torque and the displacement of the output link. The mechanisms analyzed in this chapter could be subjected to any type of external loading but for simplicity, external loads other than the driving force have been avoided. This external loading, if included, would change the relationship between the input and output displacements of the flexible link mechanism.

4.1 One Flexible Member - Flexible Strip as a Coupler

A flexible link mechanism with one flexible link (member) selected for the analysis is depicted in Figure 15. The flexible link is a spring steel strip which connects two rigid links and acts as a flexible coupler. For purposes of this analysis, the flexible coupler is divided into 4 elements of equal lengths. One element is assumed for the two "rigid" input and output links. Therefore, a total of 6 elements are required for this model of the flexible link mechanism in Figure 15 for the analysis by the finite element method.

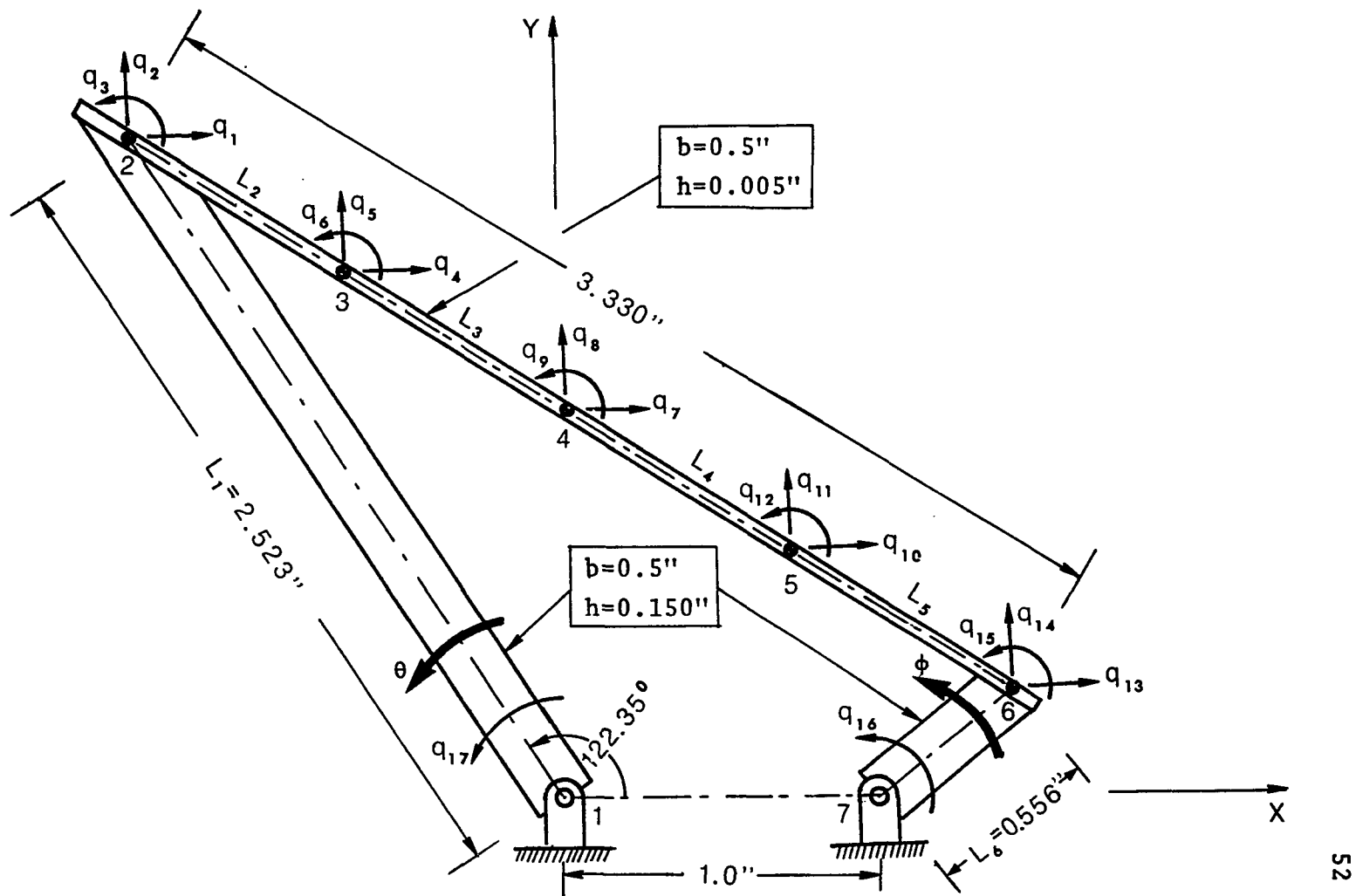


Figure 15. Flexible Coupler Mechanism

From Table 1 and the geometry of the mechanism, it is clear that the two pin joints for the input and output shafts will permit rotation only for the nodal displacements at those joints. The joints at the other ends of the input and output links (where they are connected to the flexible coupler) can be looked at as fixed joints with respect to the coupler. However, the motion of these links relative to the frame of the mechanism causes these joints (or nodes 2 and 6) to move relative to the ground, thus they have all three nodal displacements. The total of 17 nodal displacements as depicted in Figure 15, q_1 to q_{17} , are required at 7 nodal points for the analysis of the mechanism. If any external load is applied on the mechanism, and it happens that the point of application is not one of the 7 nodal points, then an additional nodal point and displacements are selected at the application point of the load.

The physical dimensions of the mechanism and the beam elements are included in Figure 15. The flexible strip is 0.5 inch wide and is 0.005 inch thick. All the links of the mechanism are assumed to be of steel for which the elastic modulus, E is 30×10^6 psi. The mechanism is analyzed to give the displacement ϕ of the output shaft, for a given displacement of the input shaft θ . The relation between the displacements θ and ϕ is depicted in Figure 16, where the input shaft is displaced in increments

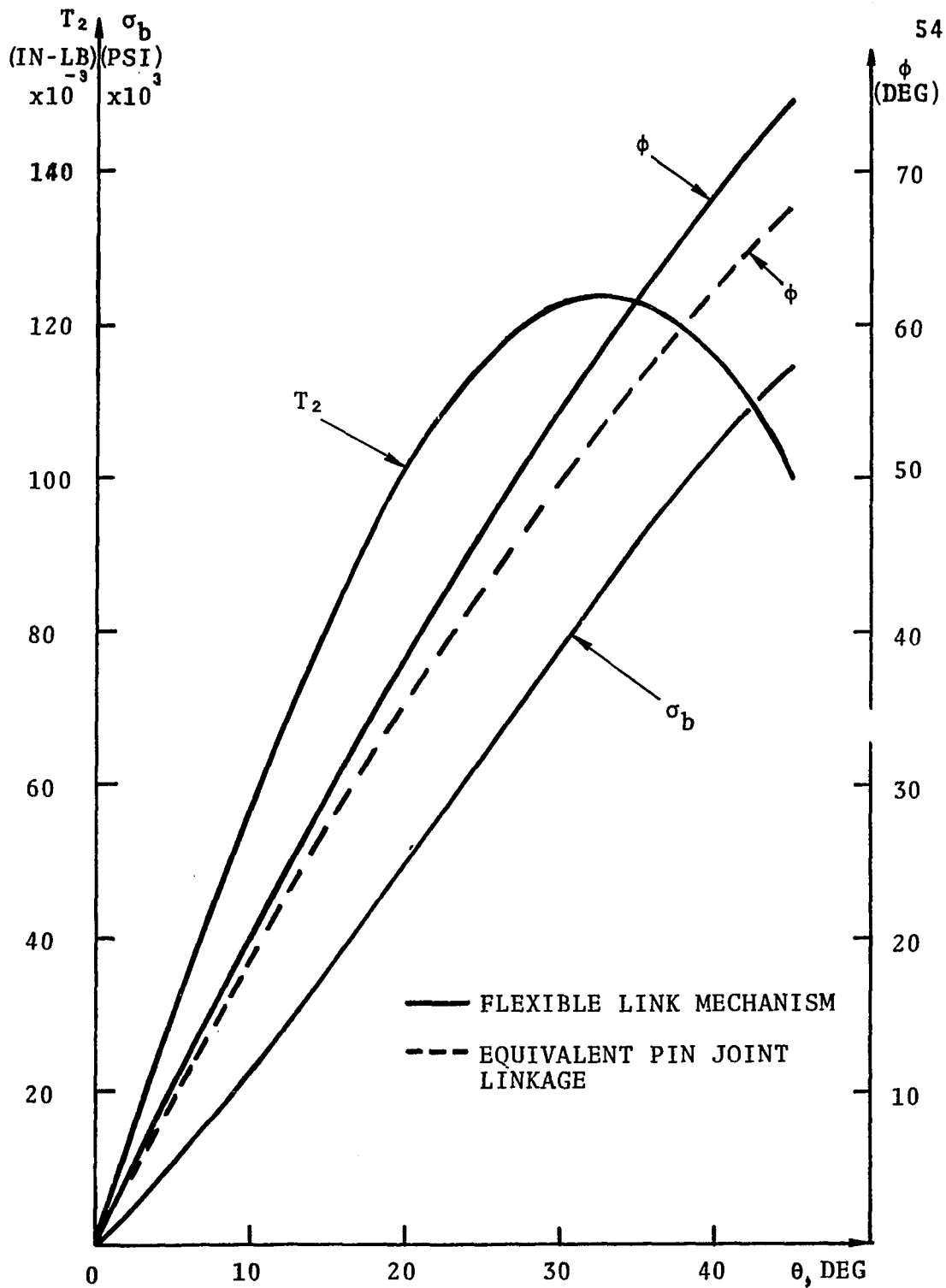


Figure 16. Result of Flexible Coupler Mechanism Analysis

of 3 degrees to a maximum rotation of 45 degrees. Also, variation of the input torque T_2 , and the bending stress in the coupler σ_b , as a function of the input shaft rotation θ , is depicted. It is interesting to notice that the input torque T_2 reaches a peak of 0.124 in-lbs. and its magnitude decreases for further rotation of the input shaft. The bending stress σ_b is the stress at the nodal point 6 on the coupler near the output link. The maximum stress of 115,000 psi is reached which is still within the elastic limit of spring steel. The bending stress can be calculated only at the nodal points. There are ways to find the maximum stress if it occurs in between the two nodal points but the present analysis procedure does not account for this.

The relation between θ and ϕ for the equivalent pin joint linkage (where two fixed joints are replaced by pin joints at nodes 2 and 6) with rigid links is also shown in Figure 16 for purposes of comparison. As a result of the fixed joints and the flexible coupler, the output link rotates 7.27 degrees more than the equivalent pin joint linkage.

The deflected shapes of the flexible coupler as the mechanism rotates are depicted in Figure 17. It should be pointed out that nodal points 2 and 6 of the coupler, which also belong to the rigid input and output links respectively, do not follow the rigid link motion. This

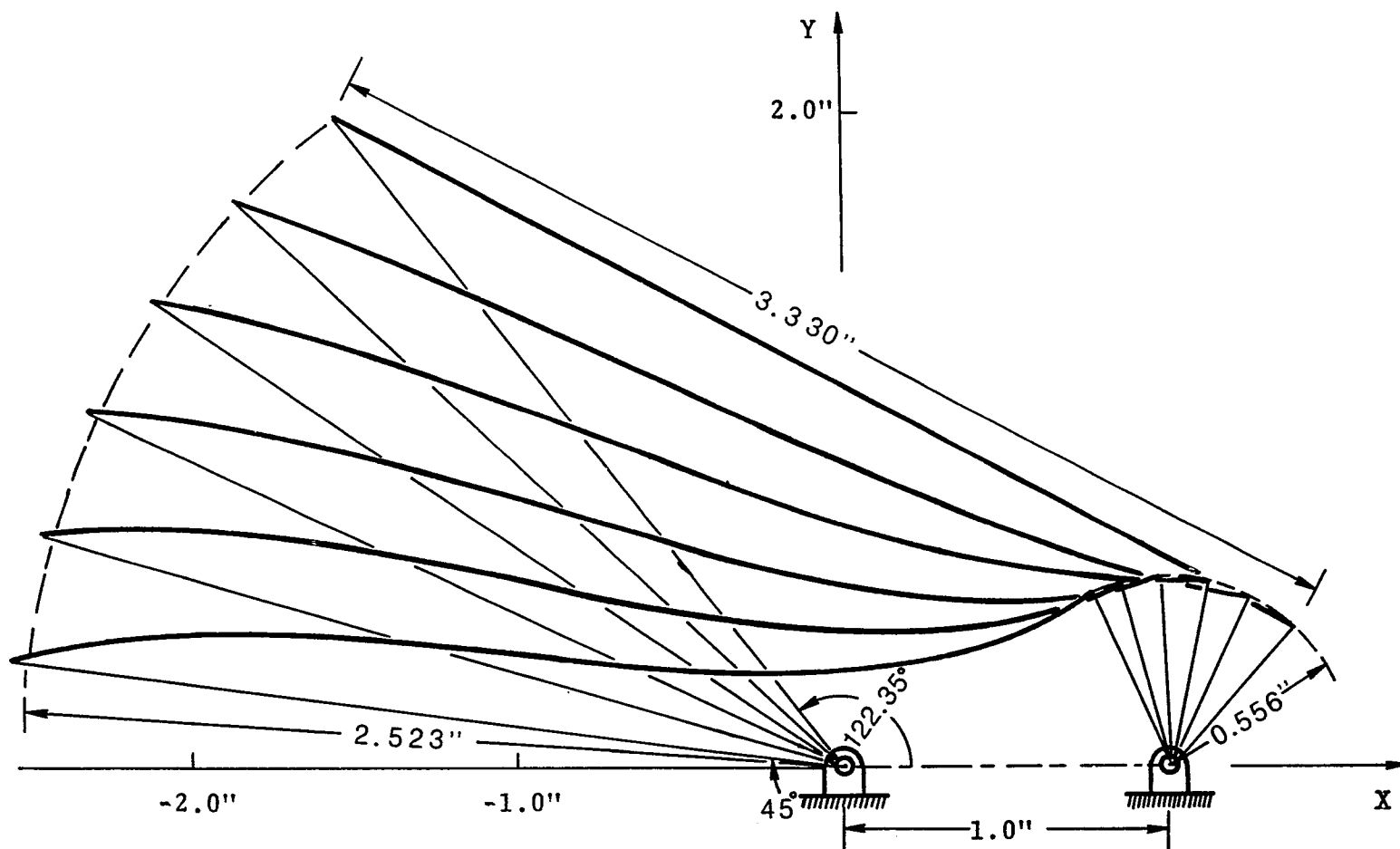


Figure 17. Deflected Shapes of the Flexible Coupler

error could be due to the truncation error which can be minimized by taking smaller increments or by double precision manipulation on the computer. In the subsequent sections, the method will be applied to the analysis of the mechanisms with two flexible members.

4.2 Two Flexible Members - Rigid Coupler Supported on Two Flexible Input and Output Links.

A hammer guide spring mechanism, as shown in Figure 3 of Chapter 1, is selected as an illustrative example to demonstrate the analysis method on the flexible link mechanism having 2 links which are flexible. The mechanism is composed of a "rigid" plastic coupler mounted on two flexible input and output links of equal length. The flexible links are 0.006 inch thick and 0.060 inch wide. One end of each link is molded in a plastic coupler and the other end is firmly fixed to the ground as depicted in Figure 18. The coupler is guided on the flexible links during its forward and return motion.

The coupler, being rigid, will be assumed to have only 1 element. Each of the two flexible links are divided into 6 elements. The total of 13 elements and 36 nodal displacements at 12 nodal points are depicted in Figure 18. The physical dimensions and elastic modulus of the links are also included in the figure.

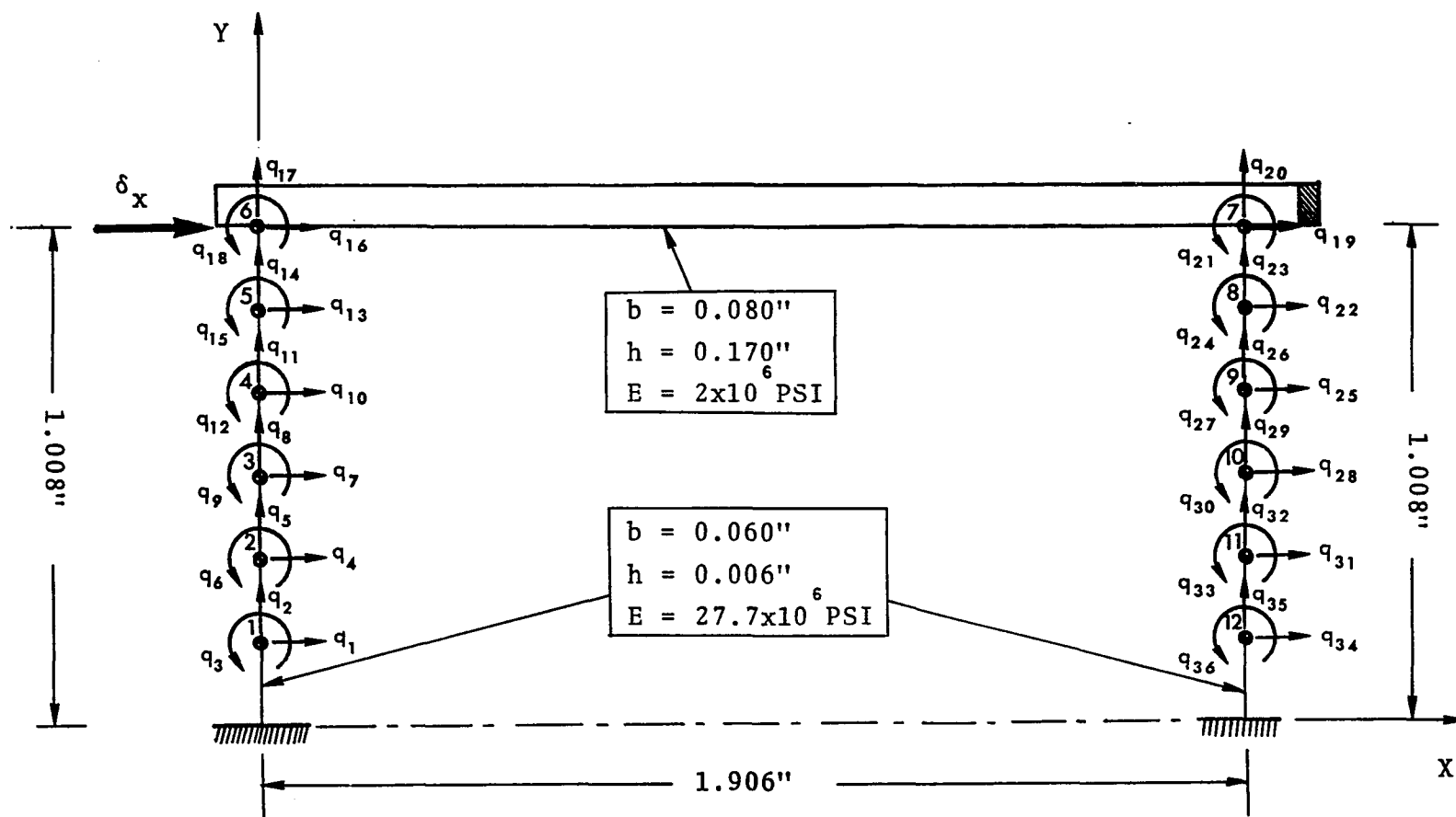


Figure 18. Flexible Input and Output Link Mechanism

The flexible input and output link mechanism was analyzed by the present analysis method for a horizontal input displacement (δ_x or q_{16}). For this analysis, δ_x was incremented by 0.010 inch up to a maximum displacement of 0.450 inch, which is almost half the length of the flexible links. The deflected shapes of the mechanism for the displacements of 0.100, 0.300 and 0.450 inch in δ_x are plotted in Figure 19. The experimental results are also included in the same figure for comparison.

The analytical results by the finite element method compare excellently to the experimental results. It can be noticed that the height of the coupler decreases as the mechanism is displaced horizontally. The following two major conclusions can be derived from the results:

- A. From the analytical results it was observed that the coupler rotates clockwise as it is displaced horizontally. This rotation of the coupler induces tensile forces in the input link and compressive forces in the output link. The compressive forces are not large enough to buckle the beam, so these results were included even though the assumption of tensile force in a flexible link was violated. It is the large displacement associated with the post-buckling

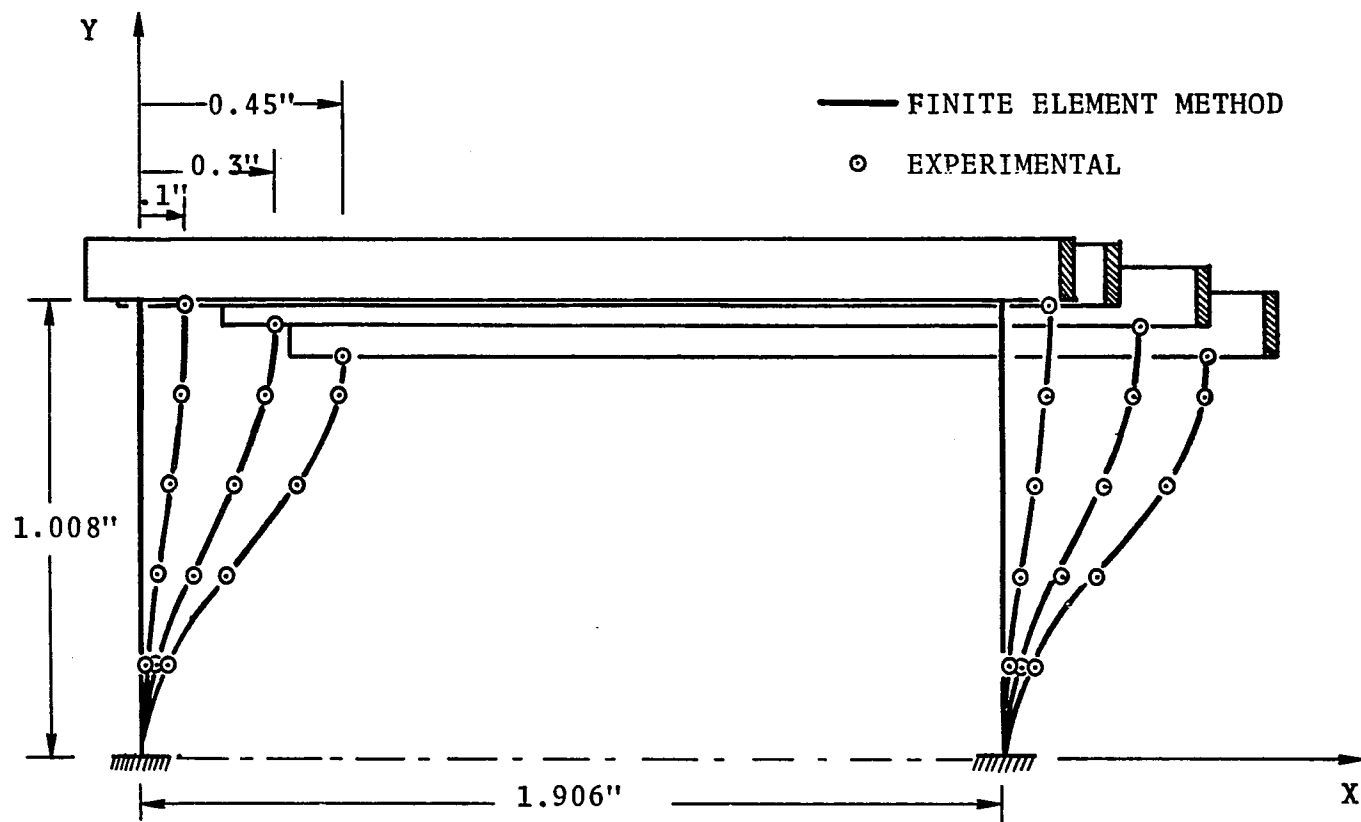


Figure 19. Shapes of the Flexible Input and Output Link Mechanism During Displacement

phenomenon that is not successfully handled by the present analysis method. The finite element method is capable of analyzing the buckling problem but modification of the present procedure would be required.

- B. In analysis by the finite element method, the stiffness of the beam (EI) is assigned to its neutral axis and the thickness of the beam does not enter into the analysis. Normally the nodal points are selected on the neutral axis of any beam. For the flexible link mechanism of Figure 18, the stiffness ratio of the coupler to the flexible link is high, so the flexible link will deflect at the lower edge of the coupler. Therefore, the nodal points are selected at the lower edge. It was also noted that the location of the nodal points at or between the lower edge and the neutral axis of the coupler changes the force vs. displacement relation of the mechanism but does not affect the displacement vs. displacement relation (deflected shapes). The best prediction of forces would come with nodes located at 0.019 inch above the lower edge of the coupler.

4.3 Two Flexible Members - Flexible Members as Flexural Joints.

A second flexible link mechanism with two flexible members will now be analyzed. In this type of linkage, flexural joints are flexible members. Such a mechanism is depicted in Figure 20, which can be considered as three rigid links connected by two flexible members. It is these two flexible members which deflect when mechanism is moved.

The mechanism of Figure 20 is a one piece part which can be made in a single punch operation, thereby reducing manufacturing cost. This makes the one piece mechanism of greater interest to engineers. Alternately, three rigid links and two flexible links could be made separately and bonded together. Similarly the other two mechanisms studied in this chapter could also be produced from a single part if so desired.

Each flexible member of the mechanism in Figure 20 is divided into 2 elements and 1 element is assumed for the rigid links. Therefore, a total of 7 beam elements with 20 nodal displacements at 8 nodal points as shown in Figure 20 are required to model this flexural joint mechanism. The flexible members are of 0.020 inch thickness and the rigid links are of 0.400 inch thickness.

The mechanism is analyzed to determine the relation between the input and the output link rotations which are

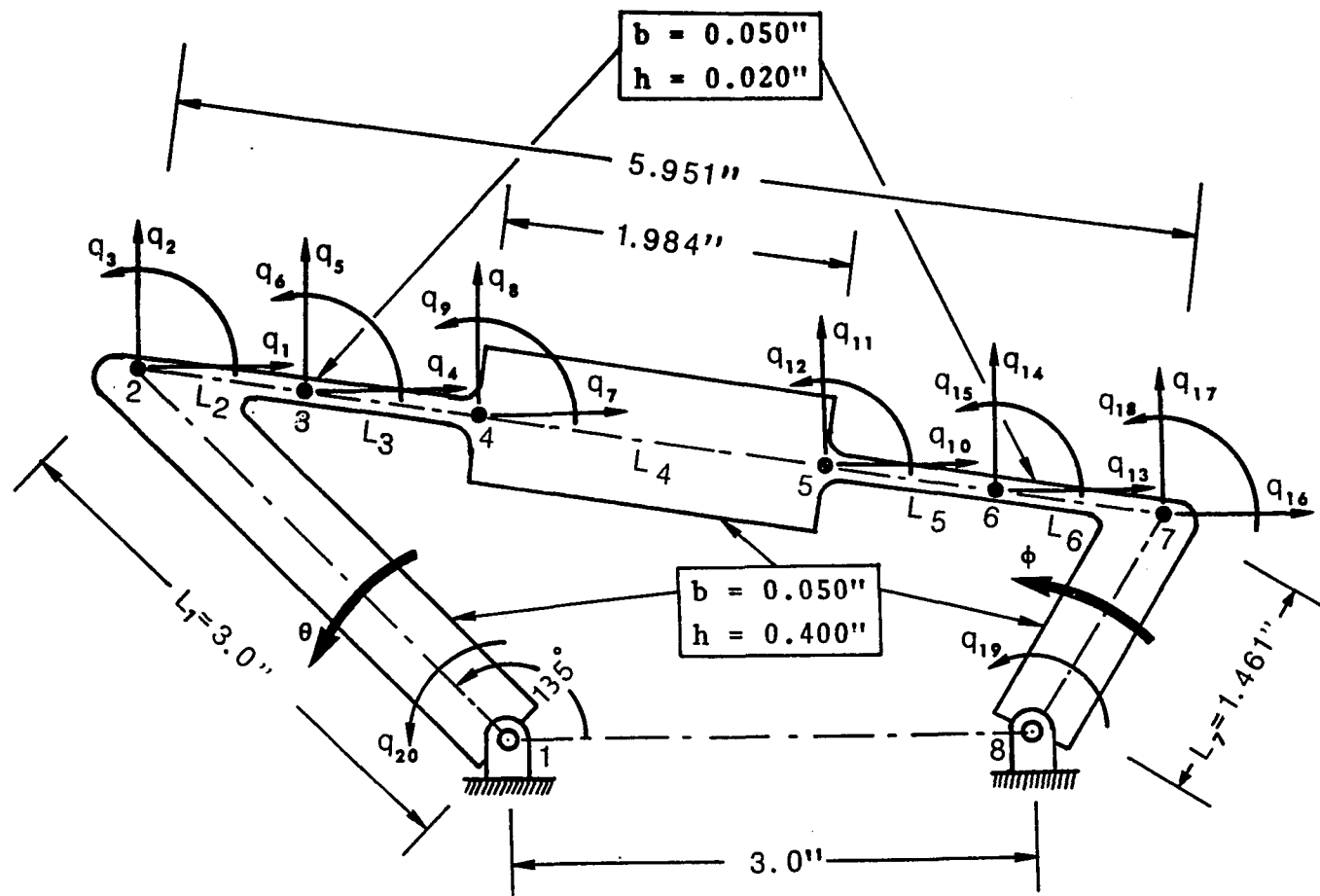


Figure 20. Flexural Joint Mechanism

depicted in Figure 21 with the variation of input torque and bending stress. The bending stress is the maximum among the stresses at the nodal points 2 to 7. The input link (θ) is rotated to a maximum rotation of 36.825 degrees in 10 increments for which the output link (ϕ) rotates by 38.85 degrees and a driving torque T_2 of 0.272 in-lbs. is required.

The results of the flexural joint mechanism, Figure 21, are similar to the results of the flexible coupler mechanism, Figure 16. In both problems, the input link (θ) rotates with an increment angle of 3 degrees or more which gives less than 15 increments. In light of the convergence study on the results of the cantilever beam (Figure 11 of Chapter 3) it could be concluded that analysis with less than 15 increments is marginal and will contribute some error to the results, which can be reduced by taking smaller increments in the input rotation.

It was concluded in the previous section that a high stiffness ratio of the rigid link to the flexible link can affect the location of the nodal point. Also, the fillet radius near the nodal points 2 and 7 will change the flexibility of flexural joint. A separate detailed investigation of the study of flexural joints

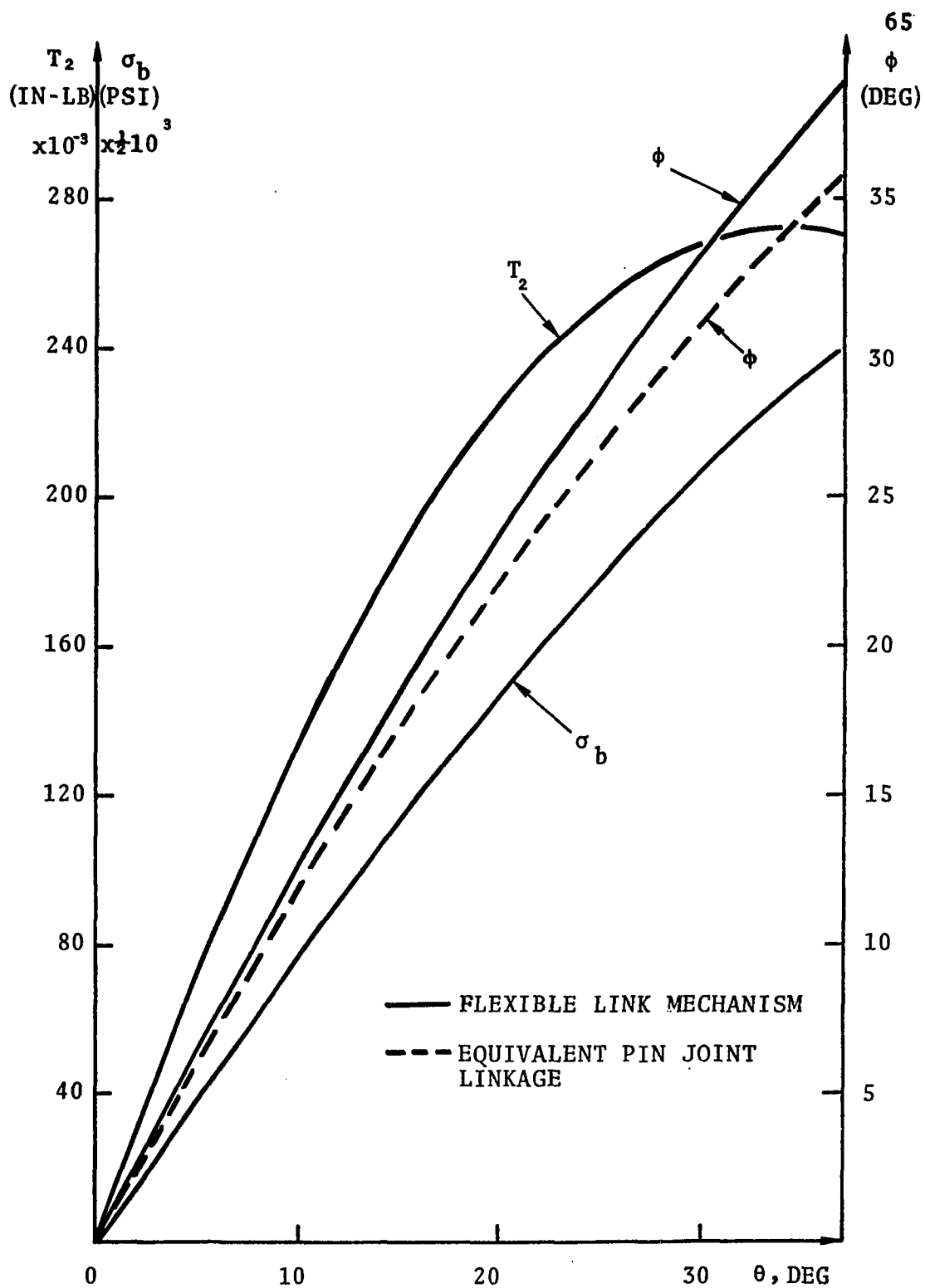


Figure 21. Results of the Flexural Joint Mechanism Analysis

with consideration to the stiffness ratio, design of the joints, etc. will be desirable for the accurate modeling of flexible link mechanisms.

CHAPTER V

OPTIMIZATION METHODS IN THE SYNTHESIS OF MECHANISMS

5.1 Introduction

Traditionally designers and kinematicians have synthesized the pin-jointed linkages by classical or direct methods. In recent years indirect methods have been developed and have been applied to the mechanism synthesis problem. Indirect methods are based on the optimization method, which evolved from structural engineering. Optimization methods are well accepted in structural, control and aerospace engineering and are slowly becoming popular in the mechanical engineering field.

Survey articles by Wasiutynski and Brant [45] cover developments in optimum design up to 1963 and Sheu and Prager [46] cover the developments up to 1968. Two recent articles by Prager [47] and Seireg [48] update the advancement in structural and mechanical design.

The survey articles by Fox and Gupta [49] and Sallam and Lindholm [50] include the references of the direct methods and the indirect methods pertaining to

mechanism design. Fox and Gupta cover in brief the general formulation for a design problem relevant to kinematic synthesis. No attempts will be made to duplicate the efforts of Fox and Sallam but a brief review will be covered in this section.

The optimization method, which is also referred to as the mathematical or nonlinear programming method, is further divided into two categories: (1) unconstrained minimization and (2) constrained minimization. The present investigation will be limited to the unconstrained minimization only.

The univariate method was the first method used for unconstrained minimization. The algorithm by Timko [52] was based on the univariate method in which one variable at a time is changed and the function generation problem was attempted by a least error-squared fit. The algorithm was not efficient but the optimization method was well demonstrated. Levenberg's damped least square method [51] was employed by Lewis et al [53-55] for a synthesis problem involving planar curve generation, higher order kinematic design, and multiple input mechanisms. Yeh [56] and Mansour and Osman [57] also followed the least square method for static force mechanism design and coupler curve generation problems, respectively. Efficient algorithms were developed for the least square method by Marquardt [58] and Powell [59].

The random-gradient method, which is a modification of Brooks' [60] method, was applied by Tomas [61, 62]. Tomas did an excellent job of formulating a mechanism synthesis problem into an optimization problem. A general formulation was sufficient for the synthesis of linkages for coupler curve generation and function generation problems. A random search procedure was popular with Garrett and Hall [63]. A library of four bar linkages, generated from the random numbers, were stored on tape. This tape was then searched for the desired function generation and a small number of good designs were selected. A subset of random linkages were generated around these to find the optimum design. Eschenback and Tesar [64] followed similar random search technique for generalized coupler positions design of linkages.

Rosenbrock's rotating coordinate method [65] was applied by Lakshminarayana and Narayanamurthi [66] to synthesize a seven-link, two degrees of freedom mechanism from precision point equations in which the starting point was selected from a brief random search. Sridhar and Torfason [67] used the same method to optimize a design of spherical four bar linkages for a path generation problem. Mueller and Osman [68] also followed the rotating coordinate method for the synthesis of a planar mechanism for coupler curve generation.

The steepest descent method [69] was used by Tull and Lewis [70] for space curve generation and by Rees Jones and Rooney [71] for planar curve generation. Kugath [72] made a comparative study of univariate, random, and pattern search, and steepest descent methods on four and six bar linkages for function generation.

Combinations of gradient and relaxation methods were applied by Nechi [73] for planar curve generation. Dimarogonas, et al [74] synthesized geared N-bar linkages with the help of the Monte Carlo optimization technique, in which the number of design variables were optimized first until better characteristics for a starting point were obtained. Bagci [75] applied the Lagrange multiplier for generation of constrained and unconstrained screws of the space mechanism.

References so far include application of design constraints externally, which means the parameters are checked for violation of constraints at the beginning of each iteration step. Fox and Willmert [78] formulated the constraints internally right in the objective function for the synthesis of planar curve generating linkages. Faicco-McCormick's sequential unconstrained minimization (SUMT) [81] was followed for the solution, but the procedure was found unsatisfactory for synthesis of four bar linkages. The modified SUMT procedure was developed and applied satisfactorily in [79]. Fletcher and Powell's

variable metric method [77] was used to minimize the unconstrained objective function. Fox and Willmert derived the necessary gradient expression for the four bar while Moore [83] used the numerically computed gradients as suggested by Stewart [85] and applied to the original variable metric method of Davidon [76]. Tranquilla [84] also followed the SUMT procedure to design four-bar linkages for specified extremes of coupler curves. Recently, Willmert and Fox [80] used the optimization method for the shock isolation system, where the topology of a system, in a limited sense, was attempted by optimizing the number of elements in the system.

Among the many methods developed for unconstrained minimization, a few are worth mentioning, even though they did not find application in the mechanism field. They are: (1) the conjugate gradients method of Fletcher and Reeves [86], and Powell [87], and (2) the rank one method of Powell [88]. The computational algorithms for most of the methods covered so far and the many more for solving unconstrained and constrained optimization problems are included by Mangasrian [89].

5.2 Formulation of Equations for the Optimization Method

The formulation of equations for a kinematic synthesis problem, as a mathematical programming problem, will be

presented before the explanation of the optimization method.

In general, the mathematical programming problem is as follows:

Let the given function to be minimized be expressed as

$$F(\{d\}^T) = F(d_1, \dots, d_n) \quad (42)$$

where d_1, \dots, d_n are the n components of the unknown n dimensional vector $\{d\}$. Function $F(\{d\}^T)$ may or may not be subjected to constraints. In any case, during the optimization process, the components of $\{d\}$ are searched in such a way that $F(\{d\}^T)$ is driven to its minimum.

For a design problem, $F(\{d\}^T)$ is referred to as the objective function. Components d_1, \dots, d_n are referred to as design variables. The objective function could be a weight function for a structural design or a cost function for a manufacturing process. For a linkage design, the objective function will be an error function.

Let the function for the synthesis be:

$$\phi = f(\theta) \quad (43)$$

and the generated function by the linkage be:

$$\phi_g = g(\theta, \{d\}^T) \quad (44)$$

as depicted in Figure 22, where θ is the input and ϕ is the output rotation of flexible link mechanism. The components of $\{d\}$ are the design variables such as the length

and stiffness of the links, the initial position of the linkage, etc. the objective of the kinematic synthesis is to generate ϕ_g as close as possible to function $f(\theta)$.

The error (which leads to the objective function) is the difference between the two curves as shown in Figure 22. This difference can be expressed in many ways to give different objective or criteria functions, three of which are shown in Equations (45), (46), and (47), as follows:

$$F(\{d\}^T) = E_A = \sum_{i=1}^s \left| f(\theta_i) - g(\theta_i, \{d\}^T) \right| \quad (45)$$

where E_A is the sum of the absolute values of the error curve cumulated at 's' number of points. This is an approximation of the absolute area of the error curve.

$$F(\{d\}^T) = E_M = \max_i \left| f(\theta_i) - g(\theta_i, \{d\}^T) \right| \quad (i=1, \dots, s) \quad (46)$$

Where E_M is the maximum value of the error curve.

$$F(\{d\}^T) = E_R = \sqrt{\frac{1}{s} \sum_{i=1}^s [f(\theta_i) - g(\theta_i, \{d\}^T)]^2} \quad (47)$$

Where E_R is the root-mean square value of the error at 's' number of points.

In the above formulation, the desired and generated functions are assumed to be for the synthesis of a linkage

for a function generation problem. The desired function could as well be a coupler curve expressed in polar coordinates, or x or y coordinates, or combined x and y coordinates. Therefore, it should be pointed out that the above formulation is valid even for a coupler curve generation problem. But, in the present investigation, only the function generation problem will be attempted.

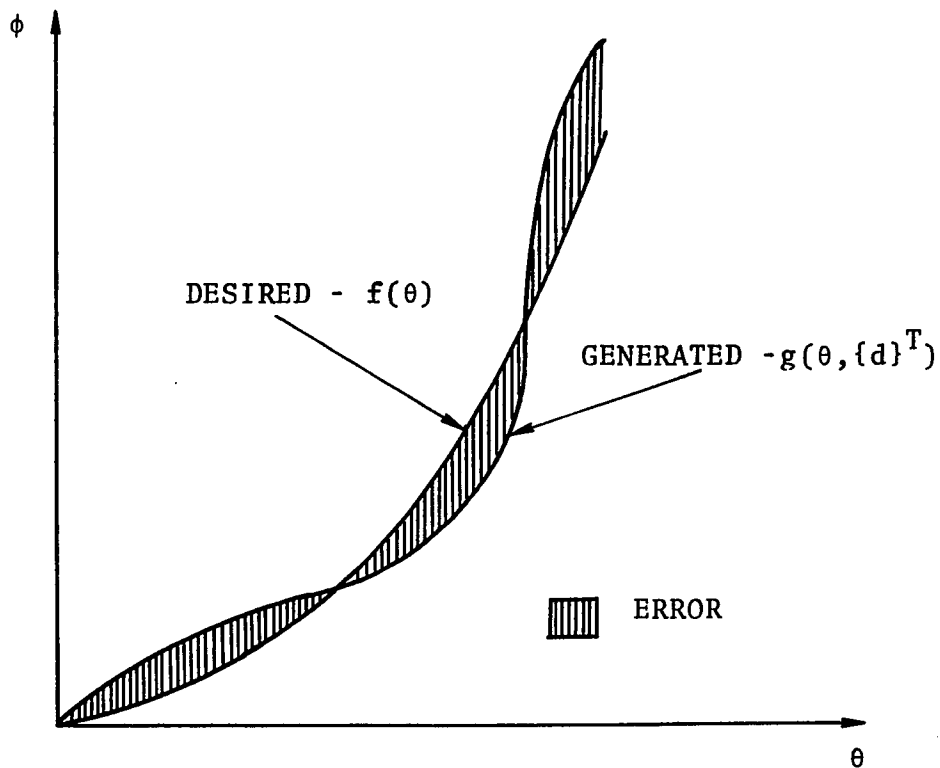


Figure 22. Desired and Generated Functions

Similarly, any one of the objective functions, Equations (45) to (47), can be minimized under design constraints such as: a limitation on the length of the links, limitation on the location of the input and output shafts, limitation on stress, etc. However, for the present investigation, design constraints will not be included.

5.3 Variable Metric Method

The variable metric method is selected as the optimization method for the synthesis of the flexible link mechanisms of this dissertation. The variable metric method was originally developed by Davidon [76] and improved by Fletcher and Powell [77]. The method requires the first partial derivative of the objective function. These derivatives (gradients) will be impossible to express in a closed form for a flexible link mechanism. Therefore, the gradients are approximated by difference quotients according to Stewart's technique [85].

The iteration procedure for converging to the optimum design by the variable metric method is depicted in the flow diagram of Figure 23. The major steps of which are as follows:

- A. The iteration starts with the initial value of design variables, $\{d_0\}$.

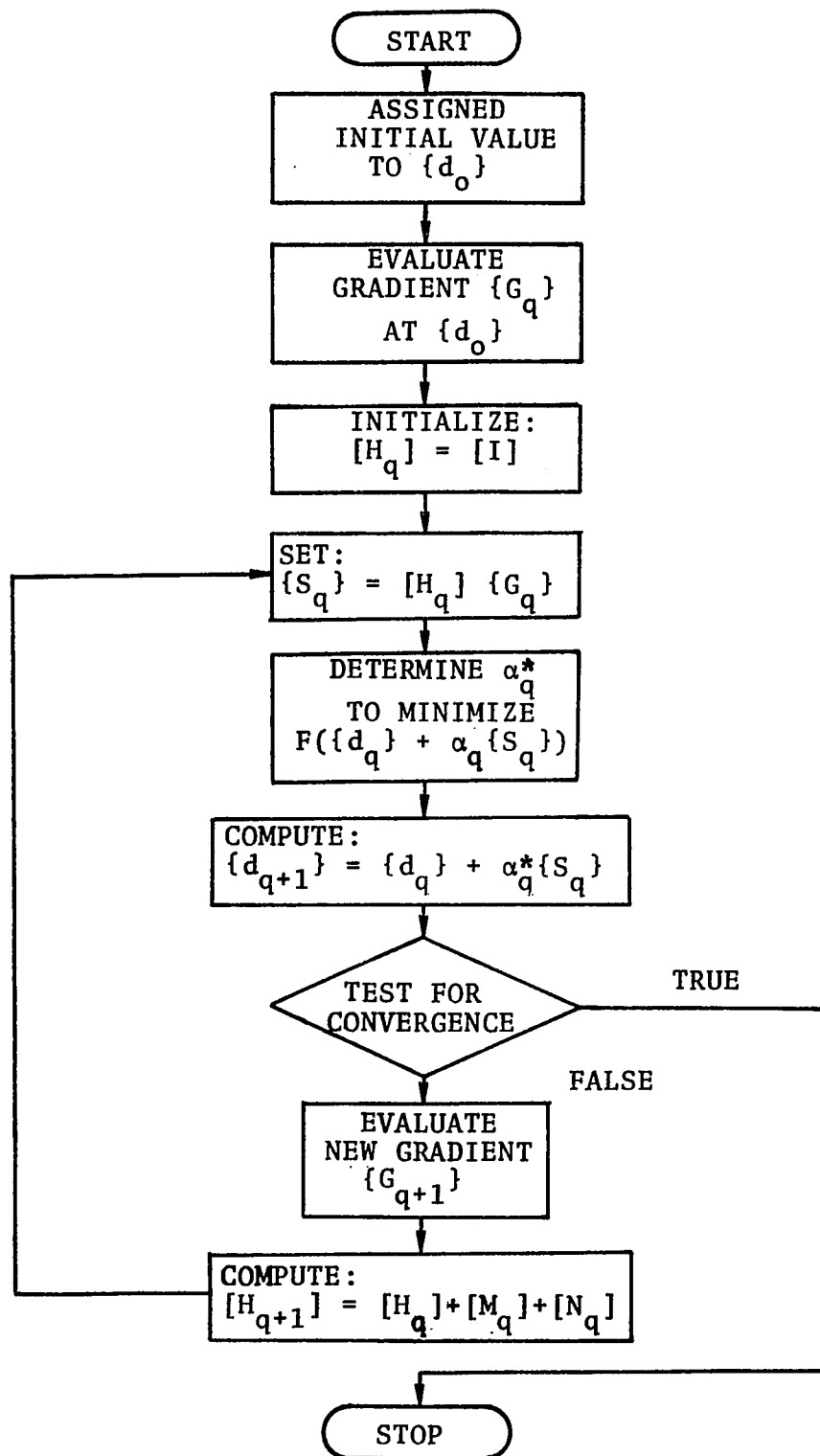


Figure 23. Flow Diagram of the Variable Metric Method

B. At the minimum point the first partial derivative of the objective function will be zero and the matrix of the second partial derivative will be positive definite. This matrix is referred to as the Hessian matrix. Proper estimation of the Hessian matrix leads the method with rapid convergence to the optimum point but its evaluation is difficult for most of the problems. The basis of the variable metric method is to replace the Hessian matrix by an approximate matrix $[H_q]$. At the end of each iteration step, $[H_q]$ is improved which eventually leads to convergence of the local Hessian matrix at the minimum point. At the beginning of the iteration cycle $[H_q]$ is initialized to the identity matrix as:

$$[H_q] = [I] \quad (48)$$

where $[I]$ is the identity matrix.

C. The components gradients (the $\{G_q\}$ of the objective function) at the initial point are evaluated by:

$$G_i = \frac{F(d_i + \Delta d_i) - F(d_i)}{\Delta d_i} \quad (49)$$

(i=1, ..., n)

where Δd_i is the given initial increment in d_i .

- D. The direction of line $\{S_q\}$, along which the minimization will be searched, is set by:

$$\{S_q\} = - [H_q] \{G_q\} \quad (50)$$

- E. The function $F(\{d_{q+1}\}^T)$ is evaluated at three points along the line whose equation is:

$$\{d_{q+1}\} = \{d_q\} + \alpha_q \{S_q\} \quad (51)$$

where α_q is the increment along the line.

With the help of quadratic interpolation, α_q^* is determined at which the function $F(\{d_q\} + \alpha^* \{S_q\})$ will be minimum. A new minimum point, $\{d_{q+1}\}$ can be evaluated from Equation (51) and α_q^* .

- F. Convergence of $\{d_{q+1}\}$ to $\{d_q\}$ is checked based on the desired accuracy. If the test is satisfactory, the iteration cycle terminates. If it is not satisfactory, then $[H_q]$ is improved and the cycle is repeated until the convergence is achieved.
- G. Before computing $[H_{q+1}]$, the gradients are evaluated at the new point $\{d_{q+1}\}$. The gradient components are computed from Equation (50) but the increments in $\{d_{q+1}\}$, $\{\Delta d_{q+1}\}$, are now determined based on special techniques developed by Stewart [87]. Stewart developed an algorithm

which accounts for the accuracy to which a function is computed and the truncation error of the machine. This algorithm was used for determining the increment size which is very crucial for accurate evaluation of the gradient components.

H. $[H_{q+1}]$ is computed as follows:

$$[H_{q+1}] = [H_q] + [M_q] + [N_q] \quad (52)$$

where

$$[M_q] = \alpha_q^* \frac{\{S_q\} \{S_q\}^T}{\{S_q\}^T \{R_q\}} \quad (53)$$

$$[N_q] = - \frac{([H_q] \{R_q\}) ([H_q] \{R_q\})^T}{\{R_q\}^T [H_q] \{R_q\}} \quad (54)$$

and

$$\{R_q\} = \{G_{q+1}\} - \{G_q\} \quad (55)$$

The cycle is repeated from step D.

The variable metric method has proven to be rapid in convergence and it possesses good stability; stability in the sense that it requires very little special attention for the progress of the minimization procedure even for a highly distorted and eccentric function. It is the most general method for finding the local minimum of an objective function for an unconstrained minimization.

The subroutine DMIN2 in Appendix A, is the program for the flow diagram of Figure 23. The subroutine FX4BAR is called whenever evaluation of the objective function is required in DMIN2. The objective function (Equation (45), (46) or (47)) is included in FX4BAR. The subroutine INITPM performs the quadratic interpolation required in step E.

In the next two chapters the variable metric method will be applied to: (1) the design of a nonlinear spring for a desired force vs. displacement relation, and (2) the synthesis of a flexible link mechanism for a function generation problem.

CHAPTER VI

OPTIMUM DESIGN OF NONLINEAR SPRINGS

6.1 Design of Cantilever Beam

The analysis by the finite element method of a cantilever beam subjected to large displacements was demonstrated in Chapter 3. Now a cantilever beam will be designed for a desired force vs. displacement relation by the optimization method. This problem was selected to check the accuracy and the convergence of the variable metric method described in the previous chapter.

The design problem is to determine the length, L , of the cantilever beam so that the force vs. displacement relation is generated as close as possible to the desired relation (function). A cross-sectional area of 0.5 inch width and 0.006 inch thickness, and an elastic modulus of 30×10^6 psi for the beam are assumed to be fixed parameters for this design.

As the accuracy of the optimization method is to be checked, the desired function (force vs. displacement) of Figure 24 was determined by the finite element method for a 10 inch length of beam. The design by optimization

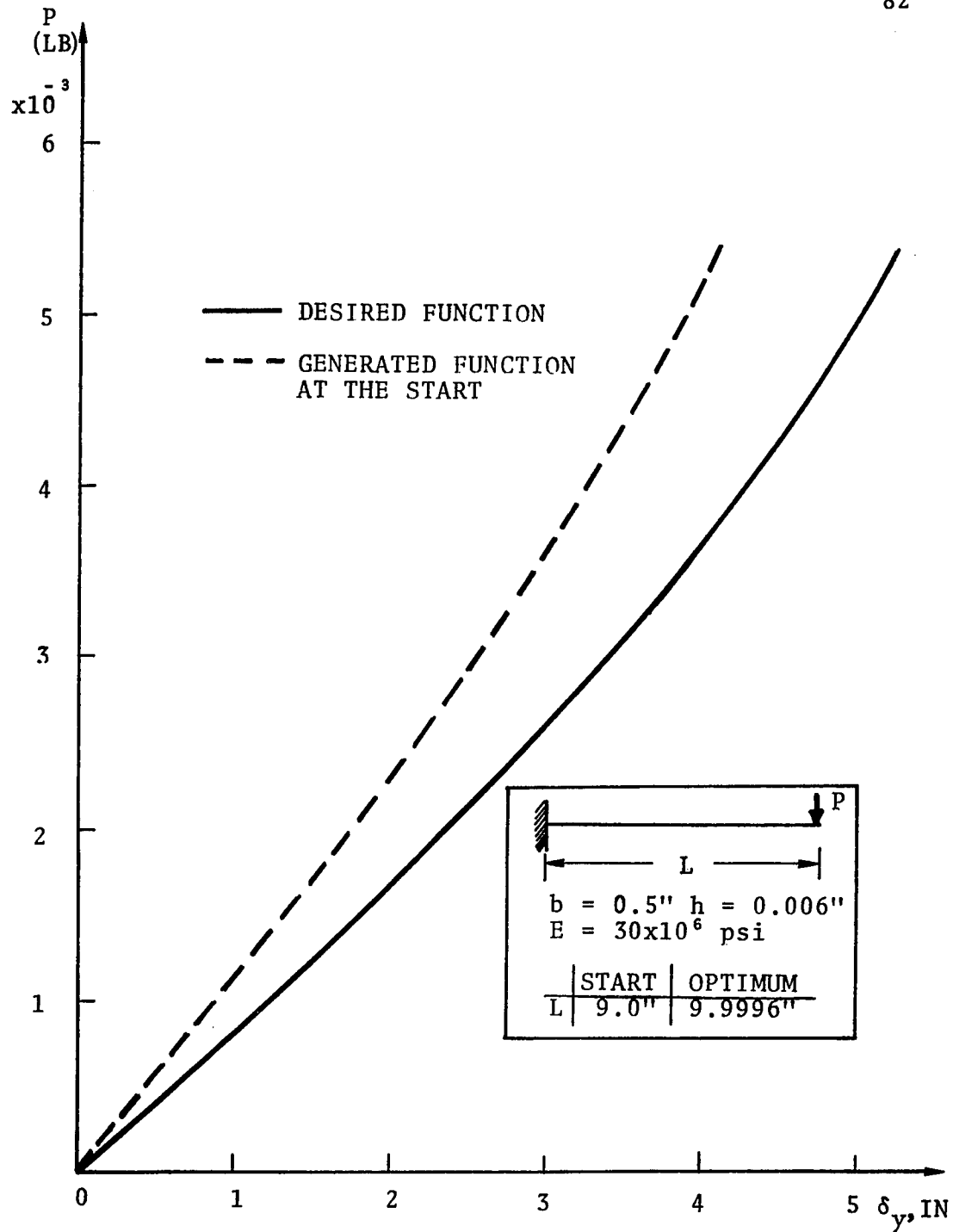


Figure 24. Design of Cantilever Beam for a Desired Force vs. Displacement Relationship.

method started with an initial value of 9 inches for the length of the beam. If the variable metric method of optimization converges the length of the beam to 10 inches then this will demonstrate the accuracy of the optimization method for one variable.

The variable metric method, as depicted in the flow diagram of Figure 23, Chapter 5, is now applied to this design of a cantilever beam. For each time the objective function is evaluated during the optimization process, the analysis based on the finite element method is performed. A total of 30 points 's' are selected at equal increments of the input force for the analysis and accumulation of error for the objective function. Also, the analysis assumes 3 elements for the cantilever beam.

The optimization method started with an initial value of 9 inches for the length L of the beam. The force vs. displacement relation for this initial design is shown in Figure 24 along with the desired function. The difference between the two gives the error curve. The sum of the absolute errors E_A , was selected as the objective function for the optimization method. The results of the optimization by the variable metric method is tabulated in Table 2. Examination of this table indicates that at the end of 3 iteration steps 'q', the length L of the beam has converged from 9.0 to 9.9996 inches which is

TABLE 2

OPTIMUM DESIGN OF A CANTILEVER BEAM USING
THE OBJECTIVE FUNCTION, E_A

q	j	{d} L	{G}	Objective Functions		
				E_A	E_M	E_R
0	1	9.0000		22.0942	1.1524	0.8093
	2	9.0010	-18.4396	22.0757	1.1514	0.8086
1	3	11.3964		35.1739	1.6931	1.2701
	4	9.9245		1.7719	0.0895	0.0646
	5	10.8491		20.8369	1.0220	0.7549
	6	9.9255	-29.4604	1.7424	0.0883	0.0635
2	7	10.0448		1.0453	0.0528	0.0380
	8	10.0002		0.0059	0.0005	0.0002
	9	9.9993		0.1818	0.0090	0.0066
	10	10.0093		0.2181	0.0114	0.0080
	11	10.0012	21.4905	0.0274	0.0016	0.0010
3	12	9.9996		0.0043	0.0004	0.0002
	13	9.9999		0.0059	0.0003	0.0003
	14	9.9992		0.0155	0.0007	0.0006
	15	9.9998	-20.0059	0.0020	0.0002	0.0001

within 0.0004 inch of the correct value of 10 inches. The method required 15 evaluations (j) of the objective function which includes the evaluation required for the gradients and for the quadratic interpolation. The results of the quadratic interpolation are underlined in Table 2. At this design point, the minimum of the objective function is achieved along a line of search for each iteration step.

The objective function E_A reduced from 22.0942 to 0.0043 at the optimum design of 9.9996 inches length of the beam. Table 2 includes the estimates of the other two objective functions, E_M , the maximum value of the error, and E_R , the root-mean square error which are also minimized along with the objective function E_A .

From the results of Table 2 it can be concluded that the optimization method of the variable metric is rapidly converging and very accurate. The optimization method is dependent on the analysis method, thus the accuracy of the analysis can affect the progress of optimization. This effect of accuracy is noticed during the 3rd iteration step. The design variable L, length of the beam at the 13th evaluation of the function (j) is 9.9999 inches which is closer to the correct length of 10 inches than the length of 9.9996 inches of the 12th evaluation of the objective function. But, the objective function E_A , for the 13th evaluation was estimated to be more than the

12th evaluation which lead to 9.9996 inches as an optimum length. This was investigated in detail and was concluded that the present analysis by the finite element method is accurate only to 4 digits in the length, L . Beyond this the method breaks down due to the truncation error and this error was detected in the results.

The magnitudes of the gradients at each iteration step are listed in Table 2. The gradients fluctuate from negative to positive and the magnitude is increased instead of decreased at the optimum point. This increase in the magnitude could be false because of the truncation error. The fluctuation in the gradients is valid and the true minimum can be achieved by continuing the optimization beyond the 3rd iteration step. But the error in the objective and the gradient functions can divert the search away from the local minimum. Thus, the extra iteration may not be worthwhile so the optimization method was terminated at the end of 3rd iteration.

A separate design of a cantilever beam was also optimized by the variable metric method for the remaining two objective functions, maximum value of the error E_M and root-mean-square error E_R . The results of these as well as the first optimization at termination of 3 iteration steps are tabulated in Table 3, in which the optimum designs are listed for each objective function with

evaluation of the three objective functions at these optimum designs. With one exception, the results indicate that the minimum of the objective function is achieved when that objective function is used for optimization of the design. The exception is for the objective function E_R , where the minimum of E_R was achieved for the design with E_A . Continuation of the optimization with E_R beyond 3 iteration steps would drive E_R to its minimum. The objective function E_A , will be the only one used for the remaining part of the investigation.

TABLE 3

COMPARISON OF THE THREE OBJECTIVE FUNCTIONS

Optimization With Objective Function	Optimum L	Objective Functions		
		E_A	E_M	E_R
E_M	9.9988	0.0139	0.0002	0.0005
E_R	9.9992	0.0096	0.0005	0.0004
E_A	9.9996	0.0043	0.0004	0.0002

In the next chapter, optimization by the variable metric method will be applied to the synthesis of flexible link mechanisms.

CHAPTER VII
OPTIMUM SYNTHESIS OF
FLEXIBLE LINK MECHANISMS

7.1 Synthesis for Function Generation, $y=x^2$

Various types of flexible link mechanisms were analyzed by the finite element method in Chapter 4. The analysis determined the relationship between the input and output link rotations. The optimization method was demonstrated on the design of a cantilever beam in a previous chapter. In this chapter, the method is applied to the synthesis of flexible link mechanisms for a function generation problem.

A parabolic function, $y=x^2$, will be generated by flexible coupler and flexural joint mechanisms to demonstrate the method. The independent variable x and dependent variable y of the function can be related to input θ and output ϕ rotations of linkage by the following linear relations:

$$\frac{\theta - \theta_s}{\theta_f - \theta_s} = \frac{x - x_s}{x_f - x_s} \quad (56)$$

$$\frac{\phi - \phi_s}{\phi_f - \phi_s} = \frac{y - y_s}{y_f - y_s} \quad (57)$$

where subscript 'f' stands for the final position of the links and 's' stands for the initial position.

Major consideration for the synthesis of flexible link mechanism will be to choose the angle of rotation for the ranges of θ and ϕ . Also, the proportion of the links should be selected so that during the range of motion the flexible members do not deflect to their extreme and produce a locking position for the mechanism.

7.2 Synthesis of a Flexible Coupler Mechanism

The flexible coupler mechanism of Figure 15 (Chapter 4) will be synthesized to generate $y=x^2$, for $1 \geq x \geq 0.5$. The range of rotation for the input link (θ) is limited to 45 degrees and that of the output link (ϕ) to 67.5 degrees. The x and y coordinates can be related to θ and ϕ by Equations (56) and (57).

A flexible coupler mechanism which has similar dimensions to Freudenstein's [41] pin joint linkage (for function $y=x^2$) was taken as the initial estimate to a solution for this problem. The results of the analysis of the flexible coupler mechanism and the Freudenstein's pin joint linkage analysis are depicted in Figure 16 (Chapter 4), which indicates that Freudenstein's linkage has a maximum error of 0.0673 degree compared to 7.266 degrees for the flexible linkage. Similarly, the sum of the absolute

error (E_A), at 15 points 's' through the range of rotation for the pin joint linkage is 0.998 and that for the flexible coupler mechanism is 53.293. It is the objective of the optimization method to reduce this error E_A of 53.293 to an acceptable level.

As depicted in Figure 25, the flexible coupler mechanism has seven possible design variables: 3 lengths of the links d_1 , d_2 , and d_3 , the initial position of the input link θ_s , the thickness h and width b of the flexible coupler and the length of the fixed link (distance between the input and output shaft), d_0 . For the present synthesis, only four design variables, d_1 , d_2 , d_3 , and θ_s , will be considered. Before attempting optimization with the four design variables, one variable at a time was studied for the flexible coupler mechanism of Figure 15. From the study it was discovered that θ_s is the most effective parameter. The decrease of the objective function E_A as a function of θ_s is depicted in Figure 26. The lowest magnitude of E_A (4.564) occurs at θ_s of 128.059 degrees.

The flexible coupler mechanism of Figure 15, with this new value of θ_s is now selected as the starting design for the optimization by the variable metric method. The results of the optimization method are tabulated in Table 4. The objective function E_A , sum of the absolute error, was used for the optimization method. In 3 itera-

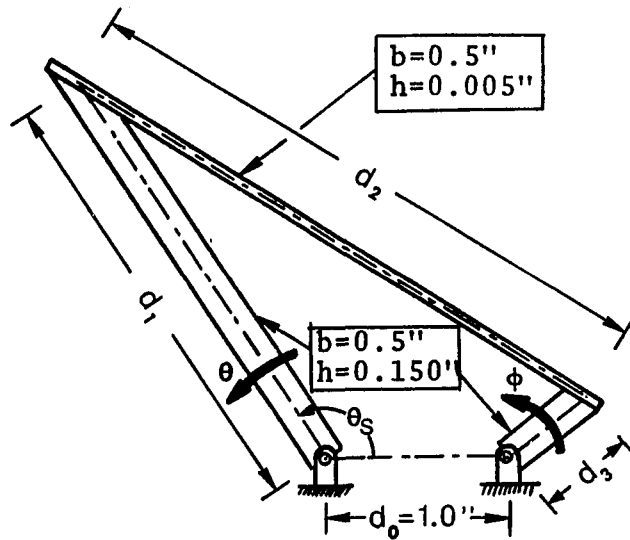


Figure 25. Design Variables For a Flexible Coupler Mechanism

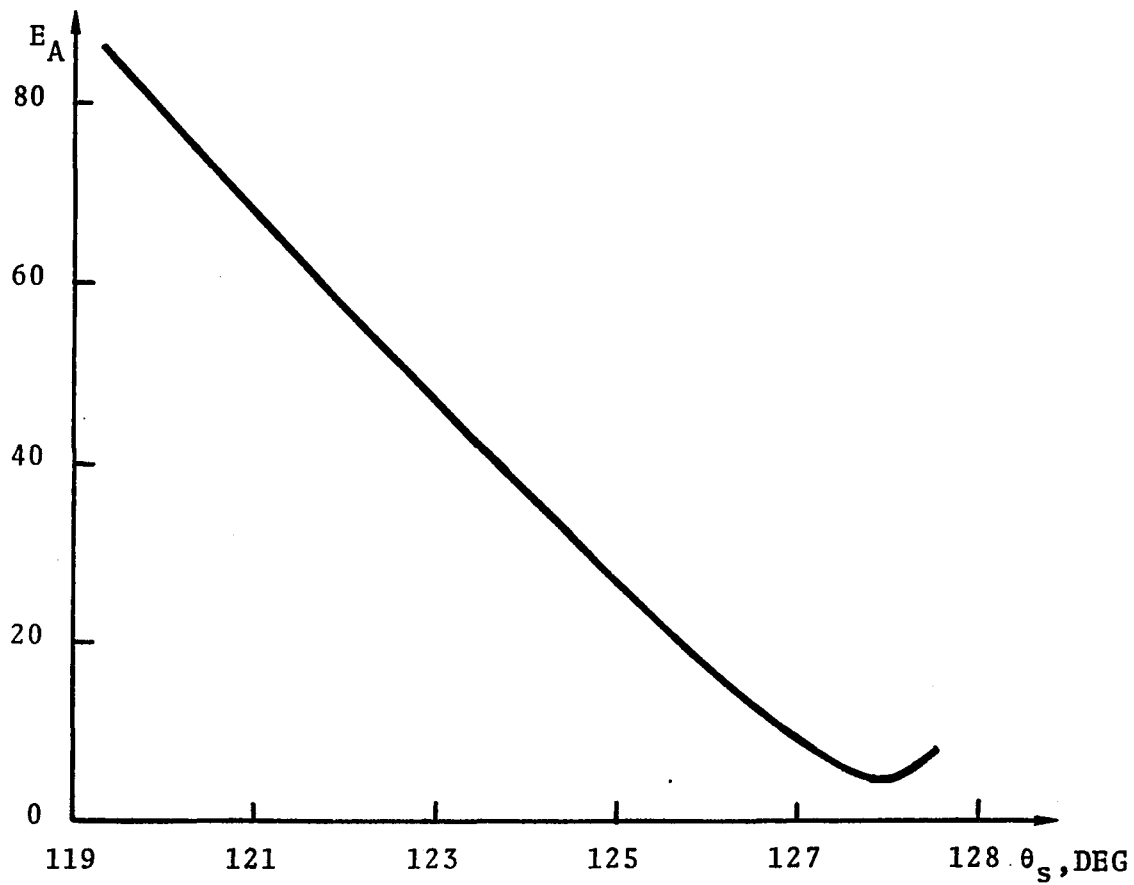


Figure 26. Relationship Between E_A and θ_s

TABLE 4

OPTIMUM SYNTHESIS OF A FLEXIBLE COUPLER MECHANISM

q	j	{d}				i	G_i	E_A
		d_1	d_2	d_3	θ_s			
0	1	2.5234	3.3296	0.5560	128.059			4.5638
	2	2.5224	3.3296	0.5560	128.059	1	-36.372	4.5274
	3	2.5234	3.3286	0.5560	128.059	2	39.606	4.6034
	4	2.5234	3.3296	0.5570	128.059	3	-107.754	4.6716
	5	2.5234	3.3296	0.5560	128.065	4	40.936	4.5597
1	6	2.5028	3.3520	0.4952	129.382			30.8794
	7	2.5207	3.3325	0.5481	128.229			4.9483
	8	2.5244	3.3285	0.5589	127.995			4.9865
	9	2.5229	3.3301	0.5545	128.091			4.5082
	10	2.5219	3.3301	0.5545	128.091	1	36.661	4.4715
	11	2.5229	3.3291	0.5545	128.091	2	-35.908	4.5441
	12	2.5229	3.3301	0.5555	128.091	3	-2.617	4.5056
	13	2.5227	3.3301	0.5545	128.097	4	-101.746	4.4980
2	14	2.4913	3.3624	0.5187	131.918			23.0241
	15	2.5154	3.3378	0.5460	128.995			5.3793
	16	2.5255	3.3274	0.5575	127.771			5.0496
	17	2.5215	3.3315	0.5530	128.251			4.2866
	18	2.5538	3.3315	0.5530	128.251	1	43.461	5.6896
	19	2.5215	3.3275	0.5530	128.251	2	-34.047	4.4233
	20	2.5215	3.3315	0.5534	128.251			4.2997
	21	2.5215	3.3315	0.5525	128.251	3	13.609	4.2870
	22	2.5215	3.3315	0.5530	128.263			4.2757
	23	2.5215	3.3315	0.5530	128.240	4	-51.140	4.2961
3	24	2.4010	3.4032	0.5464	129.150			15.1972
	25	2.4950	3.3473	0.5515	128.449			3.3364
	26	2.4924	3.3489	0.5514	128.469			3.2550
	27	2.4871	3.3520	0.5511	128.508			3.0017
	28	2.4764	3.3583	0.5505	128.587			2.2398
	29	2.4552	3.3709	0.5494	128.745			1.2944
	30	2.4398	3.3801	0.5485	128.860			3.3403
	31	2.4612	3.3674	0.5497	128.701			1.2230
	32	2.4623	3.3674	0.5497	128.701	1	12.455	1.2367
	33	2.4612	3.3655	0.5497	128.701	2	-9.316	1.2407
	34	2.4612	3.3674	0.5499	128.701			1.2149
	35	2.4612	3.3674	0.5495	128.701	3	-41.500	1.2313
	36	2.4612	3.3674	0.5497	128.707	4	-9.568	1.2220

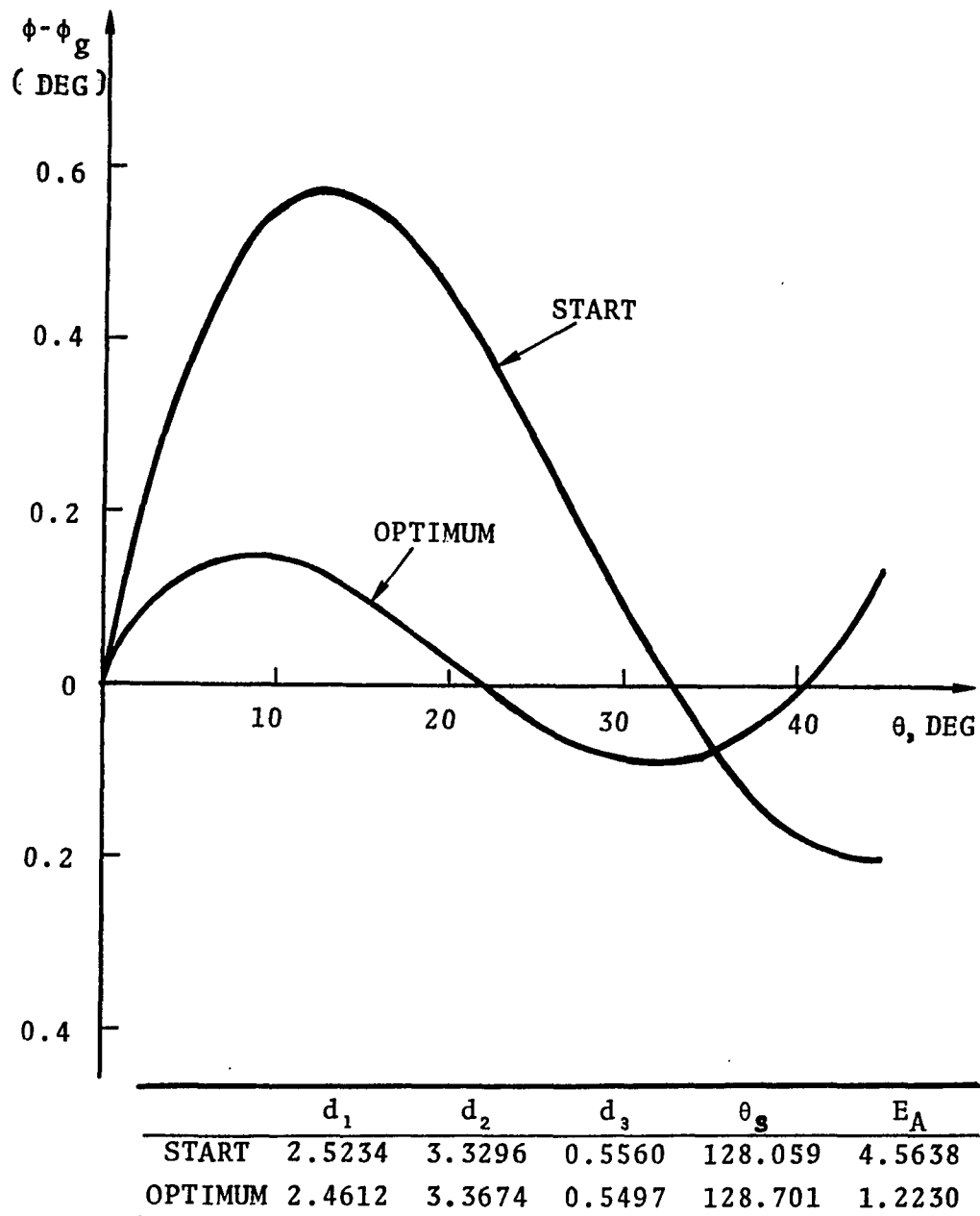


Figure 27. Synthesis of a Flexible Coupler Mechanism

tive steps 'q', the value of the objective function E_A , was further reduced from 4.5638 to 1.2230. A total of 36 evaluations of the function 'j' was required for the optimization method. The minimum objective function achieved during each step is underlined in Table 4.

The error (structural error) curves for the starting design and the optimum design are depicted in Figure 27. The error curve has a maximum of 0.1490 degrees of error which amounts to 0.221% error of the output range.

7.3 Synthesis of a Flexible Coupler Mechanism from a Different Starting Design

A second starting point was also investigated for this type of linkage. The schematic diagram for the linkage is shown in Figure 28. For this linkage, it is desired to generate the function $y=x^2$ for $0 \leq x \leq 1$. The range of rotation for the input link θ was selected to be 60 degrees and for the output link ϕ to be 50 degrees.

The optimization method was also applied to the linkage of Figure 28. Only the three lengths of links d_1 , d_2 , and d_3 were selected as the design variables for the optimization. For the given three initial lengths of links, the initial position of the input link θ_s , was determined so that the coupler would be in line with the input link. This assures that the first derivative of the

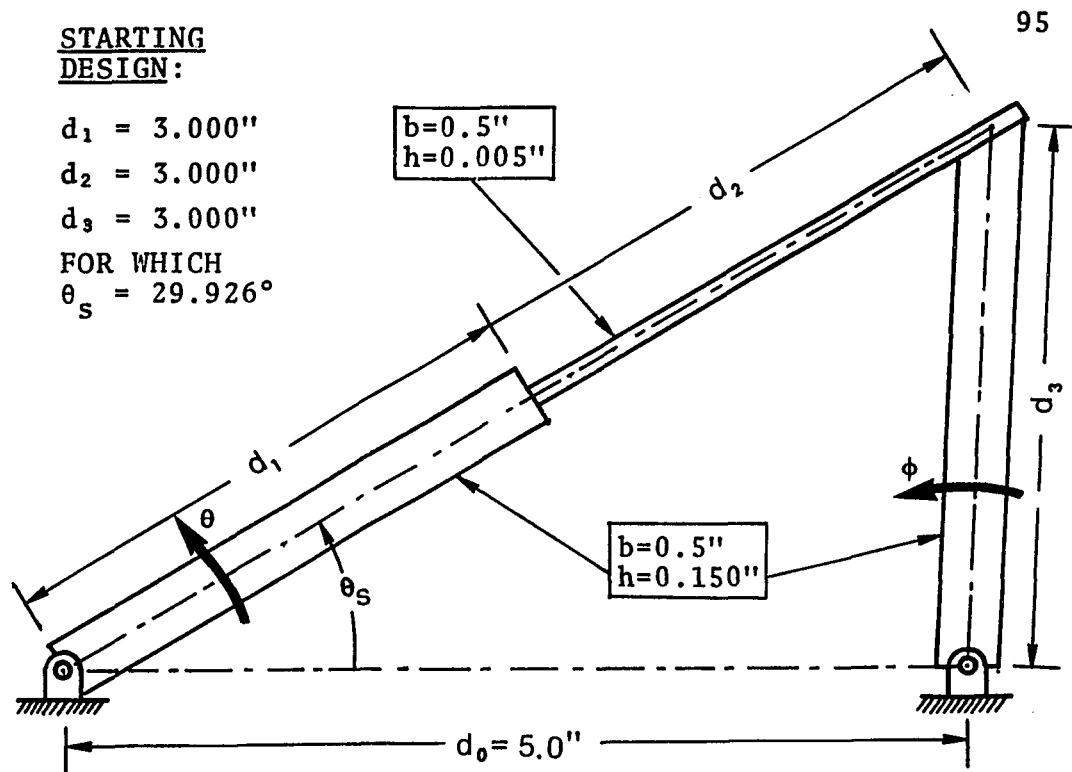


Figure 28. Second Flexible Coupler Mechanism

TABLE 5

OPTIMUM SYNTHESIS OF A SECOND FLEXIBLE COUPLER MECHANISM

q	{d}			θ_s^a	E_A
	d_1	d_2	d_3		
0	3.0000	3.0000	3.0000	29.926	39.0028
1	2.8612	3.0567	3.1224	31.844	14.8834
2	2.5261	2.5754	3.0380	34.987	8.3910

Total Number of Evaluations (j) of $E_A = 17$

a θ_s was determined from:

$$\theta_s = \cos^{-1} \left\{ \frac{(d_1 + d_2)^2 + d_0^2 - d_3^2}{2d_0(d_1 + d_2)} \right\}$$

function, $y=x^2$, $\frac{dy}{dx}$ will be zero or close to zero at $x=0$.

The results of the optimization method are tabulated in Table 5. Table 5 includes only the results of the quadratic interpolation at which the objective function is minimum during each iteration step. The optimization method was terminated after 2 iteration steps during which the objective function E_A , sum of the absolute error at 20 points (s) was reduced from 39.003 to 8.391. The error curves for the starting and the optimum design reached are depicted in Figure 29, which indicates E_A is reduced even though the maximum error is increased. If the flexible coupler mechanism is limited to move 51 degrees for θ (i.e. $x = 0.85$) the maximum error of 0.223 degree results and the sum of the absolute error, E_A will be 1.880 only. This is a reasonable design, unless the motion in the neighborhood of $x=1$ is important.

7.4 Study of the Remaining Design Variables (d_0 , h and b) of the Flexible Link Mechanism

The optimum design of the flexible coupler mechanism of Figure 28 is selected as representative of flexible link mechanisms to study the effect of the remaining design variables.

Even for the case where the input rotation θ was

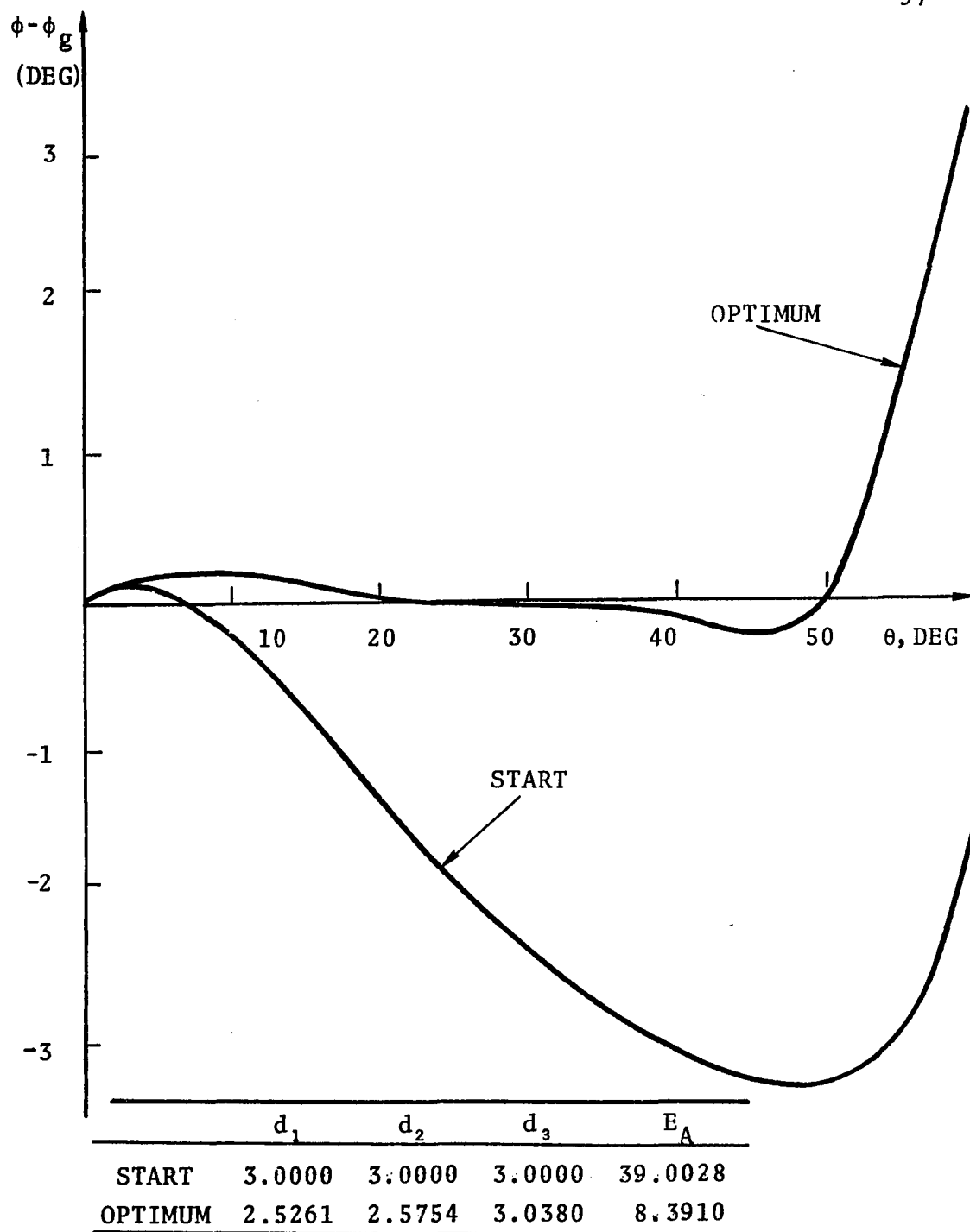


Figure 29. Synthesis of a Second Flexible Coupler Mechanism

limited to 51 degrees only, the bending stress ' σ_b ' in the coupler near the output link reaches 410,773 psi, which is very high, but can be reduced within the elastic limit of the spring steel with help of the remaining parameters.

The flexible coupler mechanism selected for this investigation was analyzed for increase and decrease in length d_o of the fixed length and thickness h of the flexible coupler. The results of this investigation are depicted in Figure 30. For the variation in d_o , it was assumed that the increase or decrease in the size of the linkage was in the same proportion as the length d_o . The results indicate that the bending stresses decrease in the same proportion as the increase in the length of the fixed link d_o , and the decrease in thickness h of the flexible coupler. By decreasing the thickness h of the flexible coupler by 5 times, it will reduce the bending stresses to 82,509 psi, which is within the elastic limit. The variation of the length d_o in Figure 30 was studied with a thickness h of 0.001 inch.

It should be pointed out that for the magnitude of variations of d_o and h as depicted in Figure 30, the functional characteristic between θ and ϕ was not altered significantly. The maximum variation in the objective function E_A was from 1.880 to 2.118 only.

Obviously, the effect of the variation of width b of the flexible coupler will be similar to the thickness h .

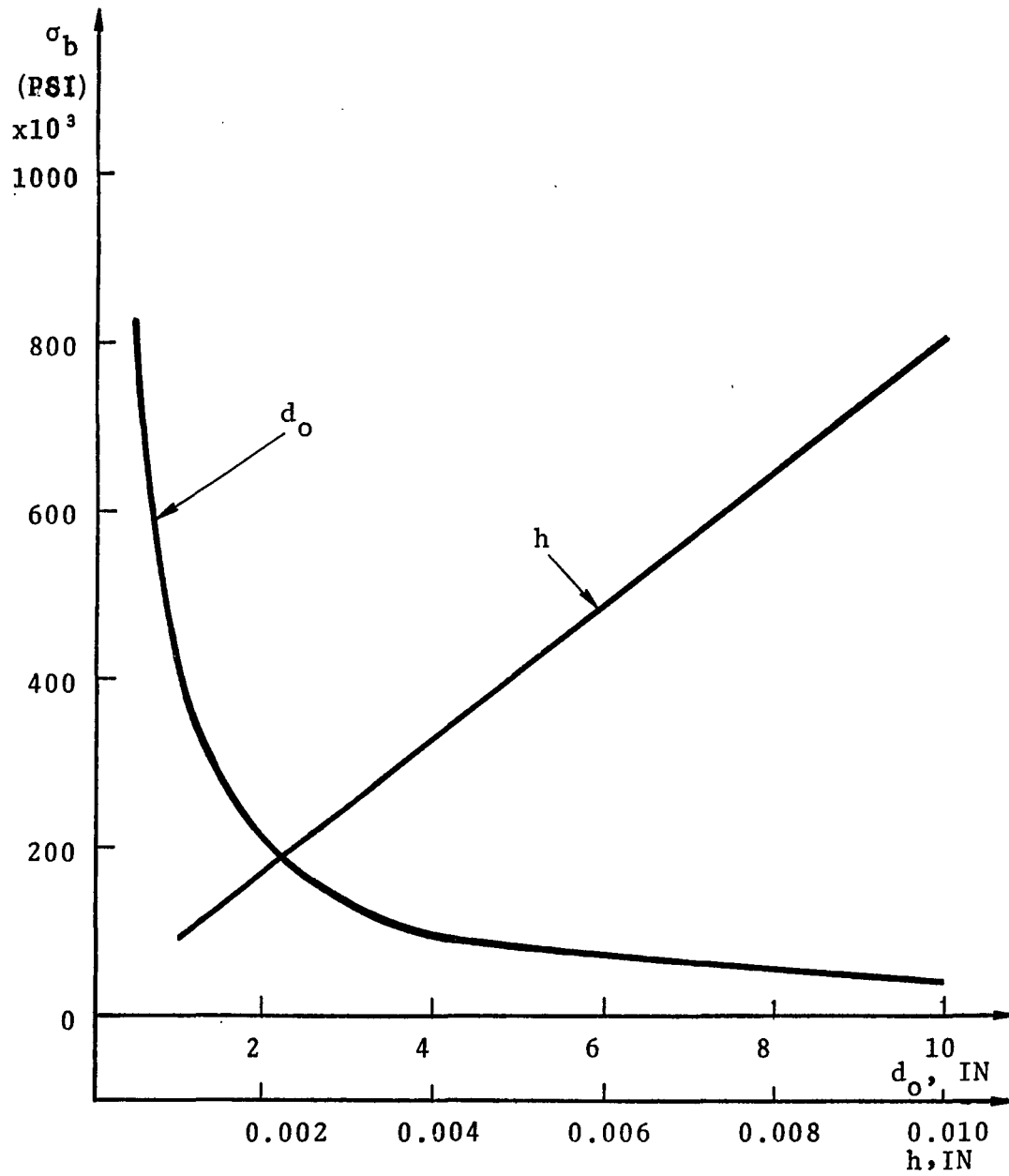


Figure 30. Study of Effects of the Fixed Length d_o and Coupler Thickness h on the Maximum Stress in the Coupler

Therefore, the study for the design variable 'b' was omitted.

7.5 Synthesis of a Flexural Joint Mechanism

The synthesis of a flexural joint mechanism for a function generation problem will now be attempted by the optimization method. The flexural joint linkage as shown in Figure 20 (Chapter 4) is analyzed by the finite element method. A flexural joint linkage as depicted in Figure 31 has two more design variables than a flexible coupler mechanism. The extra two variables come from the fact that besides the length of coupler d_2 , the lengths of two flexural joints d_4 and d_5 are also to be determined.

The starting design for the synthesis of the flexural joint linkage was selected to be the same as the starting design of the flexible coupler mechanism whose dimensions are listed in Table 4 for $j=1$. When this linkage was analyzed it was discovered that a bending stress of 406,448 psi was reached in the flexural joint near the output link. From the conclusion of the previous section, the linkage size was increased by 3 times which reduced the stresses to 135,144 psi. This 3 times increased linkage was the starting design for the optimization method. From an independent study, it was determined that if d_2 was selected as a design variable then, this

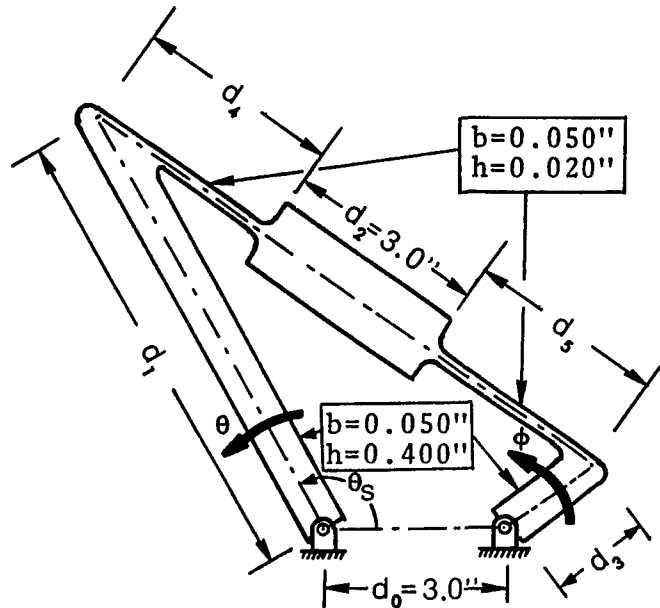


Figure 31. Design Variables for a Flexural Joint Mechanism

TABLE 6

OPTIMUM SYNTHESIS OF A FLEXURAL JOINT MECHANISM

q	{d}					E_A
	d_1	d_4	d_5	d_3	θ_s	
0	7.5701	3.4944	3.4944	1.6678	128.410	6.1339
1	7.5699	3.4945	3.4946	1.6672	128.371	6.0951
2	7.5671	3.4962	3.4965	1.6679	128.298	6.0803
3	3.4836	3.5559	3.5632	1.6508	128.578	4.0213
4	7.2283	3.2117	3.7850	1.5885	130.259	1.6293
5	7.2798	3.1856	3.9169	1.6099	130.117	1.2405

Total Number of Evaluations (j) of $E_A = 60$

would lead to an optimum design in which the length of the rigid coupler d_2 would vanish to zero. Then this would be a flexible coupler mechanism. To avoid the repetition of the design, the length of the rigid coupler d_2 was assumed to be constant at 3.0 inches during the synthesis of the flexural joint linkage.

The results of the optimization by the variable metric method for 5 design variables: d_1 , d_4 , d_5 , d_3 and θ_s , is summarized in Table 6. In 5 iteration steps, the objective function E_A , (accumulated at 15 points 's') was reduced from 6.1339 to 1.2405, for which a total of 60 evaluations (j) of the objective function was required. One more design variable and slower convergence for the first two steps are responsible for these many evaluations of the function. The error curves for the starting design and the optimum design are depicted in Figure 32. For the optimum design, a maximum error of 0.3410 degree (0.505%) resulted at the extreme of the input rotation. The optimized flexural joint mechanism will generate $y=x^2$ for $1 \geq x \geq 0.5$ for which the range of rotation for the input link (θ) is 45 degrees and for the output (ϕ) is 67.5 degrees.

7.6 Common Characteristics of the Results

The variable metric method of optimization produced acceptable results for the synthesis of flexible link

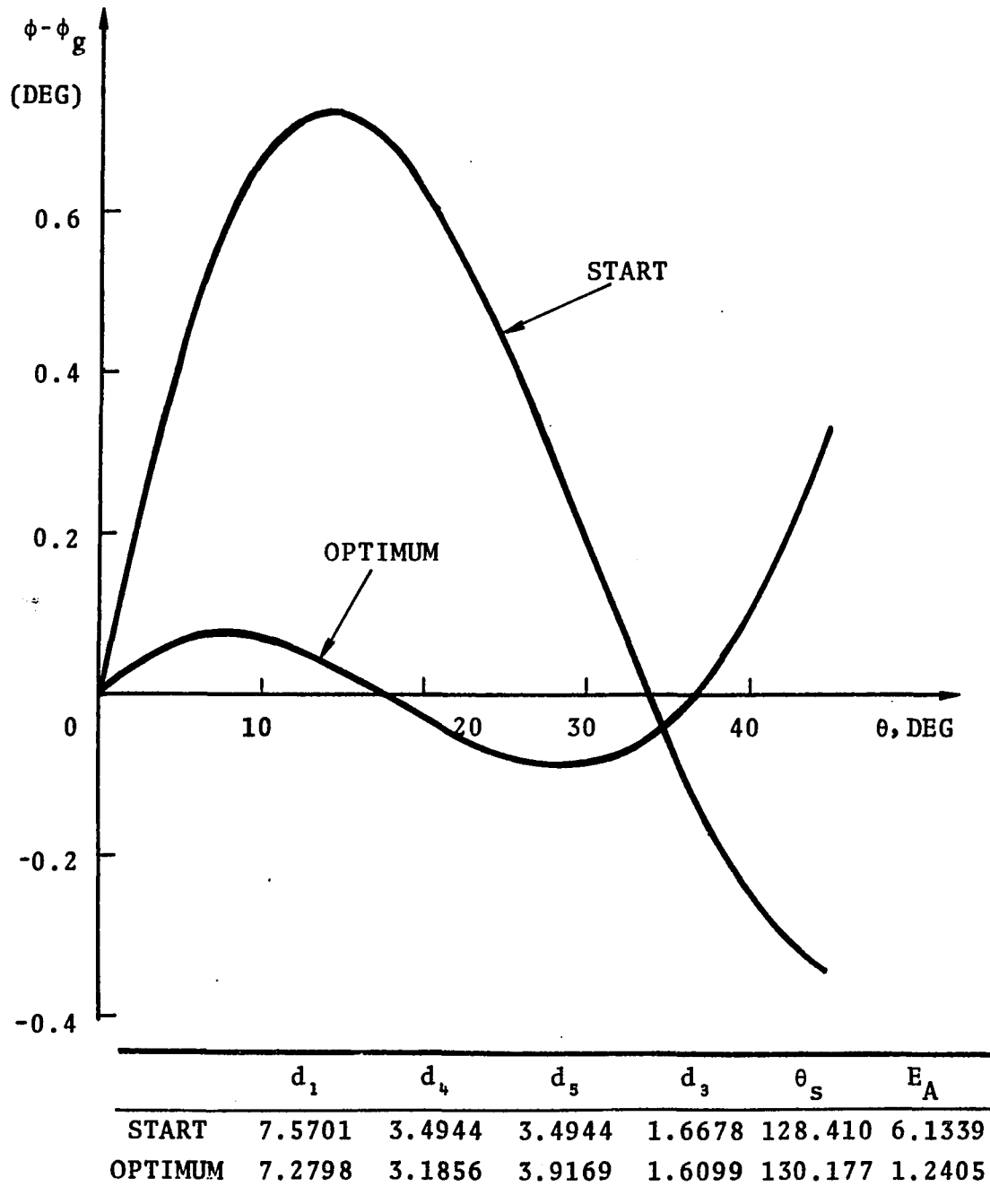


Figure 32. Synthesis of a Flexural Joint Mechanism

mechanisms. This method is very powerful which, in these cases, reduced the magnitude of the objective function (error) by at least 3 or more within 3 iteration steps.

Some common characteristics of the results are as follows:

- A. The number of points 's' at which the error E_A is accumulated can be more than the precision points for the direct method. Thus the sum of the absolute error E_A , can usually be driven to a minimum value, but not to zero by the optimization method.
- B. The results of the optimization method indicate that the sum of the absolute error E_A reaches the magnitude in the neighborhood of 1.2 in two out of three syntheses. It should be expected that any design will reach a plateau of acceptable design and no improvement beyond this is to be expected
- C. The external type of constraint was used during the optimization method. At the beginning of each evaluation of the function, the length of the links were checked to test the viability of the linkage. For a given set of 3 lengths of the links, if the linkage could not be assembled, then a large number was assigned to the objective function E_A and the method was continued.

- D. It can be noticed from Table 4 that after determination of the gradient G_i , the first search point for the quadratic interpolation ($j=6, 14$ and 24) falls far away resulting in a large value for the objective function E_A . This leads to more evaluations of the function for the quadratic interpolation. This was common with the other two synthesis problems too.
- E. The (structural) error curve of the optimum design in Figures (27), (29) and (32) shows clearly that 3 true precision points resulted. More investigation is required if control of the number of true precision points on the error curve is desired.

CHAPTER VIII

CONCLUSION

8.1 Discussion of the Results

In this investigation flexible link mechanisms were analyzed by the finite element method and were synthesized for a function generation problem by the optimization method. From the results, the following conclusions and recommendations have been reached.

The cantilever beam subjected to large deflections was analyzed by the finite element method and the results were within an acceptable degree of accuracy for engineering purposes. This method was also applied to the analysis of various types of flexible link mechanisms with one or two flexible members where the mechanisms were displaced by a linear force or torque. These mechanisms were synthesized to give minimum structural error for the function generation problem by the variable metric method of optimization.

The greatest advantage of the present analysis and synthesis methods is that they are very general. Only the four-bar flexible link mechanism was accounted for in this investigation but a six link mechanism or any complex mechanism with even multiple loads or deflections can be

handled very easily by these methods. With only slight modification of the finite element method, spatial mechanisms can be analyzed or synthesized.

Besides the capabilities of the present method, an added attraction to the designer is that all design information concerning the flexible link mechanism such as the driving torque, the bending stress, and (when extended to cover dynamics) the buckling load, the natural frequencies, etc. can be obtained from this one analysis, which is essential for the completion of the design of the mechanism. Also, the optimization method demands no knowledge of kinematic synthesis and the design obtained will be an optimum under the conditions specified by the designer.

Of the analysis and synthesis methods, the synthesis method has proven to be more accurate. This was best demonstrated by the cantilever beam design of Chapter 6. The optimization method is capable of achieving accurate results but the finite element method imposes limits on it.

Inaccuracies in the finite element method arise from two areas: (1) the formulation of the method and (2) truncation errors. The truncation errors can be improved by using double precision for the computation, while the accuracy of the linear increment method can be improved by including the higher order terms in Equation (12) or reducing the unequilibrated force to zero. The iteration at the end of each selected increment step can

be performed to improve the force equilibrium. These double precision and iteration procedures will increase the computation time which should be justified only if the accuracy is critical.

Inaccuracy also lies in modeling the flexible link mechanisms as was discussed in Chapter 4. The large difference in the thicknesses of the flexible link and the rigid link near the fixed or flexural joint, presents a problem in defining an accurate location of the nodal point. The situation will be more critical if a joint has a fillet at the corner or other design features. A separate detailed investigation for study of joints would be both desirable and significant.

The results of the flexible link mechanism when compared with an "equivalent" pin joint linkage indicated that the flexible linkage performed in a similar manner to the pin joint linkage. Thus the synthesis of the flexible linkage was conducted with the dimensions of the pin joint linkage which possesses minimum (structural) error as the starting design. The optimization method reduced the error of the flexible link mechanism to a level comparable to that of a pin joint linkage. It was noted during the synthesis that a different starting design may lead to a different optimum design. This indicates that the objective function E_A has many minimum points in a

close neighborhood. Depending upon the starting design, a specific local minimum is achieved but the global minimum is unlikely to be achieved. It might be advisable to investigate more than one starting point, in order to find possibly better optima. From a theoretical standpoint, the question of the global minimum is unanswered, but from a practical point of view, it is not relevant. A minimum is achieved and optimum design is obtained without a cut and try approach which is very time consuming for the designer.

8.2 Possibilities for Future Research

The present investigation can be extended in two areas: analysis and synthesis. First, the analysis by the finite element method can be extended to include the compressive load on the links of the flexible link mechanism. Also, the method should be able to predict the post buckling behaviour.

A very valuable investigation would be to analyze a flexible link mechanism subjected to large deflections under dynamic loading. Also, information on the natural frequency would be useful for the application of such a linkage in a vibrational environment.

During the optimization procedure, the analysis was performed many times. An economy in computation time

could be gained by an efficient optimization method but a greater saving can be attained by a faster analysis method. The doors are thus still open to originate a simpler and faster analysis method for the analysis of the flexible link mechanisms.

A very practical extension of the optimization method would be to include design constraints such as limitations on the length of links, locations of the input and output shafts, and limitation on stresses for the synthesis of flexible link mechanisms.

The finite element method for the analysis and the optimization method for the synthesis of flexible link mechanisms are very general in their formulation, thus they hold great promise for a completely automated computer aided design.

APPENDIX A

COMPUTER PROGRAM

```

C
C   THE FOLLOWING IS THE LISTING OF THE COMPUTER
C   PROGRAM FOR THE SYNTHESIS OF THE FLEXIBLE
C   LINK MECHANISM.
C
C   MAIN PROGRAM
C
EXTERNAL FX4BAR
COMMON /SYN/NEVAL, MEVAL
DIMENSION XL(5), DRV(5), EPS(5)
NIT = 10
IW = 3
FO = 0.
N = 5
ETA = 1.E-04
DRV(1) = -0.001
DRV(2) = -0.001
DRV(3) = 0.001
DRV(4) = 0.001
DRV(5) = 0.001
EPS(1) = 0.001
EPS(2) = 0.001
EPS(3) = 0.001
EPS(4) = 0.001
EPS(5) = 0.001
ISTART = 1
NEVAL = 0
MEVAL = 37
CALL DMIN2 (XL,ERSUM, N, FO, EPS, DRV,
1 FX4BAR, ETA, NIT, IW, IC)
PRINT 1011, IC, ERSUM, (XL(I),I=1,5)
1011 FORMAT (1X, I3, 5X, 6I3, 6X, 4E16.6)
END

```

```

C
C      THE SUBROUTINE DMIN2 IS FOR UNCONSTRAINED      113
C      MINIMIZATION OF A FUNCTION.
C      DMIN2 IS BASED ON THE VARIABLE METRIC
C      METHOD OF FLETCHER AND POWELL • WHERE THE
C      GRADIENTS ARE EVALUATED ACCORDING TO AN
C      ALGORITHM BY STEWART.
C
C      SUBROUTINE DMIN2(X0,FO,NN,FMIN,EPS,DRV,
1  EVAL,ETA,NLIN,WRITE,CONV)
C      DIMENSION X0(20),EPS(20),DRV(20),H(20,20),
1  X(20),G(20),G1(20),Y(20),
2  DEL(20),C(20),E(4),EE(4),F(4)
C      LOGICAL IDENT
C      INTEGER CONV,WRITE,COUNT
C
C      INITIALIZE THE PROGRAM
C
C      EM= .1E-10
C      FM= FMIN
C      N= NN
C      ILIN= 0
C      COUNT= 1
C      LOWEST= 1
C      E(1)= 1.
4  CALL EVAL(X0,FO)
C      IF(WRITE.GT.0) PRINT 2000, FO,(X0(I),I=1,N)
C      IF(WRITE.GT.2) PRINT 2007
C      DO 10 I=1,N
C      X(I)= X0(I)
5  X0(I)= X(I)+ DRV(I)
C      CALL EVAL(X0,FG)
C      COUNT= COUNT+ 1
C      IF(WRITE.GT.2) PRINT 2001, FG,(X0(J),J=1,N)
C      IF(FG.NE.FO) GO TO 7
C      DRV(I)= 2.*DRV(I)
C      GO TO 5
7  G(I)= (FG- FO)/DRV(I)
10 X0(I)= X(I)
C
C      SET H EQUAL TO THE IDENTITY MATRIX
C
C      20 IDENT= .TRUE.
C      DO 30 I=1,N
C      DO 25 J=1,N
25 H(I,J)= 0.
C      H(I,I)= 1.
30 C(I)= 1.
C      IF(WRITE.GT.0) PRINT 2002, (G(I),I=1,N)
C      IF(WRITE.GT.0) PRINT 2003, (C(I),I=1,N)
C
C      SET UP FOR A MINIMIZATION ALONG A LINE
C
50 D= 0.

```



```

EP = 1.
EQ = 1.
DO 60 I=1,N
DEL(I) = 0.
DO 55 J=1,N
55 DEL(I) = DEL(I) - H(I,J)*G(J)
IF(DEL(I).EQ.0.) GO TO 60
EP = AMIN1(EP,ABS(EPS(I)/DEL(I)))
EQ = AMIN1(EQ,1.E-7*ABS(X0(I)/DEL(I)))
D = D + G(I)*DEL(I)
60 CONTINUE
EP = .05*EP
IF(D.LT.0.) GO TO 70
IF(.NOT.IDENT) GO TO 20
CONV = 2
GO TO 500
70 IF(F0.LE.FM) FM = -1.E20
E(2) = AMIN1(1.,2.*(FM-F0)/D)
E(2) = AMAX1(E(2),EQ)
100 IF(WRITE.GT.0) PRINT 2004, EP,(DEL(I),I=1,N)
IF(WRITE.GT.0) PRINT 2005, F0,(X0(I),I=1,N)
F(1) = F0
E(1) = 0.
KKK = 0
103 DO 105 I=1,N
105 X(I) = X0(I) + E(2)*DEL(I)
CALL EVAL(X,F(2))
COUNT = COUNT + 1
IF(WRITE.GT.1) PRINT 2001, F(2),E(2)
IF(F(2).NE.F(1)) GO TO 107
E(2) = 2.*E(2)
GO TO 103
107 ED = .5*D*E(2)**2/(D*E(2)+(F(1)-F(2)))
IF(ED.LE.0.) ED = 2.*E(2)
IF(ED.LT.0.001*E(2)) ED = 0.001*E(2)
IF(F(2).LT.F(1)) GO TO 120
E(2) = ED
KKK = KKK + 1
IF(KKK.LT.2) GO TO 103
F(2) = F0
F(3) = F(2)
E(3) = E(2)
E(2) = 0.
E(1) = -E(3)
DO 110 I=1,N
110 X(I) = X0(I) + E(1)*DEL(I)
CALL EVAL(X,F(1))
COUNT = COUNT + 1
IF(WRITE.GT.2) PRINT 2001, F(1),E(1)
GO TO 150
120 LOWEST = 2
IF(ED.GT.3.*E(2)) ED = 3.*E(2)
IF(ABS(E(2)-ED).LT.EP) ED = E(2) + 1.1*EP
IF(ABS(E(2)-ED).LT..03*ABS(E(2))) ED = 1.1*E(2)
DO 130 I=1,N

```

115

```

130 X(I) = XO(I) + ED*DEL(I)
    IF(ED.GT.E(2)) GO TO 140
    E(3) = E(2)
    E(2) = ED
    F(3) = F(2)
    CALL EVAL(X,F(2))
    COUNT = COUNT + 1
    IF(WRITE.GT.1) PRINT 2001, F(2),E(2)
    GO TO 150
140 E(3) = ED
    CALL EVAL(X,F(3))
    COUNT = COUNT + 1
    IF(WRITE.GT.1) PRINT 2001, F(3),E(3)
150 CALL INITPM(E,F,EE,A,0)
160 LOWEST = 1
    DO 165 I=2,3
    IF(F(I).LT.F(LOWEST)) LOWEST = I
165 CONTINUE
    IE = 2. + SIGN(1.,EE(2))
    IF(A.EQ.0.) IE = 2. + SIGN(1.,F(1)-F(2))
    IF(A.LT.0.) IE = 4-IE
    IF(A.LE.0. .OR. ABS(EE(2)).GT.ABS(3.*EE(IE)))
1 EE(2) = 3.*EE(IE)
    EEE = E(2) + EE(2)
    IF(ABS(EEE-E(LOWEST)).LT.EP) GO TO 250
    IF(ABS(EEE-E(LOWEST)).LT..03*ABS(E(LOWEST)))
1 GO TO 250
    IF(EE(IE).LT.EE(2)) IE = IE + 1
    IF(IE.EQ.4) GO TO 180
    DO 170 LL=IE,3
    L = 3-LL+IE
    E(L+1) = E(L)
170 F(L+1) = F(L)
180 E(IE) = EEE
    DO 190 I=1,N
190 X(I) = XO(I) + EEE*DEL(I)
    CALL EVAL(X,F(IE))
    COUNT = COUNT + 1
    IF(WRITE.GT.1) PRINT 2001, F(IE),E(IE)
    IF(IE.EQ.1) GO TO 150
    KKK = 1
    IF(IE.EQ.4) GO TO 220
    IF(F(1).GT.F(4)) GO TO 200
    CALL INITPM(E,F,EE,A,0)
    IF(E(2)+EE(2).LT.E(4) .AND. A.GT.0.) GO TO 160
    GO TO 210
200 KKK = 2
    CALL INITPM(E,F,EE,A,1)
    IF(E(3)+EE(2).GT.E(1) .AND. A.GT.0.) GO TO 220
210 KKK = 1
    IF(F(2).LT.F(1) .AND. F(2).LE.F(3) .OR.
1 F(2).LE.F(1) .AND. F(2).LT.F(3)) GO TO 150
220 DO 230 I=1,3
    E(I) = E(I+1)
230 F(I) = F(I+1)

```

```

      GO TO (150,160),KKK
C
C      END OF MINIMIZATION ALONG DEL
C
250 IF(WRITE.GT.0) PRINT 2005, F(LOWEST),E(LOWEST)
    IF(WRITE.GT.0) PRINT 2006, COUNT
C
C      IF THERE WAS NO MOTION, RETURN.
C
      IF(E(LOWEST).NE.0.) GO TO 260
      CONV = 3
      GO TO 500
C
C      IF THE FUNCTION VALUE WAS NOT CHANGED, RETURN.
C
260 IF(F(LOWEST).NE.F0) GO TO 270
      CONV = 4
      GO TO 500
C
C      TEST FOR CONVERGENCE
C
270 F0 = F(LOWEST)
      CONV = 1
      ETEST = AMAX1(1.,ABS(E(LOWEST)))
      DO 280 I=1,N
        IF(ABS(ETEST*DEL(I)).GT.ABS(EPS(I))) CONV = 0
        DEL(I) = E(LOWEST)*DEL(I)
        X0(I) = X0(I) + DEL(I)
280 G1(I) = G(I)
        IF(CONV.EQ.1) GO TO 500
C
C      IF THERE HAVE BEEN TOO MANY MINIMIZATIONS
C      ALONG A LINE, RETURN.
C
      ILIN = ILIN + 1
      CONV = 5
      IF(ILIN.GE.NLIN) GO TO 500
C
C      CALCULATE A NEW GRADIENT
C
      IF(WRITE.GT.2) PRINT 2007
      DO 300 I=1,N
        X(I) = X0(I)
        IF(F0.EQ.0.) GO TO 285
        IF(IDENT) GO TO 285
        IF(G(I).EQ.0.) GO TO 285
        ETAM = AMAX1(ETA,ABS(1.E-8*G(I)*X0(I)/F0))
        IF(G(I)**2.GT.C(I)*ABS(F0)*ETAM) GO TO 282
        DRV(I) = 2.*(ABS(F0)*ABS(G(I))*ETAM/C(I)**2)
        1***33333333
        DRV(I) = DRV(I)*(1. - ABS(G(I))/(1.5*C(I)*
        1DRV(I) + 2.*ABS(G(I))))
        GO TO 283
282 DRV(I) = 2.*SQRT(ETAM*ABS(F0)/C(I))
      DRV(I) = DRV(I)*(1.-C(I)*DRV(I)/(3.*C(I)*

```

```

1DRV(I)+4.*ABS(G(I)))
283 DRV(I) = SIGN(DRV(I),G(I))
IF(.5*ABS(C(I)*DRV(I)/G(I)) .GT. .01) GO TO 295
285 XO(I) = X(I) + DRV(I)
CALL EVAL(XO,FG)
COUNT = COUNT + 1
IF(FG.NE.FO) GO TO 290
IF(WRITE.GT.2) PRINT 2001, FG,(XO(J),J=1,N)
DRV(I) = 2.*DRV(I)
GO TO 285
290 G(I) = (FG - FO)/DRV(I)
GO TO 300
295 DRV(I) = 100.*ABS(FO*ETAM/G(I))
DRV(I) = ABS(G(I)) + SQRT(G(I)**2 + 200.*
1ABS(FO)*C(I)*ETAM)
DRV(I) = 100.*ABS(FO)*ETAM/DRV(I)
XO(I) = X(I) + DRV(I)
CALL EVAL(XO,FP)
COUNT = COUNT + 1
IF(WRITE.GT.2) PRINT 2001, FP,(XO(J),J=1,N)
XO(I) = X(I) - DRV(I)
CALL EVAL(XO,FMI)
COUNT = COUNT + 1
IF(WRITE.GT.2) PRINT 2001, FMI,(XO(J),J=1,N)
G(I) = .5*(FP-FMI)/DRV(I)
300 XO(I) = X(I)
C
C IF THE MINIMUM WAS FOUND ALONG -DEL,
C GO SET H EQUAL TO C INVERSE
C
IF(E(LOWEST).LT.0.) GO TO 20
C
C MODIFY H AND GO BACK FOR ANOTHER ITERATION
C
IDENT = .FALSE.
A = 0.
DO 310 I=1,N
Y(I) = G(I) - G1(I)
310 A = A + Y(I)*DEL(I)
IF(WRITE.GT.0) PRINT 2002, (G(I),I=1,N)
AA = A/E(LOWEST)
C1 = 1./A - D/AA**2
C2 = 2./AA
B = 0.
DO 330 I=1,N
C(I) = C(I) + C1*Y(I)**2 + C2*Y(I)*G1(I)
X(I) = 0.
DO 320 J=1,N
320 X(I) = X(I) + H(I,J)*Y(J)
330 B = B - X(I)*Y(I)
IF(WRITE.GT.0) PRINT 2003, (C(I),I=1,N)
DO 340 I=1,N
IF(C(I).LE.0.) GO TO 20
DO 340 J=I,N
H(I,J) = H(I,J) + DEL(I)*DEL(J)/A + X(I)*X(J)/B

```

```

340 H(J,I) = H(I,J)
    PRINT 2002, ((H(I,J), J=1,N), I=1,N)
    PRINT 2005, F0, (X0(I), I=1,N)
    PRINT 2007
    GO TO 50
C
C
C    RETURN
500 IF(WRITE.GT.0) PRINT 2005, F0, (X0(I), I=1,N)
    IF(WRITE.GT.0) PRINT 2006, CONV
    RETURN
C
C
2000 FORMAT(3H1 *1PE15.7,2X,6E15.7/(3H 17X,6E15.7))
2001 FORMAT(3H *1PE15.7,2X,6E15.7/(3H 17X,6E15.7))
2002 FORMAT(3H0 G17X,1P6E15.7/(3H 17X,6E15.7))
2003 FORMAT(3H C17X,1P6E15.7/(3H 17X,6E15.7))
2004 FORMAT(3H D1PE15.7,2X,6E15.7/(3H 17X,6E15.7))
2005 FORMAT(3H F1PE15.7,2X,6E15.7/(3H 17X,6E15.7))
2006 FORMAT(1H I5)
2007 FORMAT(1H )
3000 FORMAT (5E15.7)
3010 FORMAT (I3)
3011 FORMAT (1X, I3)
    END

```

```

SUBROUTINE INITPM(E,F,EE,A,I)
C
C    THE SUBROUTINE INITPM IS FOR THE QUADRATIC
C    INTERPOLATION
C
    DIMENSION E(1),F(1),EE(1)
    EE(1) = E(I+1) - E(I+2)
    EE(3) = E(I+3) - E(I+2)
    DF1 = EE(1)*(F(I+3) - F(I+2))
    DF3 = EE(3)*(F(I+1) - F(I+2))
    EE(2) = .5*(EE(1)*DF1-EE(3)*DF3)/(DF1-DF3)
    A = (DF3-DF1)*SIGN(1.,EE(1))*SIGN(1.,EE(3))*
1 SIGN(1.,EE(1)-EE(3))
    RETURN
    END

```

```

C      THE SUBROUTINE FX4BAR IS FOR THE ANALYSIS
C      OF A FLEXIBLE LINK MECHANISM SUBJECTED TO
C      LARGE(NONLINEAR) STATIC DEFLECTIONS.
C      THE ANALYSIS IS BY THE FINITE ELEMENT METHOD
C      WITH LINEAR INCREMENTAL PROCEDURE
C
      SUBROUTINE FX4BAR (XL, ERSUM)
      COMMON /SYN/ NEVAL, MEVAL
      COMMON      KB(6,15), EL(15), EAL(15), AF(15),
1PT(2,15), EKT(6,90), BST(15), AST(15),
2EB(15), EH(15), ALK(3), TLK(3), LLK(10),
3EALD(15), DQ(48), DP(48), LV(48), MV(48),
4SK(20,20), ADQ(48), EK(6,6), ET(6,6), RK(6,6),
5RT(6,6), TR(6,6), EF(6), TE(6), DEL(6)
      DIMENSION SK11(19,19), SK12(19), TRF(19)
      DIMENSION XL(1)
      EQUIVALENCE (SK,SK11)
1001 FORMAT (39H1LARGE DEFLECTION BY LINEAR INCREMENTAL
140H PROCEDURE - FLEXIBLE FOUR-BAR LINKAGE
2//, 11H INPUT DATA/)
1002 FORMAT (4H LNE 12X 4H KB 18X 4H EL 12X
14H EB 12X 4H EH /)
1003 FORMAT ( 9H1OUTPUT -//5H STEP 18X 4HTH2 12X
14HTH4 12X 4HT2 12X
240HX AND Y COORDINATES OF THE NODAL POINTS //)
1010 FORMAT (I2,8X,6I3,2X,3F15.8)
1011 FORMAT (1X, I3, 5X, 6I3, 6X, 4E16.6)
1020 FORMAT (5F15.5)
1021 FORMAT (1X, 6E16.6)
1031 FORMAT (1X, I3, 13X, 6E16.6/(17X,6E16.6))
1032 FORMAT (1X, I3, 13X, 6I16 /(17X, 6I16))
1040 FORMAT (10A1)
1041 FORMAT (1X, 10A1)
1050 FORMAT (//)
1052 FORMAT (/)
1060 FORMAT (I2, 8X, 10I3)
1061 FORMAT (1X, I3, 5X, 10I3)
      PI = 3.141592654
      DTR = PI/180.
      RTD = 1./DTR
      PRINT 1001
      IF (NEVAL .GT. 0) GO TO 22
      PRINT 1050
C      READ AND PRINT INPUT DATA
      READ 1010, NE
      PRINT 1011, NE
      READ 1010, JE, NS, NLD, NST, NMP, NKD, NPS
      PRINT 1011, JE, NS, NLD, NST, NMP, NKD, NPS
      READ 1020, A1, TH4AD, TH2SD, THMD, THID, E
      PRINT 1021, A1, TH4AD, TH2SD, THMD, THID, E
      READ 1020, XS, XF, YS, YF, DTHD, DPHID
      PRINT 1021, XS, XF, YS, YF, DTHD, DPHID
      READ 1060, JE, (LLK(I), I=1,10)

```

120

```

PRINT 1061, JE, (LLK(I), I=1,10)
DX = XF - XS
DY = YF - YS
PRINT 1002
DO 10 J = 1, NE
  READ 1010, JE, (KB(I, JE), I = 1,6),
1EL(JE), EB(JE), EH(JE)
  PRINT 1011, JE, (KB(I, JE), I = 1,6),
1EL(JE), EB(JE), EH(JE)
10 CONTINUE
PRINT 1050
NSMK = NS - NKD
NSMB = NS - NKD + 1
NSM1 = NS - 1
NSM2 = NS - 2
NDSX = 0
NDSY = 0
TH4A = TH4AD*DTR
TH2S = TH2SD*DTR
DO 21 II = 1,5
  J = II + II - 1
  K = LLK(J)
  L = LLK(J+1)
  XL(II) = 0.
  DO 20 I = K, L
20 XL(II) = XL(II) + EL(I)
21 CONTINUE
ALK(1) = XL(1)
ALK(2) = XL(2) + XL(3) + XL(4)
ALK(3) = XL(5)
CEL4 = XL(3)
XL(3) = XL(4)
XL(4) = XL(5)
XL(5) = TH2S
A2 = ALK(1)
A3 = ALK(2)
A4 = ALK(3)
22 NEVAL = NEVAL + 1
IF (NEVAL .GT. MEVAL) STOP
IZPLOT = 0
IPIC = 0
INPS = 1
SQSUM = 0.
ERSUM = 0.
ERMAX = 0.
BSTMAX = 0.
ASTMAX = 0.
BSTEX = 0.
A2 = XL(1)
A3 = XL(2) + CEL4 + XL(3)
A4 = XL(4)
TH2S = XL(5)
AA5 = TH2S
IF (AA5 .GT. PI) AA5 = PI + PI - TH2S
A5 = SQRT (A1*A1 + A2*A2 - 2.*A1*A2*COS(AA5))

```

```

IF (A3 .GT. ABS(A5 - A4)) GO TO 23
GO TO 523
23 IF (A3 .LT. (A5 + A4)) GO TO 24
523 ERSUM = 10.E 10
PRINT 1021, A5
GO TO 410
24 CONTINUE
IFL = 0
CALL A4BAR (A1, A2, A3, A4, TH2S, TH3, TH4,
10., VA3, VA4, 0., AA3, AA4, TH4A, IFL)
25 TLK(1) = TH2S
TLK(2) = TH3
TLK(3) = TH4 + PI
IJ = 0
IK = 0
DO 30 II = 1, 5
J = II + II - 1
K = LLK(J)
L = LLK(J+1)
VNE = L - K + 1
IF (II .EQ. 3) GO TO 26
IJ = IJ + 1
SL = XL(IJ)/VNE
GO TO 27
26 SL = CEL4
27 IF (II .EQ. 3 .OR. II .EQ. 4) GO TO 528
IK = IK + 1
528 DELX = COS(TLK(IK))
DELY = SIN(TLK(IK))
DO 29 I = K, L
EL(I) = SL
EAL(I) = TLK(IK)
EALD(I) = EAL(I)*RTD
IF (I .EQ. 1) GO TO 28
PT(1, I) = PT(1, I-1) + EL(I)*DELX
PT(2, I) = PT(2, I-1) + EL(I)*DELY
GO TO 29
28 PT(1, I) = EL(I)*DELX
PT(2, I) = EL(I)*DELY
29 CONTINUE
30 CONTINUE
DO 32 J = 1, NE
AF(J) = 0.
BST(J) = 0.
32 AST(J) = 0.
PRINT 1011, NS, NSMK, NDSX, NDSY, NSM1, NSMB
TH3D = TH3*RTD
TH4D = TH4*RTD
TH2SD = TH2S*RTD
PHISD = TH4D
THSD = TH2SD
PRINT 1021, A2, A3, A4, TH3D, TH4D, (EALD(I),
11 = 1, NE), (PT(1, I), PT(2, I), I = 1, NE)
PRINT 1021, (XL(I), I=1, 5), (EL(I),
11 = 1, NE), PHISD, THSD, A5

```



```

PRINT 1003
DO 35 I = 1, NS
  DQ(I) = 0.
  DP(I) = 0.
35 ADQ(I) = 0.
  ISTEP = 0
  FIX = 0.
  FIY = 0.
  FIM = 0.
  DSXC = 0.
  DSYC = 0.
  DELM = 1.0
  DELMC = 1.25
  IPHASE = 1
  IFD = 1
  DQ(NLD) = THID*DTR
  ND = NKD
  MD = NS - ND
  TI = TH2S
  TO = TH4
  ISW = 1717
C  STIFFNESS (EK) AND INITIAL STRESS (ET) MATRICES
C  FOR INDIVIDUAL BEAM ELEMENT AND FORMATION
C  OF SYSTEM STIFFNESS MATRIX -SK
41 N = 0
  ISTEP = ISTEP + 1
  IF (DSXC .GE. THMD) GO TO 400
43 DO 44 I = 1, NS
  DO 44 J = 1, NS
44 SK(I,J) = 0.
  DO 130 LNE = 1, NE
    CALL TRET (TR, EAL(LNE))
    CALL BEMREK (EB(LNE), EH(LNE), EL(LNE), E, EK)
    CALL BEMRET (EL(LNE), AF(LNE), ET)
115 DO 120 I = 1, 6
  DO 120 J = 1, 6
    JJ = N + J
120 EKT(I,JJ) = EK(I,J) + ET(I,J)
    N = N + 6
    CALL BTAB (EK, TR, RK, 6, 6)
    CALL BTAB (ET, TR, RT, 6, 6)
    DO 125 K = 1, 6
      IF (KB(K, LNE) .EQ. 0) GO TO 125
121 I = KB(K, LNE)
      DO 124 L = 1, 6
        IF (KB(L, LNE) .EQ. 0) GO TO 124
123 J = KB(L, LNE)
        SK(I,J) = SK(I,J) + RK(K,L) + RT(K,L)
124 CONTINUE
125 CONTINUE
130 CONTINUE
C  CALCULATIONS FOR THE NODAL FORCES AND
C  REMAINING NODAL DISPLACEMENTS
  CALL FORDIS (SK, SK11, SK12, SK22, TRK, TRF,
1 LV, MV, NS, ND, MD, ISW, DQ, DP, IFD, DETR)

```

123

```

150 DO 160 I=1,NS
160 ADQ(I) = ADQ(I) + DQ(I)
    PRINT 1031, ISTEP, (DQ(I), I=1,NS), (ADQ(I),
1 I=1,NS), DETR, DP(NLD), TRK
C   CALCULATIONS FOR DISPLACEMENTS AND FORCES
C   FOR THE BEAM ELEMENTS
    L = 0
    N = 1
    DO 300 LNE = 1, NE
    DO 250 I = 1, 6
    IF (KB(I, LNE) .EQ. 0) GO TO 220
    J = KB(I, LNE)
    TE(I) = DQ(J)
    GO TO 250
220 TE(I) = 0.
250 CONTINUE
    B = EB(LNE)
    H = EH(LNE)
    CALL TRET5 (TR, EAL(LNE))
    CALL MPLY (TR, TE, DEL, 6, 6, 1)
    CALL MPLY (EKT(1,N), DEL, EF, 6, 6, 1)
    AF(LNE) = AF(LNE) + EF(6)
    N = N + 6
    IF (LNE .NE. 2) GO TO 253
    BSTEX = BSTEX + 6.*EF(2)/(B*H*H)
    IF (ABS(BSTMAX) .LT. ABS(BSTEX)) BSTMAX = BSTEX
253 CONTINUE
    BST(LNE) = BST(LNE) + 6.*EF(4)/(B*H*H)
    AST(LNE) = AST(LNE) + EF(6)/(B*H)
    IF (ABS(BSTMAX) .LT. ABS(BST(LNE))) BSTMAX =
1 BST(LNE)
    IF (ABS(ASTMAX) .LT. ABS(AST(LNE))) ASTMAX =
1 AST(LNE)
C   SLOPE AND LENGTH OF THE BEAM ELEMENTS
    I = LNE
    IF (I .GE. NE) GO TO 255
    PT(1, I) = PT(1, I) + DQ(L+1)
    PT(2, I) = PT(2, I) + DQ(L+2)
    L = L + 3
255 IF (I .GT. 1) GO TO 260
    DELX = PT(1,1)
    DELY = PT(2,1)
    GO TO 265
260 DELX = PT(1, I) - PT(1, I-1)
    DELY = PT(2, I) - PT(2, I-1)
265 CONTINUE
    DELEL = DEL(6) - DEL(5)
    EL(I) = EL(I) + DELEL
    EAL(I) = ATAN2 (DELY, DELX)
    ALD = EAL(I)*RTD
300 CONTINUE
    FIX = FIX + DP(NLD)
    DSXC = DSXC + DQ(NLD)*RTD
    DSYC = DSYC + DQ(NMP)*RTD
    TI = TI + DQ(NLD)

```

```

      TO = TO + DQ(NMP)
      TID = TI *RTD
      TOD = TO *RTD
      PRINT 1031, ISTEP, DSXC, DSYC, TID, TOD,
1 FIX, FIY, FIM,
2(PT(1,I), PT(2, I), I = 1, NE),BSTMAX,ASTMAX
      THD = TID
      PHID = TOD
      X = XS + (THD - THSD)/DTHD*DX
      Y = X*X
      PHIDD = PHID + (Y -YS)/DY*DPHID
      ERR = PHIDD - PHID
      AERR = ABS(ERR)
      ERSUM = ERSUM + AERR
      SQSUM = SQSUM + ERR*ERR
      IF (ERMAX .LT. AERR) ERMX = AERR
      PRINT 1031, ISTEP, THD, PHID, X, Y, PHIDD,
1 ERR, ERSUM, ERMX, SQSUM
      PRINT 1050
      GO TO 41
400 CONTINUE
410 SSTEP = ISTEP - 1
      ERRMS = SQRT(SQSUM/SSTEP)
      PRINT 1031, NEVAL, (XL(I), I=1,5), ERSUM,
1 ERMX, SQSUM, ERRMS
      RETURN
      END

```

SUBROUTINE FORDIS (SK, SFA, SFB, SFC, RK, 125
1 TRF, LV, MV, NS, ND, MD, ISW, Q, P, IFL, DETR)

C
C
C
C
C

THE SUBROUTINE FORDIS IS FOR THE SOLUTION
OF EQUATION, $P = (K) \cdot Q$, FOR FORCE OR
DISPLACEMENT INPUT.

DIMENSION SK(NS,NS), SFA(MD,MD), SFB(MD,ND),
1 SFC(ND,ND), RK(ND,ND), TRF(MD,ND)
DIMENSION Q(1), P(1), LV(1), MV(1), ISW(1)
NB = NS - ND + 1
DO 100 I = 1, ND
K = ISW(I)/100
L = ISW(I) - K*100
IF (K .EQ. L) GO TO 100
CALL SWAP (SK, NS, NS, K, L)
TEMP = Q(K)
Q(K) = Q(L)
Q(L) = TEMP
TEMP = P(K)
P(K) = P(L)
P(L) = TEMP
100 CONTINUE
130 DO 138 J = 1, ND
L = MD + J
DO 135 I = 1, ND
K = MD + I
135 SFC(I,J) = SK(K,L)
DO 138 I = 1, MD
138 SFB(I,J) = SK(I,L)
DO 140 J = 1, MD
DO 140 I = 1, MD
140 SFA(I,J) = SK(I,J)
CALL MATINV (SFA, MD, DETR, LV, MV)
CALL MPLY (SFA, SFB, TRF, MD, MD, ND)
CALL BTAB (SFA, SFB, RK, MD, ND)
DO 148 I = 1, ND
DO 148 J = 1, ND
148 RK(I,J) = SFC(I,J) - RK(I,J)
IF (IFL .GT. 0) GO TO 160
RK(1,1) = 1./RK(1,1)
CALL MPLY (RK, P(NB), Q(NB), ND, ND, 1)
GO TO 170
160 CALL MPLY (RK, Q(NB), P(NB), ND, ND, 1)
170 CALL MPLY (TRF, Q(NB), Q, MD, ND, 1)
DO 180 I = 1, MD
180 Q(I) = -Q(I)
DO 300 I = 1, ND
K = ISW(I)/100
L = ISW(I) - K*100
IF (K .EQ. L) GO TO 300
TEMP = Q(K)
Q(K) = Q(L)
Q(L) = TEMP

```
      TEMP = P(K)  
      P(K) = P(L)  
      P(L) = TEMP  
300  CONTINUE  
      RETURN  
      END
```

```

C      SUBROUTINE BEMREK(B,H,EL,E,EK)
C
C      ELASTIC STIFFNESS MATRIX OF A BEAM ELEMENT
C      B - WIDTH OF BEAM CROSS SECTION
C      H - HEIGHT OF BEAM CROSS SECTION
C      EL - LENGTH OF BEAM ELEMENT
C      E - MODULUS OF ELASTICITY
C      EK - OUTPUT STIFFNESS MATRIX OF ORDER (6,6)
C
      DIMENSION EK(6,6)
      CF=E*B*H*H*H/(6.0*EL)
      EK(1,1)=6.0*CF/(EL*EL)
      EK(2,1)= 3.0*CF/EL
      EK(3,1)=-6.0*CF/(EL*EL)
      EK(4,1)= 3.0*CF/EL
      EK(2,2)=2.0*CF
      EK(3,2)=-3.0*CF/EL
      EK(4,2)=CF
      EK(3,3)=6.0*CF/(EL*EL)
      EK(4,3)=-3.0*CF/EL
      EK(4,4)=2.0*CF
      EK(5,5)=E*B*H/EL
      EK(6,5)=-E*B*H/EL
      EK(6,6)=E*B*H/EL
      DO 10 I=5,6
      DO 10 J=1,4
10  EK(I,J)=0.0
      DO 20 I=1,6
      DO 20 J=I,6
20  EK(I,J)=EK(J,I)
      RETURN
      END

```

```

C
C
C
C
      SUBROUTINE BEMRET (EL, P, ET)
      INITIAL STRESS STIFFNESS MATRIX OF A BEAM
      ELEMENT
      DIMENSION ET(6,6), A(4,4)
      CALL MINBEM (EL, P, A)
      DO 10 I = 1, 4
      DO 10 J = 1, 4
10    ET(I,J) = A(I,J)
      DO 20 I = 5, 6
      DO 20 J = 1, 6
      ET(I,J) = 0.
20    ET(J,I) = 0.
      RETURN
      END

```

```

      SUBROUTINE MINBEM (EL, CA, A)
      DIMENSION A(4, 4)
      CF = .1*CA
      CFT = CF
      A(2,1) = CFT
      A(4,1) = CFT
      A(3,2) = -CFT
      A(4,3) = -CFT
      CFT = 12.*CF/EL
      A(1,1) = CFT
      A(3,1) = -CFT
      A(3,3) = CFT
      CFT = .3333333333333*CF*EL
      A(4,2) = -CFT
      CFT = 4.*CFT
      A(2,2) = CFT
      A(4,4) = CFT
      DO 10 J = 1, 3
      JJ = J + 1
      DO 10 I = JJ, 4
10    A(J, I) = A(I, J)
      RETURN
      END

```

```
      SUBROUTINE TRETS (T, AL)
C
C      THIS SUBROUTINE GIVES THE COORDINATE
C      TRANSFORMATION MATRIX
C
      DIMENSION T(6, 6)
      NEM = 6
      SINB = SIN(AL)
      COSB = COS(AL)
      DO 10 I=1,NEM
      DO 10 J=1,NEM
10  T(I,J)=0.0
      T(1,1)=COSB
      T(5,1)=SINB
      T(2,2)= 1.0
      T(3,3)=COSB
      T(6,3)=SINB
      T(4,4)= 1.0
      T(1,5)=-SINB
      T(5,5)=COSB
      T(3,6)=-SINB
      T(6,6)=COSB
      RETURN
      END
```



```

      SUBROUTINE BTAB(A,BETA,R,M,N)
C     THIS SUBROUTINE COMPUTES BETA TRANSPOSE * A *
C     BETA, RESULT IS STORED IN R.
C     A = INPUT MATRIX OF ORDER M X M.
C     BETA = INPUT MATRIX OF ORDER M X N.
C     R = OUTPUT MATRIX OF ORDER N X N.
      DIMENSION A(M,M),BETA(M,N),R(N,N)
      DO 40 I=1,N
      DO 30 J=1,N
      DY=0.0
      DO 20 K=1,M
      IF(BETA(K,I).EQ.0.0) GO TO 20
      CY=0.0
      DO 10 L=1,M
      IF(BETA(L,J).EQ.0.0) GO TO 10
      CY=CY+A(K,L)*BETA(L,J)
10    CONTINUE
      DY=DY+CY*BETA(K,I)
20    CONTINUE
      R(I,J)=DY
30    CONTINUE
40    CONTINUE
      RETURN
      END

```

SUBROUTINE MATINV(A,N,D,L,M)

131

C
 C THE STORE MODE OF MATRIX A MUST BE GENERAL.
 C THIS SUBROUTINE INVERSES A MATRIX.
 C A=INPUT MATRIX, DESTROYED IN COMPUTATION
 C AND REPLACED BY ITS INVERSE.
 C N=ORDER OF MATRIX A
 C D=RESULTANT DETERMINANT
 C L=WORK VECTOR OF LENGTH N
 C M=WORK VECTOR OF LENGTH N
 C

```

    DIMENSION A(1),L(1),M(1)
    D=1.0
    NK=-N
    DO 80 K=1,N
      NK=NK+N
      L(K)=K
      M(K)=K
      KK=NK+K
      BIGA=A(KK)
      DO 20 J=K,N
        IZ=N*(J-1)
        DO 20 I=K,N
          IJ=IZ+I
10      IF ( ABS(BIGA)- ABS(A(IJ))) 15,20,20
15      BIGA=A(IJ)
          L(K)=I
          M(K)=J
20      CONTINUE
          J=L(K)
          IF (J=K) 35,35,25
25      KI=K-N
          DO 30 I=1,N
            KI=KI+N
            HOLD=-A(KI)
            JI=KI-K+J
            A(KI)=A(JI)
30      A(JI)=HOLD
35      I=M(K)
          IF (I=K) 45,45,38
38      JP=N*(I-1)
          DO 40 J=1,N
            JK=NK+J
            JI=JP+J
            HOLD=-A(JK)
            A(JK)=A(JI)
40      A(JI)=HOLD
45      IF (BIGA) 48,46,48
46      D=0.0
          RETURN
48      DO 55 I=1,N
        IF (I=K) 50,55,50
50      IK=NK+I
        A(IK)=A(IK)/(-BIGA)
  
```

```

55 CONTINUE
   DO 65 I=1,N
     IK=NK+I
     HOLD=A(IK)
     IJ=I-N
     DO 65 J=1,N
       IJ=IJ+N
       IF(I-K) 60,65,60
60    IF(J-K) 62,65,62
62    KJ=IJ-I+K
       A(IJ)=HOLD*A(KJ)+A(IJ)
65 CONTINUE
       KJ=K-N
       DO 75 J=1,N
         KJ=KJ+N
         IF (J-K) 70,75,70
70    A(KJ)=A(KJ)/BIGA
75 CONTINUE
       D=D*BIGA
       A(KK)=1.0/BIGA
80 CONTINUE
       K=N
100 K=K-1
       IF (K) 150,150,105
105 I=L(K)
       IF (I-K) 120,120,108
108 JQ=N*(K-1)
       JR=N*(I-1)
       DO 110 J=1,N
         JK=JQ+J
         HOLD=A(JK)
         JI=JR+J
         A(JK)=-A(JI)
110 A(JI)=HOLD
120 J=M(K)
       IF (J-K) 100,100,125
125 KI=K-N
       DO 130 I=1,N
         KI=KI+N
         HOLD=A(KI)
         JI=KI-K+J
         A(KI)=-A(JI)
130 A(JI)=HOLD
       GO TO 100
150 RETURN
     END

```

```

C      SUBROUTINE MPLY(A,B,R,M,L,N)
C      THIS SUBROUTINE COMPUTES  $A(M,L) \times B(L,N)$  AND
C      STORED THE PRODUCT IN  $R(M,N)$ .
C
      DIMENSION A(M,L),B(L,N),R(M,N)
      DO 20 I=1,M
      DO 20 J=1,N
      Z=0.0
      DO 10 K=1,L
10  Z=Z+A(I,K)*B(K,J)
      R(I,J)=Z
20  CONTINUE
      RETURN
      END

```

```

C      SUBROUTINE SWAP(A,M,N,L,K)
C      THIS SUBROUTINE SWAPS THE ROW L TO THE
C      ROW K AND THE COLUMN L TO THE COLUMN K
C      OF THE MATRIX  $A(M,N)$ .
C
      DIMENSION A(M,1)
10  DO 15 I=1,N
      ASWAP=A(L,I)
      A(L,I)=A(K,I)
15  A(K,I)=ASWAP
20  DO 25 I=1,M
      ASWAP=A(I,L)
      A(I,L)=A(I,K)
25  A(I,K)=ASWAP
26  RETURN
      END

```

C
C
C
C

SUBROUTINE A4BAR (A1, A2, A3, A4, TH2, TH3,
1TH4, VA2, VA3, VA4, AA2, AA3, AA4, TH4S, IFL)

THIS SUBROUTINE PERFORMES THE ANALYSIS
OF THE PIN JOINT FOUR-BAR LINKAGE

```

IF (IFL .GT. 0) GO TO 10
PIT2 = 2.*3.141592654
R1 = A1/A2
R2 = A1/A4
R3 = (A1*A1 + A2*A2 - A3*A3 + A4*A4)/(2.*A2*A4)
R4 = A3/A4
10 CA = SIN(TH2)
CB = COS(TH2) - R1
CC = R3 - R2*COS(TH2)
CD = SQRT (CA*CA + CB*CB - CC*CC)
IF (IFL .GT. 0) GO TO 20
TH4P = 2.*ATAN2((CA+CD), (CB+CC))
IF (TH4P .GE. PIT2) TH4P = TH4P - PIT2
TH4M = 2.*ATAN2((CA-CD), (CB+CC))
IF (TH4M .GE. PIT2) TH4M = TH4M - PIT2
IF (TH4S .LT. 0.) TH4S = TH4S + PIT2
IFL = 1
SN = 1.
TH4 = TH4P
IF (ABS(TH4P-TH4S) .LT. ABS(TH4M-TH4S)) GO TO 30
SN = -1.
TH4 = TH4M
GO TO 30
20 TH4 = 2.*ATAN2((CA+SN*CD), (CB+CC))
IF (TH4 .GE. PIT2) TH4 = TH4 - PIT2
30 TH3=ATAN2((A4*SIN(TH4)-A2*SIN(TH2)),
1 (A1+A4*COS(TH4)-A2*COS(TH2)))
DM = 1./(A3*SIN(TH3-TH4))
VA3 = (A2*SIN(TH4-TH2))*DM*VA2
VA4 = (A2*SIN(TH3-TH2))*R4*DM*VA2
AA3 = (A2*SIN(TH4-TH2))*AA2 -
1 A2*COS(TH4-TH2)*VA2*VA2
2-A3*COS(TH3-TH4)*VA3*VA3 + A4*VA4*VA4)*DM
AA4 = (A2*SIN(TH3-TH2))*AA2 -
1 A2*COS(TH3-TH2)*VA2*VA2
2+A4*COS(TH3-TH4)*VA4*VA4 - A3*VA3*VA3)*R4*DM
RETURN
END

```

INPUT DATA FOR THE SYNTHESIS OF A FLEXURAL JOINT MECHANISM, FUNCTION $Y = X^{**2}$

7									
0	20	20	6	19	1	0			
3.00			36.00				128.41	45.00	3.00
30000000.0									
1.00			0.50				1.00	0.25	45.00
67.50									
0	1	1	2	3	4	4	5	6	7
LNE				KB			EL	EB	EH
1	0	20	2	3	0	1	7.570080	0.050	0.400
2	2	3	5	6	1	4	1.74719	0.050	0.020
3	5	6	8	9	4	7	1.74719	0.050	0.020
4	8	9	11	12	7	10	3.00000	0.050	0.400
5	11	12	14	15	10	13	1.74719	0.050	0.020
6	14	15	17	18	13	16	1.74719	0.050	0.020
7	17	18	0	19	16	0	1.66784	0.050	0.400

BIBLIOGRAPHY

1. Seelig, F. A., "Effectively Using Flexural Pivots," Presented at the Design Engineering Conference and Show, Chicato, Ill., May 11-14, 1970, ASME Paper No. 70-DE-51, 8 pp.
2. Towfigh, K., "The Four-Bar Linkage as an Adjustment Mechanism," Proceedings of the Applied Mechanism Conference, Stillwater, Oklahoma, July, 1969, Paper No. 27, 4 pp.
3. "Random Access Prime Mover Uses Flexure Joints Instead of Pivots," Electromechanical Design, Nov. 1968, pp. 48-51.
4. Bisshopp, K.E., and Drucker, D.C., "Large Deflection of Cantilever Beams," Quarterly of Applied Mathematics, Vol. 3, No. 3, Oct. 1945, pp. 272-275.
5. Frisch-Fay, R., "Flexible Bars," Butterworth & Company Limited, London, England, 1962.
6. Tada, Y., and Lee, G.C., "Finite Element Solution to an Elastica Problem of Beams," International Journal For Numerical Methods in Engineering, Vol. 2, 1970, pp. 229-241.
7. Burns, R.H., and Crossley, F.R.E., "Structural Permutations of Flexible Link Mechanisms," Presented at the Mechanisms Conference, Lafayette, Ind., Oct. 10-12, 1966, ASME Paper No. 66-Mech-5, 4 pp.
8. Burns, R.H., and Crossley, F.R.E., "Kinetostatic Synthesis of Flexible Link Mechanisms," Presented at the Mechanisms Conference, Atlanta, Ga., Oct. 5-9, 1968, ASME Paper No. 68-Mech-36, 7 pp.
9. Shockling, L.A., "Kinematic Synthesis of Three Link Mechanisms with one Flexible Link," M.Sc. Thesis, The Ohio State University, Columbus, Ohio, 1969.

10. Shoup, T.E., "An Analytical Investigation of the Large Deflection of Flexible Beam Springs," Ph.D. Dissertation, The Ohio State University, Columbus, Ohio, 1969.
11. Shoup, T.E., and McLarnan, C.W., "On the Use of the Undulating Elastica for the Analysis of Flexible Link Mechanisms," J. Eng. Ind., Trans. ASME, Series B, Vol. 93, No. 1, 1971, pp. 263-267.
12. Shoup, T.E., "On the Use of the Nodal Elastica for the Analysis of Flexible Link Devices," J. Eng. Ind., Trans. ASME, Series B, Vol. 94, No. 3, 1972, pp. 871-875.
13. Shoup, T.E., and McLarnan, C.W., "A Survey of Flexible Link Mechanisms Having Lower Pairs," J. Mechanisms, Vol. 6, No. 1, 1971, pp. 97-105.
14. Boronkay, T.G., and Mei, C., "Analysis and Design of Multiple Input Flexible Link Mechanisms," Journal Mechanisms, Vol. 5, No. 1, 1970, pp. 29-40.
15. Winfrey, R.C., "Elastic Link Mechanism Dynamics," J. Eng. Ind., Trans. ASME, Series B, Vol. 93, No. 1, 1971, pp. 268-272.
16. Winfrey, R.C., "Dynamic Analysis of Elastic Link Mechanisms by Reduction of Coordinates," J. Eng. Ind., Trans. ASME, Series B, Vol. 94, No. 2, 1972, pp. 577-582.
17. Kaufman, R.E., and Sandor, G.N., "Operators for the Kinematic Synthesis of Mechanisms by Stretch-Rotation Techniques," Presented at the Mechanisms Conference, Columbus, Ohio, Nov. 14, 1970, ASME Paper No. 70-Mech-79, 8 pp.
18. Erdman, A.G., Imam, I., and Sandor, G.N., "Applied Kineto-Elastodynamics," Proceedings of the Applied Mechanism Conference, Stillwater, Oklahoma, Oct. 1971, Paper No. 21, 17 pp.
19. Erdman, A.G., Sandor, G.N., and Oakberg, R.G., "A General Method for Kineto-Elastodynamic Analysis and Synthesis of Mechanisms," Presented at the Winter Annual Meeting, Washington, D.C., Nov. 28-Dec. 2, 1971, ASME Paper No. 71-WA/DE-6, 13 pp.

20. Erdman, A.G., and Sandor, G.N., "Kineto-Elastodynamics - A Review of the State of the Art and Trends," Mechanism and Machine Theory (Formerly the Journal of Mechanisms), Vol. 7, No. 1, 1972, pp. 19-33.
21. Neubauer, A.H., Cohen, R., and Hall, A.S., "An Analytical Study of the Dynamics of an Elastic Linkage," J. Eng. Ind., Trans. ASME, Series B, Vol. 88, 1966, pp. 311-317.
22. Viscomi, B.V., and Ayre, R.S., "Nonlinear Dynamic Response of Elastic Slider-Crank Mechanism," J. Eng. Ind., Trans. ASME, Series B, Vol. 93, No. 1, 1971, pp. 251-262.
23. Jasinski, P.W., Lee, H.C., and Sandor, G.N., "Vibrations of Elastic Connecting Rod of a High-speed Slider-crank Mechanism," J. Eng. Ind., Trans. ASME, Series B, Vol. 93, No. 2, 1971, pp. 636-644.
24. Tobias, J.R., and Frohrib, D.A., "Stability Analysis of a Beam Element in a Planar Mechanism," Proceedings of the 12th Midwestern Mechanics Conference, Aug. 1971, Vol. 6, pp. 607-620.
25. Seevers, J.A., and Yang, A.T., "Dynamic Stability Analysis of Linkages with Elastic Members via Analog Simulation," Presented at the Mechanisms Conference, Columbus, Ohio, Nov. 1-4, 1970, ASME Paper No. 70-Mech-48, 9 pp.
26. Davidson, J.K., "Analysis and Synthesis of a Slider-Crank Mechanism with a Flexibly-Attached Slider," Journal of Mechanisms, Vol. 5, No. 2, 1970, pp. 239-247.
27. Lowen, G.G., and Jandrosits, W.G., "Survey of Investigations into the Dynamic Behaviour Mechanisms Containing Links With Distributed Mass and Elasticity," Mechanism and Machine Theory, Vol. 7, No. 1, 1972, pp. 3-17.
28. Turner, M.J., Dill, E.H., Martin, H.C., Melosh, R.J., "Large Deflections of Structures Subjected to Heating and External Loads," Journal of the Aerospace Sciences - Vol. 27, Feb. 1960, pp. 97-127.

29. Martin, H.C., "On the Derivation of Stiffness Matrices for the Analysis of Large Deflection and Stability Problems," Proceedings of the First Air Force Conference on Matrix Methods in Structural Mechanics, WPAFB, Dayton, Ohio, Nov. 1965, AFFDL-TR-66-80, pp. 697-715.
30. Martin, H.C., "Finite Elements and the Analysis of Geometrically Nonlinear Problems," Presented at Japan-U.S. Seminar on Matrix Methods of Structural Analysis and Design, Tokyo, Japan, Aug. 25-30, 1969, 53 pp.
31. Argyris, J.H., "Continua and Discontinua," Proceedings of the First Air Force Conference on Matrix Methods in Structural Mechanics, WPAFB, Dayton, Ohio, 1965, AFFDL-TR-66-80, pp. 151-169.
32. Argyris, J.H., Buck, K.E., Scharpf, D.W., Hilber, H.M., Mareczek, G., "Some New Elements for the Matrix Displacement Method," Proceedings of the Second Conference on Matrix Methods in Structural Mechanics, at WPAFB, Dayton, Ohio, 15-17 Oct. 1968, pp. 333-397.
33. Jennings, A., "Frame Analysis Including Change of Geometry," J. of Structural Division, A.S.C.E., Vol. 94, No. ST3, March 1968, pp. 627-644.
34. Purdy, D.M., and Przemieniecki, J.S., "Influence of Higher-Order Terms in the Large Deflection Analysis of Frameworks," Proceedings A.S.C.E., Joint Specialty Conference, Optimization and Nonlinear Problems, April 1968, pp. 142-152.
35. Przemieniecki, J.S., "Theory of Matrix Structural Analysis", McGraw-Hill Book Company, New York, 1968.
36. Mallett, R.H., and Marcal, P.V., "Finite Element Analysis of Nonlinear Structures," J. of Structural Division A.S.C.E., Vol. 94, No. ST9, Sept. 1968, pp. 2081-2105.
37. Powell, G.H., "Theory of Nonlinear Elastic Structures," J. of Structural Division A.S.C.E., Vol. 95, No. ST12, Dec. 1969, pp. 2687-2701.

38. Ebner, A.M., and Ucciferro, J.J., "A Theoretical and Numerical Comparison of Elastic Nonlinear Finite Element Methods," Presented at the National Symposium on Computerized Structural Analysis and Design, Washington, D.C., March 27-29, 1972, 41 pp.
39. Guyan, R.J., "Reduction of Stiffness and Mass Matrices," AIAA Journal, Vol. 3, No. 2 1965, pp. 380.
40. Freudenstein, F., "An Analytical Approach to the Design of Four-Link Mechanisms," ASME, Trans. Vol. 76, April 1954, pp. 483-492.
41. Freudenstein, F., "Four-Bar Function Generators," Machine Design, Nov. 27, 1958, pp. 119-123.
42. Freudenstein, F., and Sandor, G.N., "Synthesis of Path Generating Mechanisms by Means of a Programmed Digital Computer," J. Eng. Ind., Trans. ASME, Vol. 81, Series B, 1959, pp. 159-168.
43. McLarnan, C.W., "Synthesis of Six-Link Plane Mechanisms by Numerical Analysis," J. Eng. Ind., Trans., ASME, Series B, Vol. 85, No. 1, 1963, pp. 5-11.
44. Roth, B., and Freudenstein, F., "Synthesis of Path-Generating Mechanisms by Numerical Methods," J. Eng. Ind. Trans., ASME, Series B, Vol. 85, No. 3, Aug. 1963, pp. 298-306.
45. Wasiutynski, Z., and Brandt, A., "The Present State of Knowledge in the Field of Optimum Design of Structures," Applied Mechanics Reviews, Vol. 16, No. 5, 1963, pp. 341-350.
46. Sheu, C.Y., and Prager, W., "Recent Developments in Optimal Structural Design," Applied Mechanics Reviews, Vol. 21, No. 10, 1968, pp. 985-992.
47. Prager, W., "Optimization of Structural Design," Journal of Optimization Theory and Applications, Vol. 6, No. 1, 1970, pp. 1-21.
48. Seireg, A., "A Survey of Optimization of Mechanical Design," J. Eng. Ind. Trans. ASME, Series B, Vol. 94, No. 2, 1972, pp. 495-499.

49. Fox, R.L., and Gupta, K.C., "Optimization Technology as Applied to Mechanism Design," Report No. 47, Case Western Reserve University, Cleveland, Ohio, 1971.
50. Sallam, M.M., and Lindholm, J.C., "Synthesis and Optimization of 4-Bar and G-Bar Plane Mechanisms A Literature Survey, Presented at the Second Applied Mechanism Conference, Stillwater, Oklahoma, 1971, 8 pp.
51. Levenberg, K., "A Method for the Solution of Certain Nonlinear Problems in Least-Squares," Quarterly of Applied Mathematics, Vol. 2, 1944, pp. 164-168.
52. Timko, C.A., "Determining Linkage Proportions," Machine Design, March 31, 1966, pp. 127-130.
53. Lewis, D.W., and Gyory, C.K., "Kinematic Synthesis of Plane Curves," J. Eng. Ind. Trans. ASME, Series B, Vol. 89, No. 1, 1967, pp. 173-176.
54. Lewis, D.W., and Falkenhagen, G.L., "Displacement and Velocity Kinematic Synthesis," J. Eng. Ind. Trans. ASME, Series B, Vol. 90, No. 3, Aug. 1968, pp. 527-530.
55. Lewis, D.W., and Falkenhagen, G.L., "Synthesis of Noncyclic Multiple Input Mechanism," Presented at the Mechanism Conference, Atlanta, Ga., Oct. 5-9, 1968, ASME Paper No. 68-Mech-52, 7 pp.
56. Chi-Yeh, H., "A General Method for the Optimum Design of Mechanisms," Journal of Mechanisms, Vol. 1, 1966, pp. 301-313.
57. Mansour, W.M., and Osman, M.O.M., "The Method of Residues for the Synthesis of Coupler Curve Generating Mechanisms," Presented at the Mechanisms Conference, Columbus, Ohio, Nov. 1-4, 1970, ASME Paper No. 70-Mech-53. 7 pp.
58. Marquardt, D.W., "An Algorithm for Least-Squares Estimation of Nonlinear Parameters," Journal of the Society for Industrial and Applied Mathematics, Vol. 2, 1963, pp. 431-441.

59. Powell, M.J.D., "A Method for Minimizing a Sum of Squares of Nonlinear Functions Without Calculating Derivatives," The Computer Journal, Vol. 7, No. 4, 1965, pp. 303-307.
60. Brooks, S.H., "A Discussion of Random Methods for Seeking Maxima," Operation Research, Vol. 6, 1958, pp. 244-251.
61. Tomas, J., "The Synthesis of Mechanisms as a Nonlinear Programming Problem," Journal of Mechanisms, Vol. 3, 1963, pp. 119-130.
62. Tomas, J., "Optimum Seeking Methods Applied to a Problem of Dynamic Synthesis in a Loom," Journal of Mechanisms, Vol. 5, No. 4, 1970, pp. 495-504.
63. Garrett, R.E., and Hall, A.S., "Optimal Synthesis of Randomly Generated Linkages," J. Eng. Ind. Trans. ASME, Series B, Vol. 90, No. 3, 1968, pp. 475-480.
64. Eschenbach, P.W., and Tesar, D., "Optimization of Four-Bar Linkages Satisfying Four Generalized Coplanar Positions," J. Eng. Ind. Trans. ASME, Series B, Vol. 91, No. 1, 1969, pp. 75-82.
65. Rosenbrock, H.H., "An Automatic Method for Finding the Greatest or Least Value of a Function," The Computer Journal, Vol. 3, 1960, pp. 175-184.
66. Lakshminarayana, K., and Narayanamurthi, R.G., "Derivative Synthesis of Plane Mechanisms to Generate Functions of Two Variables," Journal of Mechanisms, Vol. 5, No. 2, 1970, pp. 249-271.
67. Sridhar, B.N., and Torfason, L.E., "Optimization of Spherical Four-Bar Path Generators," Presented at the Mechanisms Conference, Columbus, Ohio, Nov. 1-4, 1970, ASME Paper No. 70-Mech-46, 4 pp.
68. Mueller, G.S., and Osman, M.O.M., "A Computer-Oriented Numerical Approach for the Synthesis of Planar Mechanisms," Presented at the Second Applied Mechanism Conference, Stillwater, Oklahoma, 1971, 13 pp.
69. Curry, H.B., "The Method of Steepest Descent for Nonlinear Minimization Problems," Quarterly of Applied Mathematics, Vol. 2, No. 3, 1944, pp. 258-261.

70. Tull, H.G., and Lewis, D.W., "Three-Dimensional Kinematic Synthesis," J. Eng. Ind. Trans. ASME, Series B, Vol. 90, No. 3, 1968, pp. 481-484.
71. Rees Jones, J. and Rooney, G.T., "Motion Analysis of Rigid Link Mechanisms by Gradient Optimization on an Analogue Computer," Journal of Mechanism, Vol. 5, No. 2, 1970, pp. 191-201.
72. Kugath, D., "Direct Optimization Techniques Applied to Computer Aided Linkage Design," Ph.D. Dissertation, Purdue University, 1967, University Microfilm No. 67-10218.
73. Nechi, A.J., "A Relaxation and Gradient Combination Applied to the Computer Simulation of a Plane Four-Bar Chain," J. Eng. Ind., Trans. ASME, Series B, Vol. 93, No. 1, 1971, pp. 113-119.
74. Dimarogonas, A.D., Sandor, G.N., and Erdman, A.G., "Synthesis of a Geared N-Bar Linkage," J. Eng. Ind., Trans. ASME, Series B, Vol. 93, No. 1, 1971, pp. 157-164.
75. Bagci, C., "Minimum Error Synthesis of Space Mechanisms for the Generation of Constrained and Unconstrained Screws," J. Eng. Ind., Trans. ASME, Series B, Vol. 93, No. 1, 1971, pp. 165-175.
76. Davidon, W.C., "Variable Metric Method for Minimization," A.E.C. Research and Development Report, ANL-5990 (Rev.) 1959.
77. Fletcher, R., and Powell, M.J.D., "A Rapidly Convergent Descent Method for Minimization," The Computer Journal, Vol. 6, 1963, pp. 163-168.
78. Fox, R.L., and Willmert, K.D., "Optimum Design of Curve-Generating Linkages with Inequality Constraints," Engineering Design Center Report No. 2-66-11, Case Institute of Technology, Cleveland, Ohio, 1966.
79. Fox, R.L., and Willmert, K.D., "Optimum Design of Curve-Generating Linkages With Inequality Constraints," J. Eng. Ind., Trans. ASME, Series B, Vol. 89, No. 1, 1967, pp. 144-152.
80. Willmert, K.D., and Fox, R.L., "Optimum Design of a Linear Multi-Degree-of-Freedom Shock Isolation System," J. Eng. Ind., Trans., ASME, Series B, Vol. 94, No. 2, 1972, pp. 465-471.

81. Fiacco, A.V., and McCormick, G.P., "Computational Algorithm for the Sequential Unconstrained Minimization Technique for Nonlinear Programming," Management Science, Vol. 10, 1964, pp. 601-617.
82. Fox, R.L., "Optimization Methods for Engineering Design," Addison-Wesley Publishing Company, Massachusetts, 1971.
83. Moore, L.I., "Linkage Optimization Using Inequality Constraint Penalty Functions," M.S. Thesis, Case Western Reserve University, Cleveland, Ohio, June, 1968.
84. Tranquilla, M., "Optimum Design of a Four-Bar Linkage Whose Coupler Path Has Specified Extremes," J. Eng. Ind., Trans. ASME, Series B, Vol. 94, No. 2, 1972, pp. 483-487.
85. Stewart, G.W., "A Modification of Davidson's Minimization Method to Accept Difference Approximations of Derivatives," Journal of A.C.M., Vol. 14, No. 1, Jan. 1967, pp. 72-83.
86. Fletcher, R., and Reeves, C.M., "Function Minimization by Conjugate Gradients," The Computer Journal, Vol. 7, No. 2, 1964, pp. 149-154.
87. Powell, M.J.D., "An Efficient Method for Finding the Minimum of a Function of Several Variables Without Calculating Derivatives," The Computer Journal, Vol. 7, No. 3, 1964, pp. 155-162.
88. Powell, M.J.D., "Rank One Methods for Unconstrained Optimization," Presented at the International Summer School on Integer and Nonlinear Programming, NATO Advanced Study Institute, France, 1969.
89. Mangasrian, O.L., "Techniques of Optimization", J. Eng. Ind., Trans. ASME, Series B, Vol. 94, No. 2, 1972, pp. 365-372.